NUREG/CR-5741

Technical Bases for Regulatory Guide for Soil Liquefaction

U.S. Army Corps of Engineers

U.S. Nuclear Regulatory Commission
Office of Nuclear Regulatory Research
Washington, DC 20555-0001

AVAILABILITY NOTICE

Availability of Reference Materials Cited in NRC Publications

NRC publications in the NUREG series, NRC regulations, and *Title 10, Energy,* of the *Code of Federal Regulations,* may be purchased from one of the following sources:

1. The Superintendent of Documents
   U.S. Government Printing Office
   P.O. Box 37082
   Washington, DC 20402–9328
   <http://www.access.gpo.gov/su_docs>
   202–512–1800
2. The National Technical Information Service
   Springfield, VA 22161–0002
   <http://www.ntis.gov>
   1–800–553–6847 or locally 703–605–6000

The NUREG series comprises (1) brochures (NUREG/BR-XXXX), (2) proceedings of conferences (NUREG/CP-XXXX), (3) reports resulting from international agreements (NUREG/IA-XXXX), (4) technical and administrative reports and books [(NUREG-XXXX) or (NUREG/CR-XXXX)], and (5) compilations of legal decisions and orders of the Commission and Atomic and Safety Licensing Boards and of Office Directors' decisions under Section 2.206 of NRC's regulations (NUREG-XXXX).

A single copy of each NRC draft report for comment is available free, to the extent of supply, upon written request as follows:

Address: Office of the Chief Information Officer
Reproduction and Distribution
Services Section
U.S. Nuclear Regulatory Commission
Washington, DC 20555–0001
E–mail: <DISTRIBUTION@nrc.gov>
Facsimile: 301–415–2289

A portion of NRC regulatory and technical information is available at NRC's World Wide Web site:

<http://www.nrc.gov>

After January 1, 2000, the public may electronically access NUREG-series publications and other NRC records in NRC's Agencywide Document Access and Management System (ADAMS), through the Public Electronic Reading Room (PERR), link <http://www.nrc.gov/NRC/ADAMS/index.html>.

Publicly released documents include, to name a few, NUREG-series reports; *Federal Register* notices; applicant, licensee, and vendor documents and correspondence; NRC correspondence and internal memoranda; bulletins and information notices; inspection and investigation reports; licensee event reports; and Commission papers and their attachments.

Documents available from public and special technical libraries include all open literature items, such as books, journal articles, and transactions, *Federal Register* notices, Federal and State legislation, and congressional reports. Such documents as theses, dissertations, foreign reports and translations, and non-NRC conference proceedings may be purchased from their sponsoring organization.

Copies of industry codes and standards used in a substantive manner in the NRC regulatory process are maintained at the NRC Library, Two White Flint North, 11545 Rockville Pike, Rockville, MD 20852–2738. These standards are available in the library for reference use by the public. Codes and standards are usually copyrighted and may be purchased from the originating organization or, if they are American National Standards, from—

American National Standards Institute
11 West 42nd Street
New York, NY 10036–8002
<http://www.ansi.org>
212–642–4900

NUREG/CR-5741

Technical Bases for Regulatory Guide for Soil Liquefaction

Manuscript Completed: October 1999
Date Published: March 2000

Prepared by
J. P. Koester, M. K. Sharp, M. E. Hynes

U.S. Army Corps of Engineers
3909 Halls Ferry Road
Vicksburg, MS 39180-6199

E. G. Zurflueh, NRC Project Manager

Prepared for
Division of Engineering Technology
Office of Nuclear Regulatory Research
U.S. Nuclear Regulatory Commission
Washington, DC 20555-0001
NRC Job Code W6246

ABSTRACT

This document provides technical bases for development of a new U.S. Nuclear Regulatory Commission Regulatory Guide for evaluation of the potential for earthquake-induced liquefaction at nuclear facility sites, compiling current and state of the art techniques. The report summarizes the processes of acquiring and using geological, geophysical, geotechnical, and other kinds of relevant information that support design considerations with respect to liquefaction hazard and that may affect the construction or performance of a building or other engineered structure at selected sites. A historical perspective is provided to define liquefaction phenomena observed during earthquakes and to support identification of soil characteristics associated with liquefaction. Guidance is presented for site characterization studies, including the various in situ tests available for liquefaction potential evaluation. Screening techniques are described for preliminary hazard assessment; progressively more detailed procedures are presented to provide for investigations that are judged necessary once screening procedures identify soils that may pose a hazard to important facilities. Deterministic procedures are treated in this report; probabilistic approaches are detailed in a separate report, prepared by Dr. Mary E. Hynes of the U.S. Army Engineer Waterways Experiment Station.

This document is not intended to serve as a definitive manual; some specific recommendations are offered, however, it was the purpose of the authors to allow for engineering judgment, thus it is more comprehensive as a reference document. An example problem is included to illustrate the evaluation of liquefaction triggering and estimation of residual strength of liquefied soils. Current practice for evaluation and estimation of permanent deformations caused to earthen structures is discussed; deformations accompanying liquefaction are included, but limited to those resulting from inertial movements during shaking. Large, permanent deformations that may result from gravity slumping are not discussed; estimation of very large deformations is not a well-established process and is a subject of ongoing research.

TABLE OF CONTENTS

ABSTRACT . . . iii

PREFACE . . . ix

1 INTRODUCTION . . . 1
1.1 Background . . . 1
1.2 Purpose and Scope . . . 1

2 LIQUEFACTION OF SOIL DEPOSITS . . . 2
2.1 Definitions . . . 2
2.2 Mechanisms of Soil Liquefaction . . . 3
2.3 Surface Manifestations of Liquefaction . . . 3
2.4 Factors Influencing Liquefaction Potential . . . 5
2.5 Characteristics of Liquefiable Soils . . . 14
2.6 Residual Strength of Liquefied Soils . . . 14
2.6.1 Use of In Situ Testing Procedures . . . 14
2.6.2 Laboratory Based Method . . . 16

3 LIQUEFACTION POTENTIAL EVALUATION PROCEDURES . . . 22
3.1 Liquefaction Potential Assessment - Overview . . . 22
3.1.1 Site Characterization - General . . . 22
3.1.2 In Situ Testing . . . 23
3.1.2.1 Standard Penetration Test (SPT) . . . 23
3.1.2.2 Cone Penetration Test (CPT) . . . 23
3.1.2.3 Becker Penetration Tests . . . 31
3.1.2.4 Large Penetrometer Tests . . . 40
3.1.2.5 Pressuremeter Applications . . . 40
3.1.2.6 Seismic Wave Velocity Measurements . . . 40
3.1.2.7 Other . . . 44
3.1.3 Undisturbed Sampling . . . 47
3.2 Screening Techniques . . . 47
3.2.1 General . . . 47
3.2.2 Liquefaction Hazard Screening Evaluation . . . 48
3.2.2.1 Are Potentially Liquefiable Soil Types Present? . . . 49
3.2.2.2 Are They Saturated and/or May They Become Saturated? . . . 49
3.2.2.3 Is the Geometry of Potentially Liquefiable Deposits Such that They Pose No Risk? . . . 49
3.2.3 Quantitative Evaluation of Liquefaction Resistance . . . 51
3.3 Evaluation of Liquefaction Susceptibility - General . . . 51
3.3.1 Analytical Methods . . . 51
3.3.2 Physical Modeling . . . 52
3.3.3 Empirical Procedures . . . 53
3.3.4 Laboratory Cyclic Strength Testing . . . 53
3.4 Procedures for Empirical Evaluation of Liquefaction Susceptibility . . . 54
3.4.1 Evaluation of Earthquake-Induced Cyclic Stress Ratios . . . 54
3.4.1.1 Method 1. Simple, Empirical Evaluation Based on Prior Analyses . . . 54

3.4.1.2 Method 2. Direct Calculation of $\tau_{hv,cyclic,max}$ or $a_{max,z}$ at Each Point of Interest .. 58
3.4.2 Evaluation of In Situ Liquefaction Resistance 60
3.4.2.1 "Standardized" SPT criteria 60
3.4.2.2 Corrections to SPT N_m Values to Yield $(N_1)_{60}$ Values 62
3.4.3 Correction for Earthquake Magnitudes other than M = 7-1/2 67
3.4.4 Correction of CRR for Effective Overburden Stress 69
3.4.5 Correction of CRR for Initial Static Shear Stress 69
3.5 Energy Approach 71
3.6 Evaluation of Factor of Safety and Residual Excess Pore Pressure Generation 71
3.7 Example Calculations 74
3.7.1 Given 74
3.7.2 Problem 77

4 ANALYSIS OF DISPLACEMENTS ACCOMPANYING LIQUEFACTION 81
4.1 Background 81
4.2 Inertial Deformations (Newmark Sliding Block Analogy) 81
4.3 Lateral Spreading Estimation 88
4.4 Settlements Consequent to Liquefaction 89

5 CONCLUSIONS 91

REFERENCES 91

APPENDIX A STEADY STATE STRENGTH TESTING A-1

LIST OF FIGURES

Figure 1. Changes in soil fabric during cyclic loading (Walker and Stewart, 1989, after Youd, 1977) 4
Figure 2. Limiting shear strains in Monterey No. 0 sand as a function of relative density (after DeAlba, Seed and Chan, 1976) 7
Figure 3. Influence of initial principal stress ratio on liquefaction resistance of clean sands in simple shear tests (Walker and Stewart, 1989, after Seed, 1979) 9
Figure 4. Relationship between cyclic strength and OCR (Walker and Stewart, 1989, after Ishihara and Takatsu, 1979) 10
Figure 5. Comparison of overburden pressure correction factor for liquefaction resistance, K_σ, for various soils (after Hynes, 1988) 11
Figure 6. Initial static shear stress liquefaction resistance correction factor, K_α as a function of initial static shear stress ratio, α (Rollins, 1987) 12
Figure 7. Liquefaction occurrence as a function of magnitude and distance, R_{MAX}, from the zone of faulting (adapted from Carter and Seed, 1988) 13
Figure 8. Relationship between equivalent clean sand SPT blowcount $(N_1)_{60}$ and undrained residual shear strength (Seed and Harder, 1990) 17
Figure 9. Typical stress-strain and pore pressure response in monotonic triaxial tests on sands (Department of the Army, 1970) 19
Figure 10. Charts relating normalized SPT resistance $(N_1)_{60}$ and residual shear strength (S_r) to vertical overburden pressure (σ'_{vo}) for saturated nongravelly silt-sand deposits that have experienced large deformation (Baziar and Dobry, 1995) 21

Figure 11. NCEER (1997) recommended cyclic resistance ratio (CRR) for clean sands under level ground conditions based on CPT 25
Figure 12. Stress exponents for cone resistance on the CPT soil characterization chart (Olsen and Mitchell, 1995) 27
Figure 13. Depiction of cone resistance trends toward the stress focus for any relative density (Olsen, 1994) 28
Figure 14. Estimation of the normalized liquefaction cyclic resistance ratio (CRR_1) using the CPT soil characterization techniques (Olsen, Koester, and Hynes, 1996) 29
Figure 15. CPT estimation of SPT N_1 using both CPT measurements (Olsen 1994, 1988, 1986, 1984) 30
Figure 16. Graphical procedural steps for CPT-based determination of the SPT blowcount, fines content, equivalent clean sand SPT blowcount, and normalization liquefaction cyclic resistance ratio (CRR_1) (Olsen, 1988) 32
Figure 17. SPT blowcount fines content correction (Olsen, 1988) 33
Figure 18. Curves recommended by NCEER workshop for calculation of CRR from SPT and fines content data (NCEER, 1997) 34
Figure 19. Schematic diagram of Becker Hammer sampling operation 36
Figure 20. Correction curves adopted to correct Becker hammer blowcounts to constant combustion curve adopted for correction (from Harder and Seed, 1986) 37
Figure 21. Correlation between corrected Becker hammer and SPT blowcounts (from Harder and Seed, 1986) 38
Figure 22. Concept of dynamic penetration test (Kokusho, 1989) 41
Figure 23. Soil profile at T-site (Tanaka, et al., 1989) 42
Figure 24. SPT vs. LPT relationship for gravelly soils (Kokusho, 1989) 43
Figure 25. Chart to predict liquefaction in clean sands from shear wave velocity and maximum acceleration (Stokoe et al., 1988) 45
Figure 26. Recommended liquefaction assessment chart based on V_{S1} and CSR for magnitude 7.5 earthquake and uncemented soils of Holocene age (NCEER, 1997) 46
Figure 27. Schematic of cyclic triaxial test equipment (Department of the Army, 1986) 55
Figure 28. Typical analog recordings of load, deformation, and pore pressures during a cyclic triaxial test (Department of the Army, 1986) 56
Figure 29. Cyclic triaxial strength curves for Monterey No. 0 sand (Department of the Army, 1986) 57
Figure 30. Variations of the parameter r_d with depth (NCEER, 1997) 59
Figure 31. Correlation between correction factor C_N and effective overburden pressure (Marcuson and Bieganousky, 1977) 65
Figure 32. Several proposed relationships between SPT penetration resistance and relative density (Torrey, Dunbar, and Peterson, 1988) 66
Figure 33. Relationship between K_M and magnitude (NCEER, 1997) 68
Figure 34. K_σ recommendations from NCEER (1997) workshop 70
Figure 35. K_α recommendations from NCEER (1997) workshop 72
Figure 36. Observed liquefaction data plotted as a function of fines content and Arias Intensity I_{hb} (after Kayen, 1983) 73
Figure 37. Relationship between residual excess pore water pressure ratio and factor of safety against liquefaction, from laboratory data (Marcuson, Hynes, and Franklin, 1990) 75
Figure 38. Example problem soil profile with raw SPT blowcounts 76
Figure 39. Principal components of the sliding block analysis (Franklin and Chang, 1977) 83
Figure 40. Comparison of peak base and crest transverse accelerations measured at earth dams (from Harder, et al. 1990, as modified by Cameron, 1996) 85

Figure 41. Relationship of the variation of maximum acceleration ratio with depth of sliding mass (Makdisi and Seed, 1978) 86
Figure 42. Variation of displacement with yield acceleration for various earthquake magnitudes (Makdisi and Seed, 1978) 87
Figure 43. Curves for estimating volumetric strain at liquefiable sites (Youd, 1988, after Tokimatsu and Seed, 1987) 90
Figure A-1. Typical undrained triaxial test result on loose sand (Castro, Poulos, and France, 1985) A-3
Figure A-2. State diagram for compacted specimens (Castro, Poulos, and France, 1985) A-5
Figure A-3. Correction of steady state strength for void ratio changes (Castro, Poulos, and France, 1985) A-7

LIST OF TABLES

Table 1 Estimated Susceptibility of Sedimentary Deposits to Liquefaction During Strong Seismic Shaking Based on Geological Age and Depositional Environment (After Youd and Perkins 1978) 15
Table 2 Summary of liquefaction occurrences in gravel deposits (after Sy, Campanella, and Stewart, 1995, supplemented by the author) 35
Table 3 Relative liquefaction susceptibility of natural deposits as a function of groundwater table depth (Youd, 1998) 50
Table 4 Summary of energy ratios (ER) for some common SPT procedures (after Seed, et al., 1984, 1986) 61
Table 5 Corrections to SPT N-values (NCEER, 1997, modified from Skempton, 1986) 63
Table 6 Corrections to N-values for Example Problem 78
Table 7 Calculation of Factor of Safety and Residual Excess Pore Pressure Ratio 79
Table 8 Evaluation of Residual Strength of Liquefied Soil for Example Problem 82

PREFACE

The study covered by this report was performed by the U.S. Army Engineer Waterways Experiment Station (WES) for the U.S. Nuclear Regulatory Commission (NRC) under Inter-Agency Agreement RES-95-008 during the period June, 1995 to January, 1999. The study was directed by Mr. Robert Kornasiewicz, Office of Nuclear Regulatory Research, NRC.

The report was prepared by Dr. Joseph P. Koester, Mr. Michael K. Sharp, and Dr. Mary E. Hynes of the Earthquake Engineering and Geosciences Division (EEGD), Geotechnical Laboratory, WES. General supervision was provided by Dr. Mary E. Hynes, Chief, Earthquake Engineering and Geophysics Branch, and Dr. Lillian D. Wakeley, Acting Chief, EEGD.

At the time of publication of this report, Commander and Acting Director of WES was COL Robin R. Cababa, EN.

1 INTRODUCTION

1.1 Background

Soils subjected to earthquake shaking may undergo either transient or permanent reduction in undrained shear resistance (stiffness and/or strength) as a consequence of excess pore water pressures or disruption of the soil structure accompanying cyclic loading. Cyclic strength degradation may range from slight diminution of shear resistance to the catastrophic strength loss associated with seismically-induced liquefaction, which is a transient phenomenon. Regulatory documentation pertaining to the geotechnical engineering evaluation of potential or existing nuclear facilities reflects the concern of the Nuclear Regulatory Commission (NRC) over the effect of seismic instability of foundation soil deposits. As previously discussed by Koester and Franklin (1985) in a state-of-the-art report on liquefaction potential assessment methodologies prepared for the NRC, the reference regulation is Appendix A, "Seismic and Geologic Siting Criteria for Nuclear Power Plants," to 10 CFR, Part 100, "Reactor Site Criteria," which requires the evaluation of geologic features which could affect the foundations of nuclear facility structures, including liquefaction of soil when subjected to earthquake shaking. The National Center for Earthquake Engineering Research (NCEER; recently renamed the Multidisciplinary Center for Earthquake Engineering Research, MCEER) sponsored a January, 1996 workshop on liquefaction evaluation procedures, the proceedings of which (NCEER, 1997) will shape the state of practice for the next several years.

The NRC requires new guidelines to be developed for design basis evaluation of liquefaction potential and post-earthquake stability of soils as a consequence of recent developments in geotechnical earthquake engineering research and practice. This report provides technical bases for subsequent development of regulatory guidance that reflects both current practice and the state-of-the-art for evaluation of seismic stability of soils, with emphasis on the potential for and consequences of seismically-induced liquefaction of soils beneath foundations.

Current guidance for conducting geotechnical site investigations is provided by: Regulatory Guide 1.132, "Site Investigations for Foundations of Nuclear Power Plants (U.S. Nuclear Regulatory Commission, 1979);" and Regulatory Guide 1.138, "Laboratory Investigation of Soils for Engineering Analysis and Design of Nuclear Power Plants (U.S. Nuclear Regulatory Commission, 1978)." Substantial changes have taken place since these guides were published, particularly in the performance of in situ investigations and the interpretation and application of test results to evaluate seismic stability of foundation soils. The NRC requires that extant guidance be reevaluated in view of current practice and the state-of-the-art, and that new guidance be developed to address liquefaction potential assessment procedures. Companion reports were prepared concurrently with this document to provide technical bases to support updates of the above Regulatory Guides.

1.2 Purpose and Scope

This report was prepared for the Office of Nuclear Regulatory Research, NRC, to provide technical bases for currently accepted methods used in the evaluation of liquefaction potential of soil deposits that may be subjected to earthquake shaking. The report describes deterministic procedures and criteria that are currently applied to assess the liquefaction potential of soils ranging in gradation from gravels to clays, and provides guidance for simplified analysis of the consequences of liquefaction, i.e., lateral spreading of level or gently sloping deposits. Approaches to estimate earthquake-induced deformation of slopes are also discussed, with emphasis on the applicability of simplified techniques and the informed selection of strengths to use in these estimates. Probabilistic approaches are presented in a separate report, in view of the NRC's concern over seismic margin issues.

The scope of the report is limited to evaluation of the behavior of soils subjected to earthquake shaking, and specifically excludes non-seismic failure of sensitive clays, failure under static load conditions (such as flow slides in loose point bar deposits), and soil response to machine vibrations and blasting. The selection or synthesis of appropriate ground motion records to use for response analysis is beyond the scope of this report.

2 LIQUEFACTION OF SOIL DEPOSITS

2.1 Definitions

Several terms used in this document may be interpreted according to various perspectives; definitions are provided below to establish convention. Variables specific to a given measurement or calculation will be defined as they are introduced.

<u>Liquefaction</u>. The word *liquefaction* literally means a state change from solid to a liquid. In the context of this guidance and soil mechanics in general, the term refers to a change from a solid or stable assemblage of soil particles (structure) to a complete or substantially complete suspension of the solid particles in a fluid, such that the suspension has very low shear strength. In reality, the condition of full suspension and zero strength is seldom encountered. Small and large scale laboratory tests and observations in instrumented sites during earthquakes indicate that, under certain circumstances, the soil may deform for a limited strain range with very low shear resistance; however, shear resistance, sometimes substantial, is mobilized for larger strains (particularly in dilative granular soils). Some practitioners restrict use of the term *liquefaction* to describe flow failure, as observed to occur in a failed slope when driving shear stresses remain higher than the post-failure shear strength of the soil materials (e.g., Castro and Poulos, 1977). *Liquefaction* as treated in this report includes any drastic loss of undrained shear resistance (stiffness and/or strength) resulting from repeated, rapid straining, regardless of the state of stress prior to loading. The term is interchangeably applied to the development of either excessive cyclic strains or complete loss of effective stress within an undrained laboratory specimen under cyclic loading. The term *initial liquefaction* is also occasionally used in practice to describe the buildup of pore water pressure in laboratory tests within an undrained soil specimen to a level equal to the total confining stress applied to the confining membrane.

<u>Liquefaction resistance</u> is the capacity of a soil to resist the drastic strength loss described above. This term is generally interpretable regardless of the means of its measurement; every attempt has been made in this document to follow the convention established among contemporary researchers and practitioners to associate the term <u>cyclic strength</u> to laboratory determination of the capacity of a specimen under controlled conditions to resist development of a specified level of cyclic straining or excess pore pressures.

<u>Cyclic resistance ratio, CRR</u> is defined for the purposes of this document as the ratio of a soil's capacity to resist liquefaction to the initial effective confining stress at the point in question. This follows the recommendations published in the proceedings of a definitive National Center for Earthquake Engineering Research (NCEER, now the Multidisciplinary Center for Earthquake Engineering Research, MCEER) workshop on the subject (NCEER, 1997).

Cyclic stress ratio is defined for the purposes of this document as the ratio of the demand shear load imposed (by earthquake shaking) on a soil to the initial effective confining stress at the point in question. This also follows the recommendations published in NCEER (1997).

Excess pore pressure is defined as the differential pore water pressure induced in a soil deposit or specimen by an externally applied load, i.e., the difference between initial and present pore water pressures, and may be either positive or negative. *Residual excess pore pressure* is that value of excess pore pressure measured at the end of an applied shear stress cycle. The latter quantity, when divided by initial effective confining stress, is termed the *residual excess pore pressure ratio.*

Steady state strength, residual strength, and post-liquefaction strength are considered synonymous in this report and refer to the lowest value of shear strength potentially available in a soil deposit or specimen after liquefaction. The typically very low shear strength of liquefied materials is a vital parameter in post-earthquake stability evaluation practice. The measurement and understanding of this quantity are a matter of some controversy, e.g., whether monotonic or cyclic loading tests produce the appropriate values for use in analysis.

2.2 Mechanisms of Soil Liquefaction

Figure 1 illustrates the response of a relatively loose packing of soil grains to cyclic shear loading. With the onset of shear and at small shear strains, particles are caused to slide or roll along each other, which under undrained (constant volume) conditions causes decreased pore water pressure. For even denser soils, larger-than-initial voids form in the dilating zones, and the larger, unstable holes may ultimately collapse on stress reversal. Increased pore water pressure results from this collapse. Gravity loading also encourages net downward displacements and a tendency for volume reduction, which further contributes to the transfer of load to pore water. Soil fines present in the voids between larger grains of sand likely affect the response of the structure (fabric, anisotropy); recent research (e.g., Koester, 1992) examines the effects of the presence of fines of varying content and index properties on response of soils to undrained cyclic loading.

The following references offer a historical perspective on the early development of analyses techniques for seismic response of saturated cohesionless soil deposits and the physical mechanisms of liquefaction: Casagrande (1936); Shannon and Wilson, Inc., and Agbabian and Associates (1972); Castro (1975); and Finn and Martin (1975). Empirical techniques based on field performance data were developed and promoted during the subsequent several years: Seed (1976, 1979a, 1979b); Castro and Poulos (1977); Casagrande and Rendon (1978); Finn (1981); and Seed and Idriss (1982). Hynes (1988) extended the state of knowledge on liquefaction mechanisms with regard to large-particled soils; Kaufman (1981); Puri (1984); Walker and Stewart (1989); Koester (1992); and others examined mechanisms of earthquake-induced liquefaction of sands containing fines and mixtures of silt and clay, both plastic and nonplastic. Additional references will be discussed with regard to influence of particle gradation and consistency in later sections.

2.3 Surface Manifestations of Liquefaction

Excess pore water pressures generated by earthquake shaking in a soil deposit usually dissipate upward, toward the free surface. The upward migration of excess pore water pressure is often sufficient to eject mixtures of soil and water through the ground surface, depositing transported soil around the pressure venting point in "volcanoes" or "boils." The violent ejection of soil and water at the ground surface

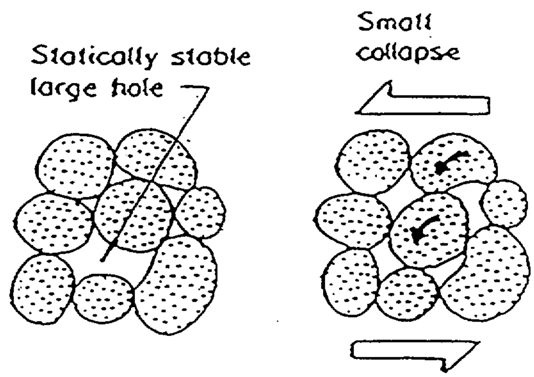

(a) Changes in initial fabric at small strains

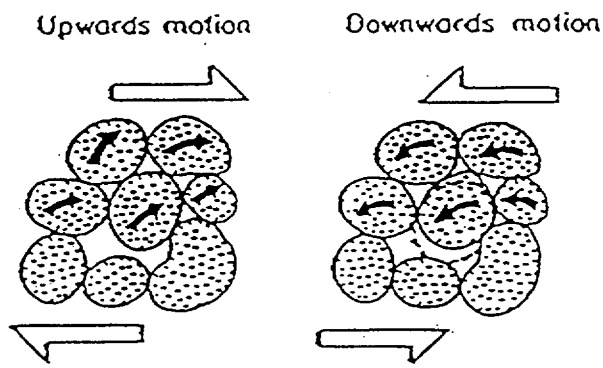

(b) Changes in fabric due to dilatancy at large strains

Figure 1. Changes in soil fabric during cyclic loading (Walker and Stewart, 1989, after Youd, 1977)

occurs only if the overburden soils are less pervious than the soils in which high pore pressures develop. The materials ejected and deposited around boils have been used to classify liquefied soils, but fine layering and in situ gradations that may have somehow impeded subsurface drainage and contributed to pore pressure buildup are lost on disturbance. Excess pore pressures sufficient to cause liquefaction may develop at depth, without provoking surface evidence; liquefaction may thus have occurred, but with no surface manifestations.

Ground fissures, lateral spreading, and sand boils are the most common level-ground manifestations of subsurface liquefaction. Sand boils and their infilled craters may be the only tangible evidence of historical liquefaction. Recent remote sensing and trench studies of remnant liquefaction sand deposits in southeastern Missouri and northeastern Arkansas have helped engineers to define the extent and delineation of the New Madrid fault system (Wesnousky, Schweig, and Pezzopane, 1989). Liquefaction features in the north central United States have provided evidence of strong historical earthquake shaking (Obermeier et al., 1991). Liquefaction has also accompanied earthquakes in the northeastern part of this country (e.g., Tuttle and Seeber, 1989), and in the southeastern region affected by strong shaking from the 1886 Charleston, South Carolina earthquake (e.g., Obermeier et al., 1985, and Obermeier et al., 1989).

Wang (1981) postulated types of locally predominant ground motions by examining the patterns formed by surface expressions of liquefaction associated with the 1976 Tangshan earthquake. He also proposed that the likelihood of liquefaction recurrence may be determined from geologic evidence. Test pits disclosed vertical sand pipes through less permeable overburden soils that apparently formed preferential drainage paths for earthquake-induced excess pore water pressures resulting from successive earthquakes. Sand boils at several sites have reactivated during subsequent moderate earthquakes.

Liquefaction-induced ground failure, in the extreme sense of surface manifestation, may take the form of *flow failure*, *lateral spread* as mentioned, and *ground oscillation*. Youd (1993) distinguishes these as follows: *flow failures* are most often associated with steep slopes in contractive soils and are characterized by displacements on the order of tens of feet (several meters) or greater, and involve disruption of the moving mass of soil; *ground oscillation* is, as the name implies, associated with observations of large-amplitude ground waves during shaking of flat ground, resulting in generally small, random, permanent displacements, with visible fissures that may open and close, sometimes ejecting groundwater dramatically; *lateral spreads* are defined between the two. Lateral spread deformation estimation will be discussed in a later section in more detail.

2.4 Factors Influencing Liquefaction Potential

Seed and Idriss (1982) provide a comprehensive list of the factors commonly considered as most influential on liquefaction resistance of soils, divided into three categories: *soil properties*, including dynamic shear modulus and damping characteristics, density, gradation characteristics, relative density (in the case of granular, cohesionless soils), and soil structure (fabric); *environmental factors*, such as mode of soil deposition, seismic history (prior shear straining), geologic history (aging), coefficient of lateral earth pressure at rest, K_o, overconsolidation ratio, depth to water table, and effective confining pressure; and *earthquake characteristics*, specifically ground shaking intensity and duration. A few of these factors are singled out in following paragraphs due to their relative importance to analysis procedures.

Density. Liquefaction susceptibility is strongly a function of density (typically relative density of cohesionless soils). The capacity for volume reduction in a soil is the basic cause for cyclic pore pressure development and consequent liquefaction. The dependence of cyclic strength (defined here as the cyclic shear stress ratio required to cause residual excess pore pressures to attain equivalence with total confining stress) on relative density was demonstrated in Monterey No. 0 sand by DeAlba, Seed and Chan (1976) from the results of large-scale laboratory cyclic simple shear tests. Cyclic shear strengths were shown to vary in direct proportion with relative density below relative densities of about 80 percent; cyclic strengths increased at a faster rate than relative densities above this level. Cyclic strengths were defined for 30 loading cycles to develop the relationships shown in Figure 2. This number of loading cycles corresponds, roughly, to the level of shaking associated with a Richter Magnitude 8.0 earthquake, according to a well-known study by Seed et al. (1975).

The DeAlba, Seed and Chan (1976) study also described relationships between relative densities higher than 45 percent (up to 100 percent) and limiting shear strains (i.e., beyond which shear stresses in excess of the cyclic shear stresses would be required to produce additional shear strains). Sands having relative densities lower than 50 percent should be judged unsatisfactory as regards seismic stability on the basis of their very large strain potential. Sands at relative densities higher than about 85 percent possess limited strain potential. The level of strain development must be evaluated for acceptability at intermediate relative densities. A later section on evaluation procedures discusses the most recent findings concerning adjustment factors on liquefaction resistance for various earthquake magnitudes.

Gradation characteristics. The grain size distribution of a soil deposit somewhat dictates its capacity to densify on cyclic loading. Membrane penetration compliance effects on undrained laboratory test results are also tied to gradation. Finn (1981) noted that the influence of grain size as observed by Lee and Fitton (1969) (specifically that increased mean grain size was associated with increased liquefaction resistance) may in fact be a result of membrane compliance. Mean grain size may, in view of this contention, be an unconservative delimiter of liquefaction susceptibility. Tokimatsu and Yoshimi (1983) found that soils containing up to 60 percent by weight silt-size particles and 12 percent clay-size particles (that is, particles smaller than 0.005 millimeters), if sufficiently loose, exhibited moderate-to-extensive liquefaction (in terms of affected land area) during historical Japanese earthquakes.

Age of deposit. Liquefaction resistance, as observed from both laboratory and field performance data, is increased by sustained load, i.e., aging. Finn (1981) reported the common result of a number of studies that liquefaction resistance may be increased by as much as 75 percent due to geological aging. Microscopic evidence suggests that finer particles tend to occupy intergranular voids and even separate larger sand grains in hydraulic fills and other, naturally young deposits, creating a relatively compressible soil structure; more grain-to-grain contacts in older deposits contributed to increased frictional resistance and less potential for densification on shearing (Tohno, 1975). Liquefaction most commonly occurs in Holocene deposits, far less often in Pleistocene soils, and very rarely in pre-Pleistocene deposits (Youd and Hoose, 1977). Aging may result in cementation of the grain-to-grain contacts. Cementation processes were evaluated by Mitchell and Solymar (1984). Troncoso, Ishihara, and Verdugo (1988) examined the effects of aging in tailings deposits.

Initial state of stress. Overconsolidation (generally designated by the overconsolidation ratio, OCR) and associated lateral earth pressure (generally, the higher the OCR, the greater is the coefficient of lateral earth pressure at rest, K_o, the latter defined as the ratio of horizontal to vertical effective stress) increase liquefaction resistance. Cyclic triaxial strengths of undisturbed specimens of sandy silts and silty clays were found by Campanella and Lim (1981) to be 75 percent greater when the specimens were isotropically consolidated to have an OCR of 2, and 150 percent greater when they were consolidated to have an OCR of 4.

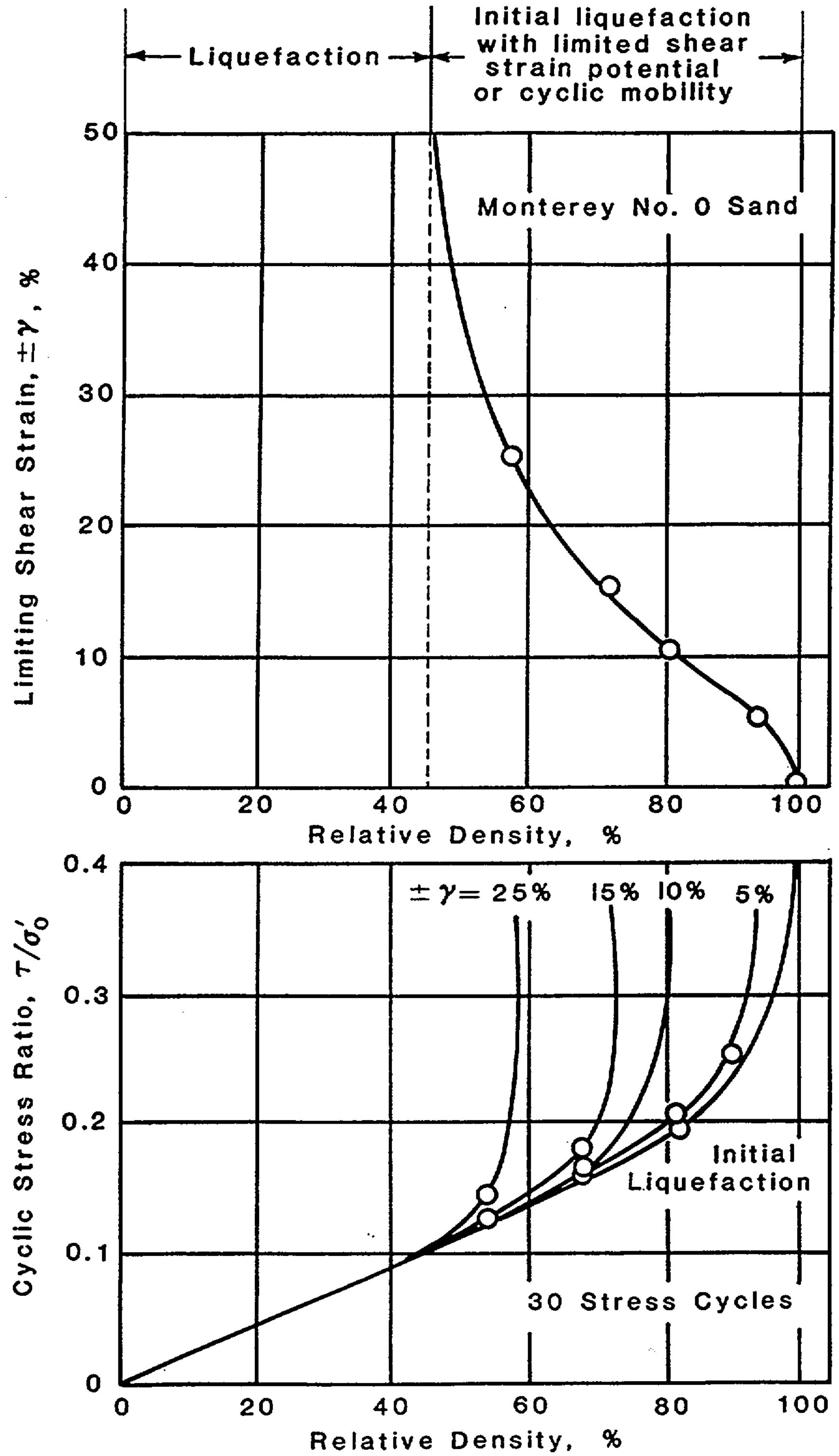

Figure 2. Limiting shear strains in Monterey No. 0 sand as a function of relative density (after DeAlba, Seed and Chan, 1976, reprinted with permission from ASCE)

2. Liquefaction of Soil Deposits

Figure 3 (Walker and Stewart, 1989, after Seed, 1979a) illustrates the effects of OCR and K_c (the latter is analogous in the laboratory to K_o, i.e., $K_c = \bar{\sigma}_{1c}/\bar{\sigma}_{3c}$, where $\bar{\sigma}_{1c}$ and $\bar{\sigma}_{3c}$ are major and minor effective principal stresses after consolidation in laboratory specimens) on liquefaction resistance of clean sands. The same trend is also shown in Figure 4 (adapted from Ishihara and Takatsu, 1979) as observed from cyclic torsional shear tests on Fuji River sand.

Higher effective confining pressure increases undrained cyclic strength as evidenced by either development of 100 percent residual excess pore pressure response or an unacceptable level of cyclic strain. The rate of this increase with confining stress is less than linear, however, and the cyclic stress ratio required to cause liquefaction (generally expressed as the ratio of cyclic applied shear stress to the effective consolidation stress) decreases with increasing effective confining pressure. An adjustment factor, K_σ (liquefaction resistance ratio at a given effective confining stress divided by liquefaction resistance ratio at 1 tsf effective confining stress) can be developed from laboratory tests on replicate specimens to relate cyclic stress ratios required for liquefaction in a given number of cycles to effective confining stress, to allow estimation of liquefaction resistance at other effective confining stresses without specific testing. Figure 5 is a collection of laboratory-determined relationships and shows the variation of K_σ with effective confining stress for several soil types. Recent recommendations for K_σ adjustments arising from the 1996 NCEER workshop will be discussed in a later section on procedures for liquefaction potential evaluation.

Field occurrence data suggest that liquefaction generally occurs within relatively shallow soil deposits (less than about 10 m), corresponding to effective overburden pressures of less than 1.5 tsf (e.g., Seed, Idriss, and Arango, 1983). A few occurrences have, however, been documented in soils as deep as 100 m (Youd and Hoose, 1977).

Initial, static shear stress (on potential failure planes in laboratory cyclic test specimens) increases liquefaction resistance in all but very loose granular soils. Figure 6 (Rollins, 1987, after the data of Szerdy, 1985; Vaid and Chern,1983; Vaid and Finn, 1979; Seed et al., 1973; Lee and Seed, 1967; Castro et al., 1982; Yoshimi and Tokimatsu, 1978; and Yoshimi and Oh-Oka, 1975), gives relationships between the factor, K_α, applied to adjust liquefaction resistance for the effects of initial static shear stress as a function of α for sands of various relative densities. Current recommendations for adjustments to liquefaction resistance for initial static shear stress arising from the 1996 NCEER workshop (NCEER, 1997) will be discussed in a later section on procedures for liquefaction potential evaluation.

Earthquake characteristics. The particular features of earthquake ground motion to which a soil deposit is subjected, particularly severity and duration of shaking, dictate whether a potentially liquefiable soil will experience significant strain or develop sufficiently high excess pore pressures to lose substantial stiffness and/or strength under ambient driving loads. Ground motion characteristics at a site are ultimately functions of three factors: (1) the source mechanism and magnitude of the earthquake; (2) wave propagation and attenuation behavior between the source and the site; and (3) wave propagation characteristics of the site itself. Figure 7 (adapted from Carter and Seed, 1988, after the data of Kuribayashi and Tatsuoka, 1975; Smart and Von Thun, 1983; and Fairless, 1984) correlates liquefaction occurrence to epicentral distance and magnitude; this compilation indicates no liquefaction occurrence for earthquake magnitudes less than about 5.2, or for distances from the zone of faulting greater than about 500 km.

Larger settlements (which, in saturated soils, are a consequence of pore water pressure buildup) have been shown to occur in soils subjected to horizontally polarized shaking than in soils shaken vertically (Puri, 1984, and Prakash and Gupta, 1967). The effects of inherently multidirectional earthquake

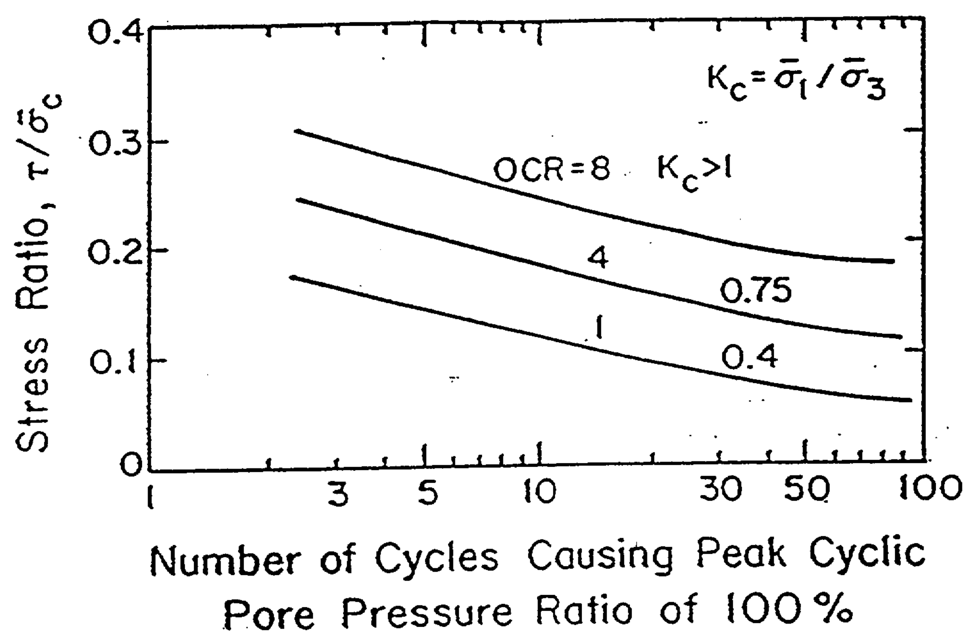

Figure 3. Influence of initial principal stress ratio on liquefaction resistance of clean sands in simple shear tests (Walker and Stewart, 1989, after Seed, 1979, reprinted with permission from ASCE)

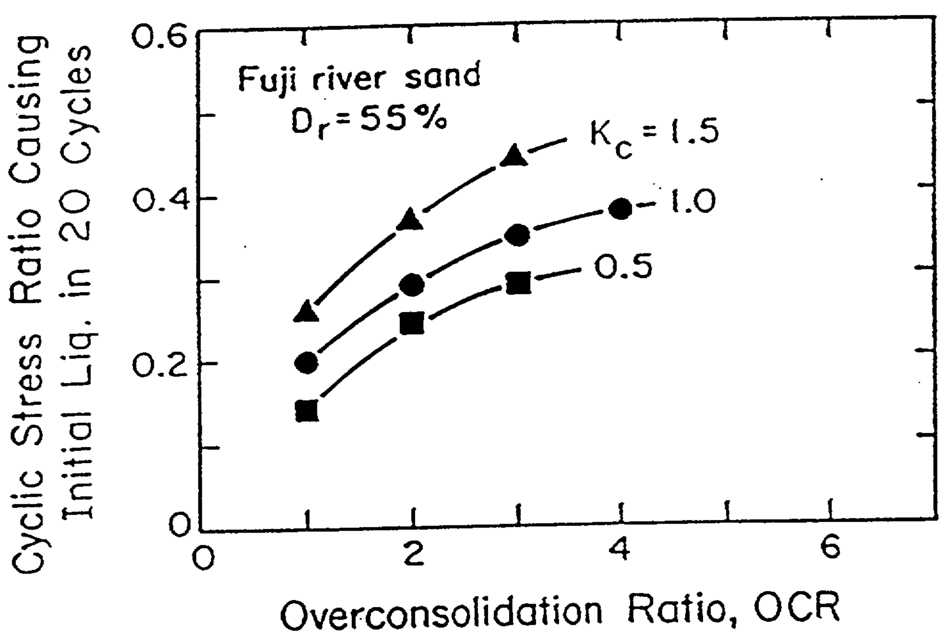

Figure 4. Relationship between cyclic strength and OCR (Walker and Stewart, 1989, after Ishihara and Takatsu, 1979)

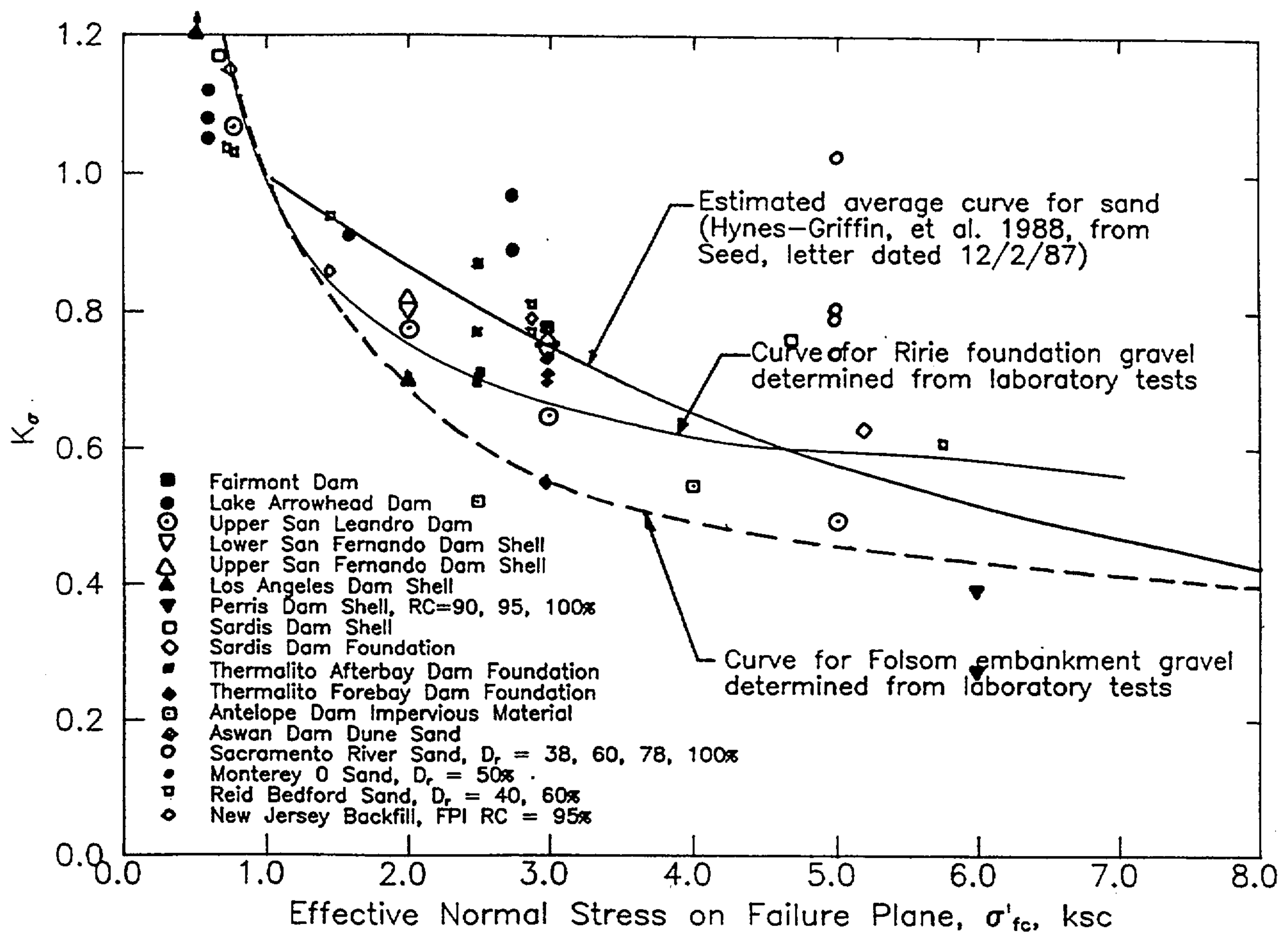

Figure 5. Comparison of overburden pressure correction factor for liquefaction resistance, K_σ, for various soils (after Hynes, 1988) (Note: 1 ksc = 14.2 psi)

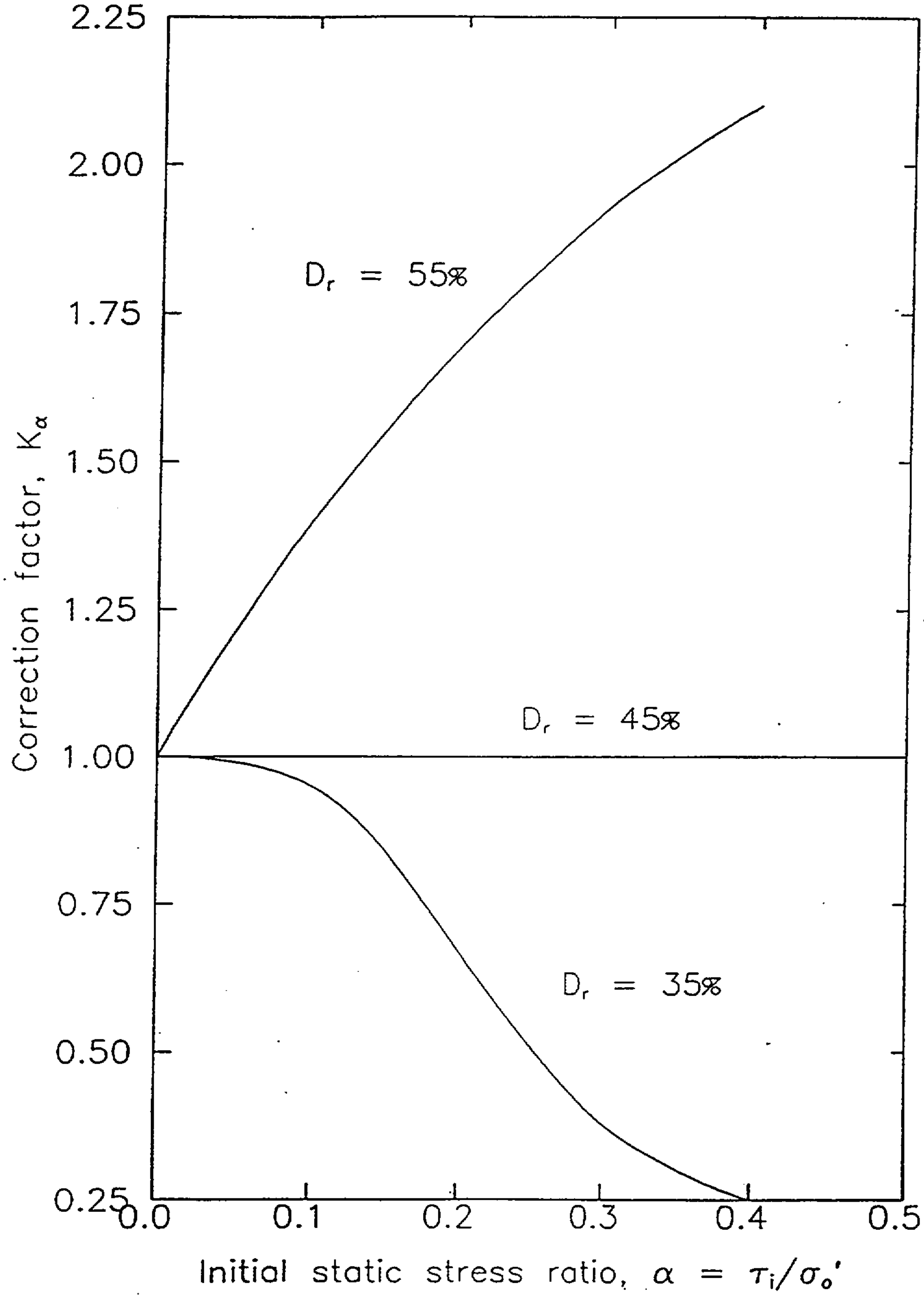

Figure 6. Initial static shear stress liquefaction resistance correction factor, K_α as a function of initial static shear stress ratio, α (Rollins, 1987)

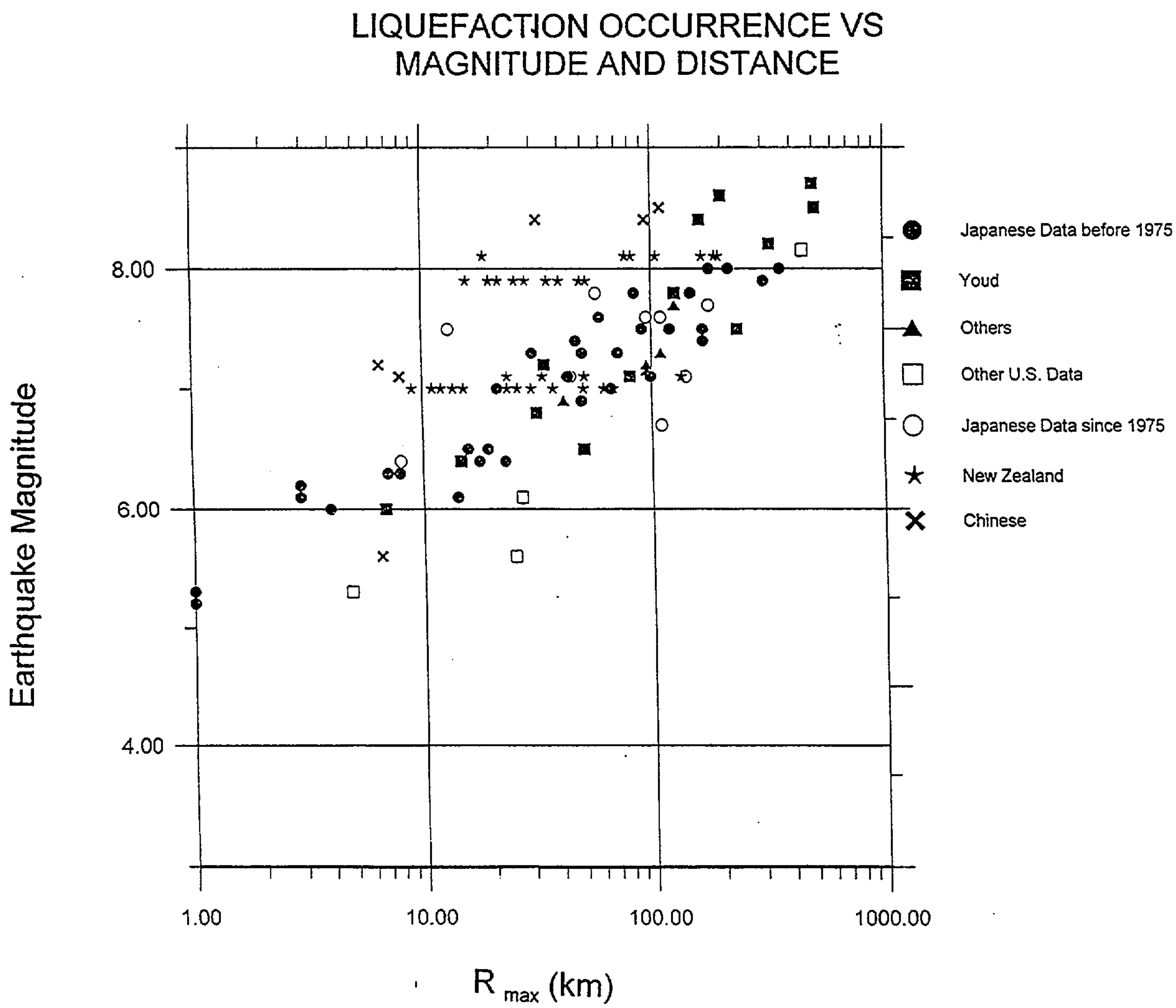

Figure 7. Liquefaction occurrence as a function of magnitude and distance, R_{MAX}, from the zone of faulting (adapted from Carter and Seed, 1988)

shaking on liquefaction resistance have been estimated by Pyke, Chan, and Seed (1974), and irregular and multi-directional loading effects have been studied in laboratory programmed tests by Ishihara and Nagase (1985). Special studies to assess particular ground motion characteristics for site specific conditions are beyond the scope of this report. Later sections will discuss approaches to evaluating liquefaction potential that are based on the relationship between shear strain development and excess pore pressure development.

2.5 Characteristics of Liquefiable Soils

Earthquake-induced liquefaction is most commonly observed in (but not restricted to) the following types of soils: (1) fluvial-alluvial deposits; (2) eolian sands and silts; (3) beach sands; (4) reclaimed land; and (5) uncompacted hydraulic fills. Environmental, geological, and depositional characteristics associated with some documented liquefaction occurrences are reported by Youd and Hoose (1977); Kuribayashi and Tatsuoka (1975); and Seed and Idriss (1971). Table 1 presents an example of geologic (and topographic) bases for preliminary estimation of liquefaction susceptibility, as summarized by Youd (1998, after Youd and Perkins, 1978).

Koester and Franklin (1985) list the following observations that may be made during preliminary site investigations at critical sites (defined according to the consequences of failure as involving loss of life or substantial property damage or both) that would indicate potential for liquefaction: (1) low penetration resistance, as measured by standard penetration tests (SPT's) or cone penetration tests (CPT's) in sands and finer grained soils, or Becker hammer penetration tests (BPT'S) in gravels; (2) artesian head conditions (it should be noted, however, that artesian head conditions have not been commonly found at historical liquefaction sites, and are therefore not currently considered as a useful screening tool); (3) persistent inability to retain soil samples in conventional sampling devices; (4) saturated zones of granular soil with impeded drainage; and (5) the presence of any clean, fine sand below the ground water table. It should be emphasized that the above are not necessarily indicative of imminent liquefaction, however, any of these occurrences should be noted on boring logs and followed up with further investigation to define their threat to the project.

2.6 Residual Strength of Liquefied Soils

As early as 1936, Casagrande postulated that soils sheared under undrained conditions would achieve a residual condition at which further shearing would cause no additional change in strength or volume or pore pressure (Casagrande, 1936). This principle is the underlying basis of "critical state" soil mechanics (Schofield and Wroth, 1968) as well as more recently proposed "steady state" analysis techniques for evaluation of post-triggering stability of liquefiable soils. There are two techniques for evaluation of undrained residual strength (S_r, S_{ur}, or S_{us}) of soils: (a) performance-based correlation with in situ tests, and (b) laboratory test methods based mainly on the relationship between void ratio and S_{us}.

2.6.1 Use of In Situ Testing Procedures

Seed (1987) recommended a technique for evaluation of in situ undrained residual strength (S_r) based on penetration test results. This procedure, which is based on the use of in situ testing (now SPT and/or CPT), is widely applied for simplified evaluation of the in situ undrained residual strengths of silty and sandy soils. Seed (1987) presented the results of back-analyses of a number of liquefaction-related slope failures from which values of the undrained residual strength could be calculated for soil zones in which

Table 1 Estimated Susceptibility of Sedimentary Deposits to Liquefaction During Strong Seismic Shaking Based on Geological Age and Depositional Environment (After Youd and Perkins 1978)

Type of Deposit (1)	General Distribution of Cohesionless Sediments in Deposits	Likelihood that Cohesionless Sediments, When Saturated, Would Be Susceptible to Liquefaction (by Age of Deposit)			
		<500 yr (3)	Holocene (4)	Pleistocene (5)	Pre-Pleistocene
(a) Continental Deposits					
River channel	Locally variable	Very high	High	Low	Very low
Flood plain	Locally variable	High	Moderate	Low	Very low
Alluvial fan and plain	Widespread	Moderate	Low	Low	Very low
Marine terraces and plains	Widespread	–	Low	Very low	Very low
Delta and fan-delta	Widespread	High	Moderate	Low	Very low
Lacustrine and playa	Variable	High	Moderate	Low	Very low
Colluvium	Variable	High	Moderate	Low	Very low
Talus	Widespread	Low	Low	Very low	Very low
Dunes	Widespread	High	Moderate	Low	Very low
Loess	Variable	High	High	High	Unknown
Glacial till	Variable	Low	Low	Very low	Very low
Tuff	Rare	Low	Low	Very low	Very low
Tephra	Widespread	High	High	?	?
Residual soils	Rare	Low	Low	Very low	Very low
Sebka	Locally variable	High	Moderate	Low	Very low
(b) Coastal Zone					
Delta	Widespread	Very high	High	Low	Very low
Esturine	Locally variable	High	Moderate	Low	Very low
Beach					
High wave energy	Widespread	Moderate	Low	Very low	Very low
Low wave energy	Widespread	High	Moderate	Low	Very low
Lagoonal	Locally variable	High	Moderate	Low	Very low
Fore shore	Locally variable	High	Moderate	Low	Very low
(c) Artificial					
Uncompacted fill	Variable	Very high	–	–	–
Compacted fill	Variable	Low	–	–	–

SPT data were available, and proposed a correlation between S_r and $(N_1)_{60-cs}$. $(N_1)_{60-cs}$ is the "corrected" penetration resistance with an additional correction for fines content to generate an equivalent "clean sand" blowcount as

$$(N_1)_{60-cs} = (N_1)_{60} + N_{corr} \tag{1}$$

where N_{corr} is a function of percent fines, as shown below.

% Fines	N_{corr} (blows/ft)
10	1
25	2
50	4
75	5

It should be noted that this is not the same "fines" correction as is used in the evaluation of liquefaction resistance, described in a later section.

Figure 8 presents the correlation between S_r and $(N_1)_{60-cs}$, based on values back-calculated from an increased number of case studies (Seed and Harder, 1990), most often used in current practice. Many of the S_r values presented are slightly different from those in earlier correlations (Seed, 1987) due to the following reasons: (a) improved techniques have been used to account for dynamic effects (e.g., momentum) in developing estimates of S_r from the field failures, and (b) additional data have recently become available for several of these case studies. The lower-bound, or near lower-bound relationship between S_r and $(N_1)_{60-cs}$ in Figure 8 is recommended for SPT-based undrained residual strength evaluation at present, due to inherent scatter and uncertainty in case history data. The relationship of Figure 8 should not be extrapolated to values of $(N_1)_{60} > 16$ blows/ft, since no supporting field case history data are available to justify extrapolation.

Finally, it should be noted that it is theoretically possible for soils to mobilize undrained strengths that are considerably higher than their fully-drained strengths (this requires that the soil be "dense" and thus dilative under uni-directional shearing). As the use of undrained residual strengths (S_r) is a relatively recent development, however, it is suggested that residual strengths based on penetration test results and assigned to any soil zone or unit for post-liquefaction stability analyses (and/or seismic deformation analyses) be conservatively taken as the lesser of either: (1) the undrained residual strength, S_r, or (2) the fully-drained shear strength (as controlled by soil friction and initial in situ effective stresses). If analyses using the lower bound residual strength values indicate the structure in question to be stable and the seismic deformations (estimated as described in a subsequent section) to be tolerable, no further action is needed. If, however, the lower bound residual strength values are associated with potential instability or excessive deformations, site-specific determinations of undrained residual strength should be made following steady state strength method such as described below or an equivalent rationale.

2.6.2 Laboratory Based Method

The penetration test - based method for residual strength estimation is not without its limitations and uncertainties, which should be duly noted in a comprehensive technical bases report for critical facilities. The determination of geotechnical parameters for analysis is always subject to uncertainties, and blind adherence to any single method without recognition of these uncertainties and limitations may be dangerous. It is traditional and prudent in geotechnical engineering that more than one method is used to

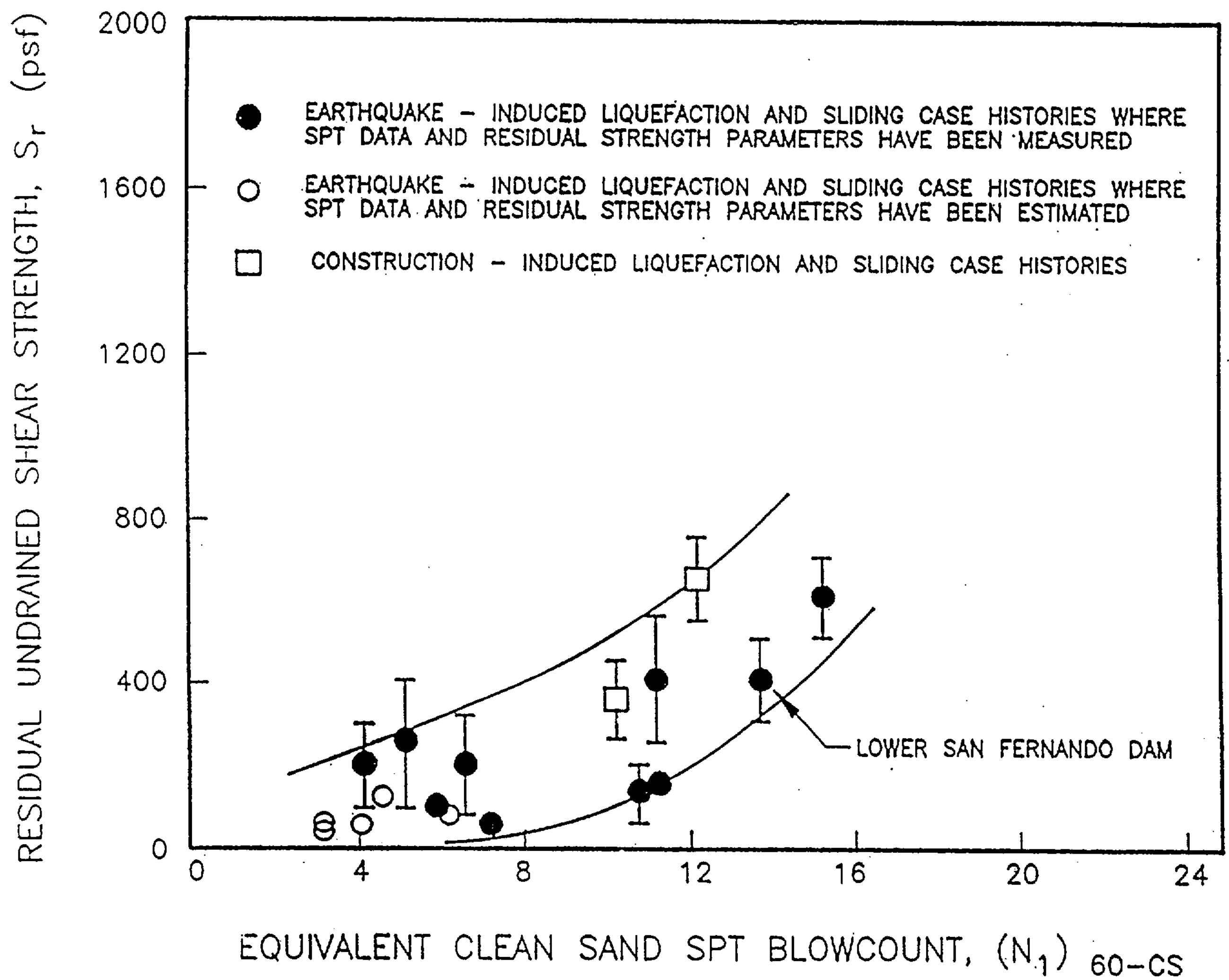

Figure 8. Relationship between equivalent clean sand SPT blowcount $(N_1)_{60}$ and undrained residual shear strength (Seed and Harder, 1990, reprinted with permission from BiTech Publishers, Ltd.)

determine vital parameters whenever more than one method is available, and the consequences of an erroneous assessment of the parameters are serious in terms of safety or of incurring large construction expenses. Determination of SPT blowcounts, for example, is affected by various factors of the performance of the penetration test and the equipment employed, as will be discussed in some detail in subsequent sections. The SPT may not properly interpret penetration resistance in potentially liquefiable layers thinner than about 3 ft (1 m); specific sampling and testing of suspect soils is a justifiable adjunct to large projects.

Poulos, Castro, and France (1985) proposed a methodology for evaluation of in situ undrained residual "steady state" strengths (S_{us}), based on obtaining high-quality soil samples with minimal disturbance, testing these in the laboratory, and then using specially developed techniques to correct the resulting laboratory S_{us} values for the effects of void ratio changes due to sampling, handling, and test set-up in order to develop estimates of the field (in situ) S_{us}. This represents a major contribution to geotechnical practice, as it has spurred considerable interest and research into the use of undrained residual strengths for post-liquefaction stability assessment. Castro, et al. (1989) report a case history application of the steady state strength approach to evaluate the damage caused to the Lower San Fernando Dam during a 1971 earthquake. In that study, the steady state approach successfully represented the behavior of both the upstream, failed slope and the minor, non-flow failure deformations observed in the downstream slope of the dam.

The steady-state strength is the shear strength at the steady state of deformation defined by Poulos (1981) as "the state in which the mass is continuously deforming at constant volume, constant normal effective stress, constant shear stress, and constant velocity. The steady state of deformation is achieved only after all particle orientation has reached a statistically steady-state condition, after all particle breakage, if any, is complete, so that the shear stress needed to continue deformation and the velocity of deformation remains constant." At steady state there is a strong correlation between void ratio and normal effective stress or shear strength (Castro, 1969). Thus, in the case of undrained behavior of a given saturated sand, the deformations that lead to steady state occur at constant void ratio, and thus the steady-state value of normal effective stress and shear strength are strongly dependent on the void ratio and appear to be independent of stress path and initial structure. The application of this laboratory test-based method is fully explained in the Appendix to this report.

Liquefaction response may be indicated by monotonic, undrained triaxial compression test results. Figure 9 illustrates typical stress-strain and pore pressure responses such as might result from isotropically consolidated, monotonic triaxial compression tests on sand specimens prepared to void ratios either side of and very close to the critical void ratio, that is, that void ratio at which a soil can deform continuously at constant shearing stress (Casagrande, 1936). A steady state of deformation developed in Test A. Tests B and C did not reach steady state within the strain and load limitations of the test equipment.

A workshop was convened at the University of Illinois, Champaign-Urbana (UIUC) in April 1997 to examine the issue of residual strength of liquefied soils. About 30 geotechnical engineering researchers and practitioners from industry, government, and the private sector met to discuss theoretical and conceptual issues, back-calculation of residual strength from field case histories, and to compare and contrast procedures and results from laboratory and in situ tests to measure residual strength. The proceedings from that workshop are synopsized by Stark, et al. (1998); a complete set of proceedings is available from the National Science Foundation, referenced to Grant Number CMS-95-31678. Significant outcome items follow:

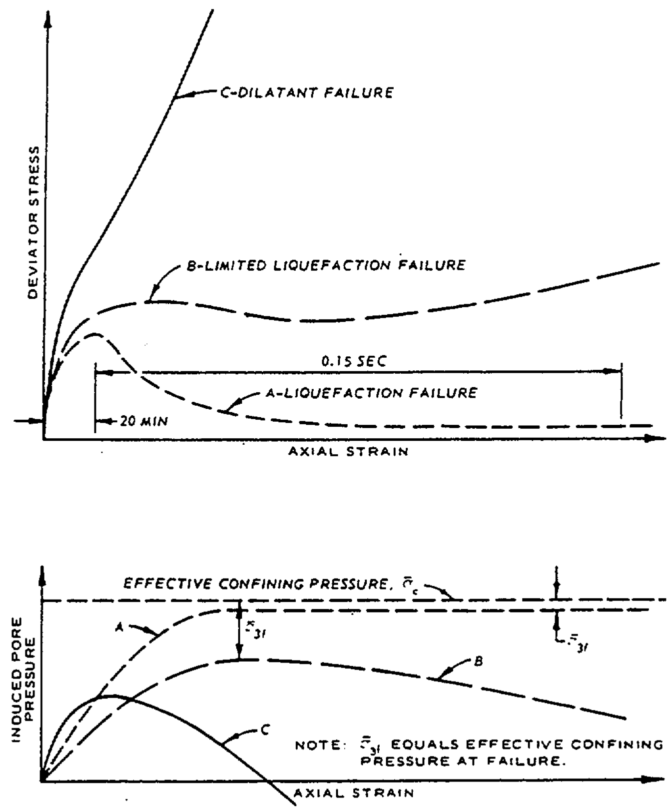

Figure 9. Typical stress-strain and pore pressure response in monotonic triaxial tests on sands (Department of the Army, 1970)

2. Liquefaction of Soil Deposits

- Terminology: the use of two terms was proposed, one to describe back-calculated values (apparent residual strength) and one for laboratory generated values (quasi-steady state). The use of two terms will hopefully allow practitioners to immediately determine the origin and applicability of the data.

- Normalization: A consensus was formed at the workshop that normalization (to effective confining stress) is appropriate, however, the range of soils that it is applicable to is a subject for additional study. For example, there is some uncertainty about normalization in clean sands but it is clearly applicable to silty or clayey sands. Dependence of residual strength on confining stress was investigated by Baziar and Dobry (1995); their data from field occurrences of embankment failures and lateral spreads is included in Figure 10 (note the caution on using lateral spread data for residual strength back-calculation, below). The relationships given in this figure are widely recognized as appropriate boundaries on available data.

- Soil Mixing: Mixing of soil types once very large deformations develop appears to play a major role in post-earthquake shear strength and behavior. This complicates determination of appropriate properties in field case studies.

- Field Case Histories: Back-calculation of shear strengths from field case histories are most applicable to silty sands. This suggests that considerable research should be conducted on the post-earthquake behavior of clean sands.

- Lateral Spreads: The mechanism(s) of lateral spreading is very different from that of flow failure. Residual shear strengths back-calculated from lateral spreads should not be included in empirical charts for residual strengths from flow slides, nor should these residual strengths be used in evaluation of flow slide potential. Conversely, residual strengths back-calculated from flow slides should not be used in analyses of lateral spread displacement.

- In Situ Tests: In situ tests appear to provide a more cost effective technique for estimating the post-earthquake shear strength than do programs of laboratory residual strength testing. However, the influence of grain characteristics and thin layers on the in situ test results needs to be understood. Lack of experience with sampling to obtain undisturbed sampling of sands makes in situ tests more desirable.

- A re-evaluation of existing case histories was strongly recommended given the uncertainties present in the currently published cases.

Sands without fines that have been liquefied typically dilate with undrained shear loading beyond some minimum value, thus gaining strength and potentially restricting deformations unless further loaded. Soils containing fines, however, may not dilate and gain undrained shear strength, depending on such factors as fines content, cohesion, and void ratio (Koester, 1992).

Residual strength of cohesive soils, included here for completeness with regard to post-earthquake deformation evaluation discussions to appear later in the document (not as a facet of liquefaction hazard analyses, per se), should be evaluated using a test device capable of imparting large deformations along a consistent surface within a soil specimen without changing its geometry and maintaining appropriate volume change characteristics. Standard laboratory triaxial or direct shear devices do not accommodate very large strain behavior. In recognition of these constraints, Stark and Contreras (1996) describe a constant volume ring shear device, based on the Bromhead (1979) ring shear apparatus to measure both peak and residual undrained strength of clays. Their device maintains specimen cross sectional area

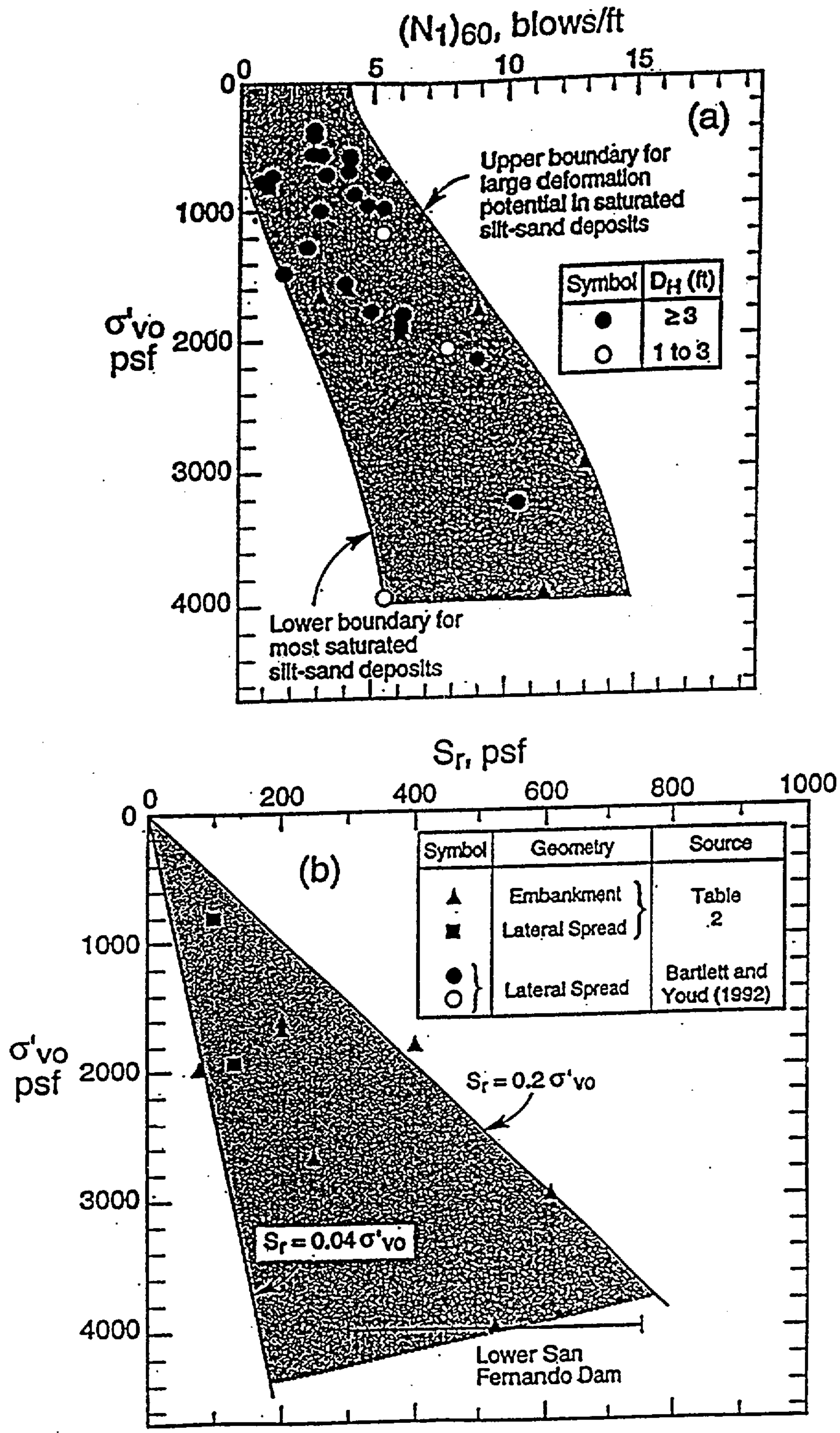

Figure 10. Charts relating normalized SPT resistance $(N_1)_{60}$ and residual shear strength (S_r) to vertical overburden pressure (σ'_{vo}) for saturated nongravelly silt-sand deposits that have experienced large deformation (Baziar and Dobry, 1995, reprinted with permission from ASCE)

during shear and accommodates trimming of the specimen directly into the holding container. Constant volume conditions are maintained in the Stark and Contreras apparatus by decreasing the normal stress applied to the specimen during shear. The authors demonstrated agreement between peak undrained shear strength values obtained in clays from direct simple shear tests and by using the constant volume ring shear device. This is included as an example, and should not be construed as an endorsement of the procedure for all cases.

3 LIQUEFACTION POTENTIAL EVALUATION PROCEDURES

3.1 Liquefaction Potential Assessment - Overview

3.1.1 Site Characterization - General

Preliminary assessments may often be made to determine whether a given site is clearly likely or not likely to liquefy in response to earthquake shaking. Previous occurrence of liquefaction in site soils, knowledge of embankment placement techniques that have historically performed well or poorly when shaken, the seismicity of the site, and degree of saturation are some of the factors that may indicate the potential for future liquefaction.

The importance of adequate site characterization to seismic stability analysis cannot be overstated. Much can and should be accomplished by acquiring and examining existing site data from the geological literature, historical records, earlier field investigations and even remote sensing imagery before additional subsurface investigation is planned or undertaken. The following information is essential to initial assessment of the potential for earthquake-induced ground failure:

(a) Site topography.

(b) At any site, minimally, a detailed soil profile, including classification of soil properties and the origin of soils at the site in question. For major projects such as involving foundations of nuclear facilities, this takes on much more significance and requires development of three-dimensional soil stratigraphy to support a site conceptual model. Torres, et al. (1998) presents technical bases for field investigations for foundations of nuclear facilities and describes conceptual site modeling procedures.

(c) Water level records, representative of both current and historical fluctuations.

(d) Evidence from project records, aerial photographs, or previous investigations of past ground failure at the site or at similar (geologically and seismologically) nearby areas (including historical records of liquefaction, topographical evidence of landslides, sand boils, effects of ground movement on trees and other vegetation, subsidence, and sand intrusions in the subsurface).

(e) Seismic history of the site.

(f) Geologic history of the site, including age and mode of deposition of site soils, glacial preconsolidation or preconsolidation by now-eroded overburden, and lateral extent and continuity of soil deposits.

Subsurface investigation should be performed in two phases, distinguished by coverage and purpose. The first of these should include cone penetration test (CPT) soundings and standard penetration tests (SPT's) for measuring penetration resistance; the latter for obtaining disturbed split-spoon samples for classification and water content determination. The author attended a workshop on new approaches for liquefaction potential evaluation, held in conjunction with the 1999 Annual Meeting of the Transportation Research Board (TRB) in Washington, DC, 9-15 January. It was the majority opinion of the group of technical specialists assembled for this workshop from academia, government, and geotechnical engineering consulting practice, that the CPT is the tool of choice for ***initial*** site characterization studies in support of liquefaction potential assessment. Final proceedings of the TRB workshop will be available in the TRB Record publication series, accessible through the World Wide Web at ***http://www.nas.edu/trb/meeting***. The CPT is considered by the profession at large to provide superior stratigraphic detail for penetration resistance and soil characteristics than does the SPT, recognizing, of course, the inherent drawback that the CPT does not provide a physical sample. The CPT results should be used to select localities and depths for subsequent SPT borings and other sampling efforts. Coverage of the site with CPT soundings and SPT borings should be adequate to (1) establish general soil conditions, distributions of soil types, homogeneity and ground water elevations; (2) identify soils that, if shaking were sufficiently intense, might liquefy; and (3) assist in specifying the locations of additional borings and geophysical surveys aimed at detailed seismic response evaluation. The second phase of subsurface investigation likely includes surveys and undisturbed sampling borings to: (1) refine preliminary interpretation of stratigraphy and the extent of potentially liquefiable soils; (2) measure in situ densities and dynamic properties for input to dynamic response analyses; and (3) recover undisturbed samples for laboratory testing when site soils are not adequately represented in the available data base.

3.1.2 In Situ Testing

3.1.2.1 Standard Penetration Test (SPT). The SPT has the most extensive history of any in situ test employed in this country (Civics, Salomone, and Yokel, 1981) and perhaps worldwide for preliminary subsurface investigation. A large data base of SPT blowcounts, normalized to account for the effects of different overburden pressure and performance conditions, has been correlated to occurrence and non-occurrence of liquefaction in a wide variety of soils (Seed, Idriss and Arango, 1983; Seed et al., 1985; and Farrar, 1988). The SPT was, until recently, the desired tool for preliminary in situ investigation of liquefaction potential as a result of its empirical correlation to field performance. The term "standard" is of dubious relevance, as the standard procedure specified for SPT performance by the American Society for Testing and Materials (1967) is not so rigid as to prevent variations in practice. Other countries have also developed indigenous versions of the test, unconstrained by the U.S. regulation. The finer points of the SPT, its performance, and interpretation of test results have been rigorously studied (e.g., McLean, Franklin, and Dahlstrand, 1975; Federal Highway Administration, 1978; Kovacs, Salomone, and Yokel, 1981; Seed, Idriss, and Arango, 1983; and Seed et al., 1985). Empirical procedures for liquefaction potential evaluation using the SPT will be discussed in more detail in a later section.

3.1.2.2 Cone Penetration Test (CPT)

3.1.2.2.1 Background

Cone penetration test (CPT) measurements (both tip resistance, q_c, and sleeve friction, f_s) are currently considered preferential to SPT N-values for use as a basis for evaluation of in situ liquefaction resistance. Historically, this has been accomplished by converting the CPT measurements into equivalent SPT blowcount values, from which liquefaction resistance (expressed as the cyclic resistance ratio, CRR) was judged using field performance charts described later in this text. The CPT has the advantage of continuous measurement, ease of use, and low cost; however, unlike the SPT, soil samples are not retrieved during CPT soundings. Consequently, for CPT-based evaluations, some effort should be expended toward soil sampling, at least initially using the SPT to obtain disturbed samples, for confirmation of soil type and for soil index testing.

3.1.2.2.2 NCEER (1997) Recommended Procedure for CPT-based Evaluation of CRR

The NCEER (1997) workshop proceedings recommend the procedure described in this section, based on tip bearing resistance measured using the CPT, for relatively clean sand deposits. CPT penetration resistance may be normalized to a dimensionless quantity and corrected for the effects of overburden stress as follows (detailed in the NCEER, 1997 proceedings paper by P. K. Robertson and C. E. Wride):

$$q_{c1N} = \left(\frac{q_c}{P_{a2}}\right) C_Q = \frac{q_{c1}}{P_{a2}} \tag{2}$$

where q_c is the measured cone tip resistance; $C_Q = (P_a/\sigma'_{vo})^n$ is a correction factor for overburden stress; n = exponent, typically equal to 0.5; P_a is a reference pressure in the same units as σ'_{vo} (i.e., P_a = 100 kPa if σ'_{vo} is in kPa); and P_{a2} is a reference pressure in the same units as q_c (i.e., P_{a2} = 0.1 MPA if q_c is in MPA). A maximum value of $C_Q = 2$ is generally applied to CPT tip resistances at shallow depths. The resulting CPT tip resistance, expressed as q_{c1N} is thus maintained as dimensionless. Available correlative field performance data have resulted in the NCEER (1997) recommended clean sand relationship between q_{c1N} and CRR shown in Figure 11.

3.1.2.2.3 CPT Measurements and Relevance to Estimating Liquefaction Potential

The CPT independently measures tip stress (cone resistance) and side friction (sleeve friction resistance). CPT cone resistance is a bearing stress influenced by many factors, of which the drained friction angle is the most dominant. The CPT sleeve friction resistance is an index of remolded strength after disruption of the soil structure and after the soil has undergone large strain. Historically, CPT cone resistance alone has been used to estimate liquefaction potential, but this is a limiting approach. Many factors influence liquefaction resistance such as confining stress, residual strength, density, soil type, fabric, etc. The use of both CPT measurements to estimate liquefaction potential may allow for yet improved accuracy; this is a subject of emergent research, particularly with regard to provisions for soil type and behavior, and several techniques are under evaluation. An approach developed by Olsen (1994, and elsewhere) to take advantage of both CPT measurements is presented in the following three sections.

3.1.2.2.4 Stress Focus Approach to CPT Cone Tip Resistance Normalization

Stress normalization is required for all CPT-based techniques for estimating normalized liquefaction cyclic resistance ratio (CRR_1). Stress normalization is very important for low confining stresses (depths less than 2 meters) and very high confining stresses (depths greater than 25 meters). For vertical effective stresses greater than one atmosphere (atm), an approximating linear stress normalization technique produces resultants which are increasingly overconservative. Recent research on the influence of confining stress on CPT and SPT measurements has resulted in a new theory - the stress focus theory (Olsen, 1994, and Olsen and Mitchell, 1995). The stress focus theory uses a variable stress exponent for stress normalization as shown in Equation 3.

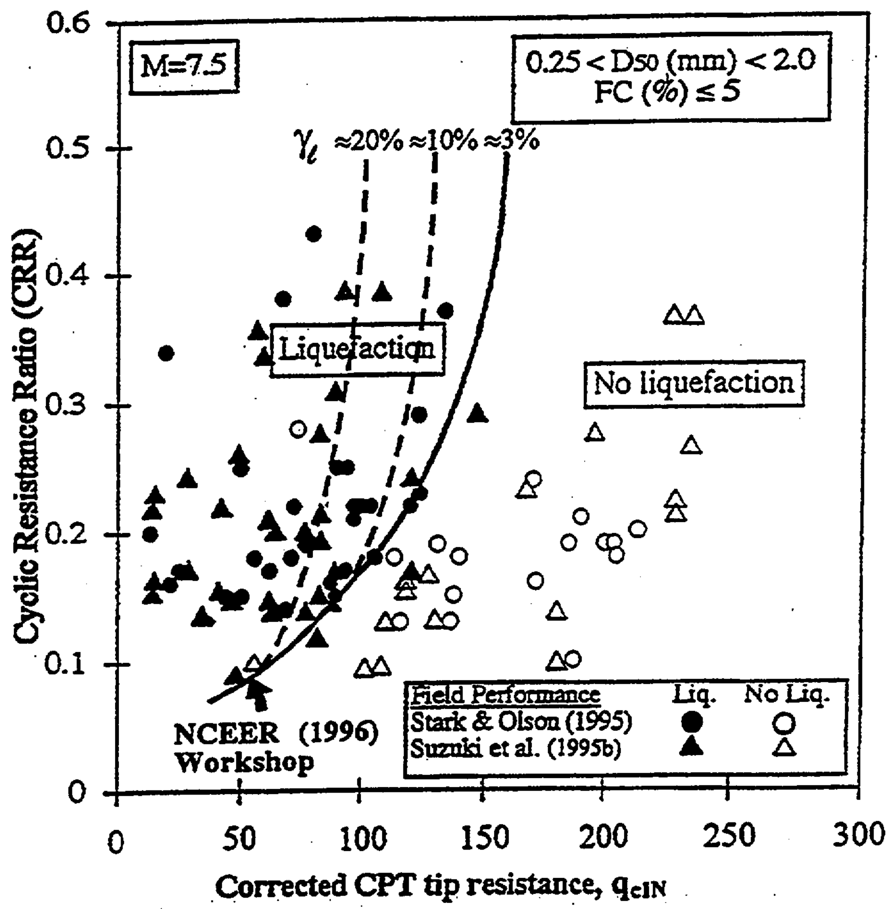

Figure 11. NCEER (1997) recommended cyclic resistance ratio (CRR) for clean sands under level ground conditions based on CPT

$$q_{c1e} = \frac{q_c - \sigma_{total}}{(\sigma_v')^c} \tag{3}$$

where

q_{c1e} = normalized cone resistance (q_{c1}) using a nonlinear variable stress exponent (equivalent value at a vertical effective stress of 1 atm)
σ_{total} = total vertical stress in atm units
c = stress exponent dependent on soil type sand relative strength level (see contours of stress exponent in Figure 12)

The stress exponent, c, shown in Figure 12, is dependent on soil type and relative strength level. For sands, it defines the log-log slope for a constant relative density trend as shown in Figure 13. The cone resistance stress exponent, c, decreases as sand relative density increases and can be approximated (for sand) as shown below using relative density, D_r (Olsen and Mitchell, 1995):

$$c = 1 - (D_r - 10\%)\,0.007 \tag{4}$$

The stress focus theory accounts for the dependence of the stress exponent for sands on initial relative density. For all overburden stress conditions, this "variable stress exponent" is believed by the authors to provide an accurate CPT cone resistance normalization.

3.1.2.2.5 Estimating Liquefaction Resistance for All Soil Types using the CPT Soil Characterization Chart Technique

The CPT soil characterization chart technique for estimating liquefaction resistance is shown in Figure 14 (Olsen and Koester, 1995). The normalized liquefaction cyclic resistance ratio (CRR_1) is determined for any depth and any soil type based on the combination of normalized cone resistance and friction ratio. This technique does not require laboratory measured soil index tests to estimate liquefaction resistance.

The CPT soil characterization chart technique for estimating liquefaction potential originated in the early 1980s (Olsen, 1984) and has been subsequently refined with additional data (Olsen, 1988; Olsen and Farr, 1986; Olsen and Koester, 1995; Olsen, Koester, and Hynes, 1996). This technique indirectly includes the effects of soil type, fines content influence, peak strength, high strain strength, and lateral stress influence. Specifically, it was developed based on: (1) correlations to cyclic laboratory tests; (2) trends of CPT estimated normalized SPT values; (3) trends observed for SPT silt corrections using CPT- estimated silt content; (4) the Seed and De Alba (1986) SPT to CRR_1 correlations; and (5) field performance data (Suzuki et al., 1995, 1995b; and elsewhere).

3.1.2.2.6 Estimating SPT Blow Count using the CPT Soil Characterization Chart Technique

The critical starting point for this chart technique was to using an accurate procedure for CPT-based estimation of SPT blow count. Contours of CPT-estimated SPT-normalized blow counts, N_1, can be established on the CPT soil characterization chart as shown in Figure 15. These SPT contours were developed using both CPT measurements (Olsen, 1984, 1988, 1994), whereas similar contours reported by Robertson, Campanella, and Wightman (1983) and Seed and De Alba (1986) are based on the q_c/N ratio. Seed

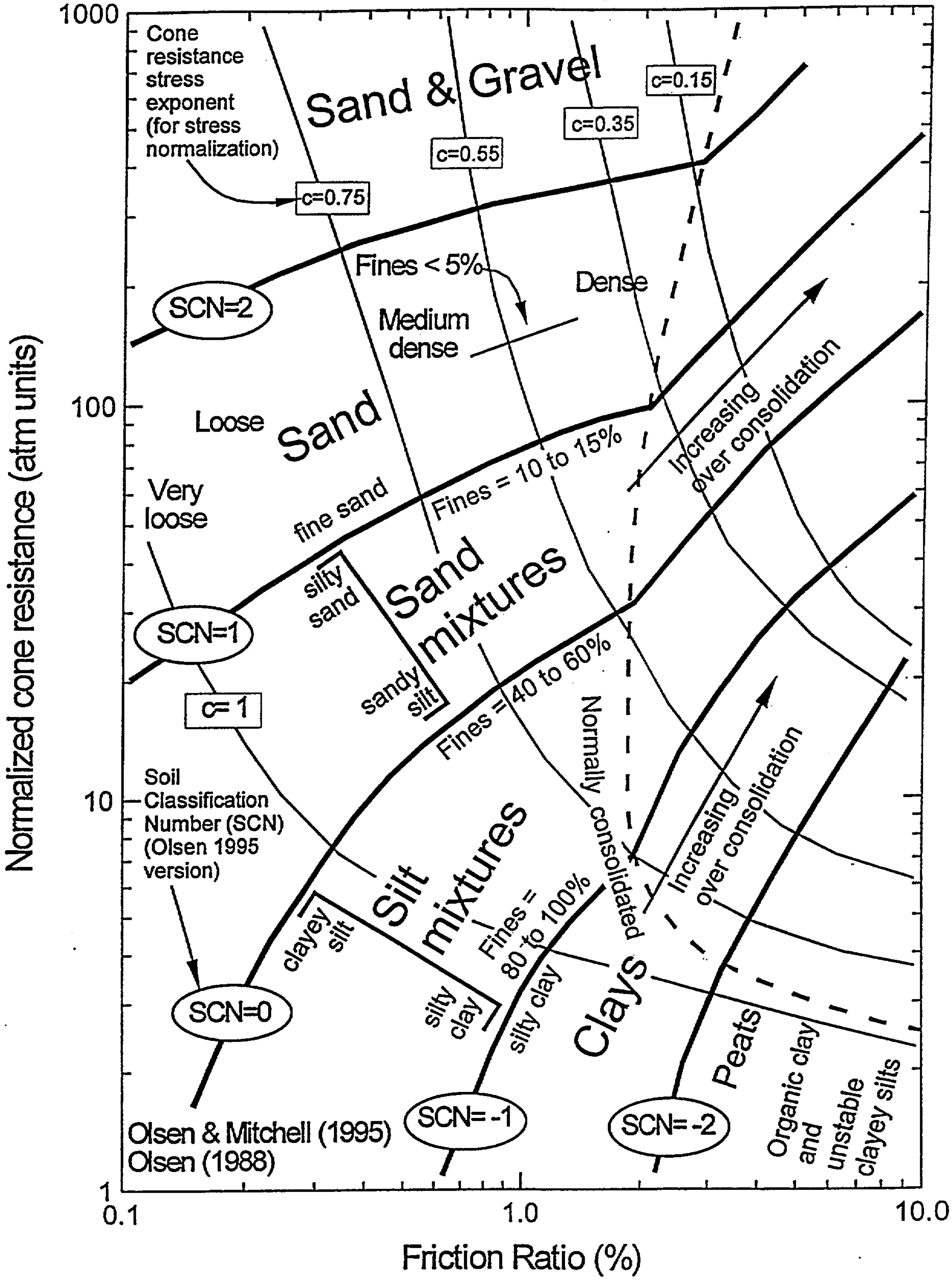

Figure 12. Stress exponents for cone resistance on the CPT soil characterization chart (Olsen and Mitchell, 1995).

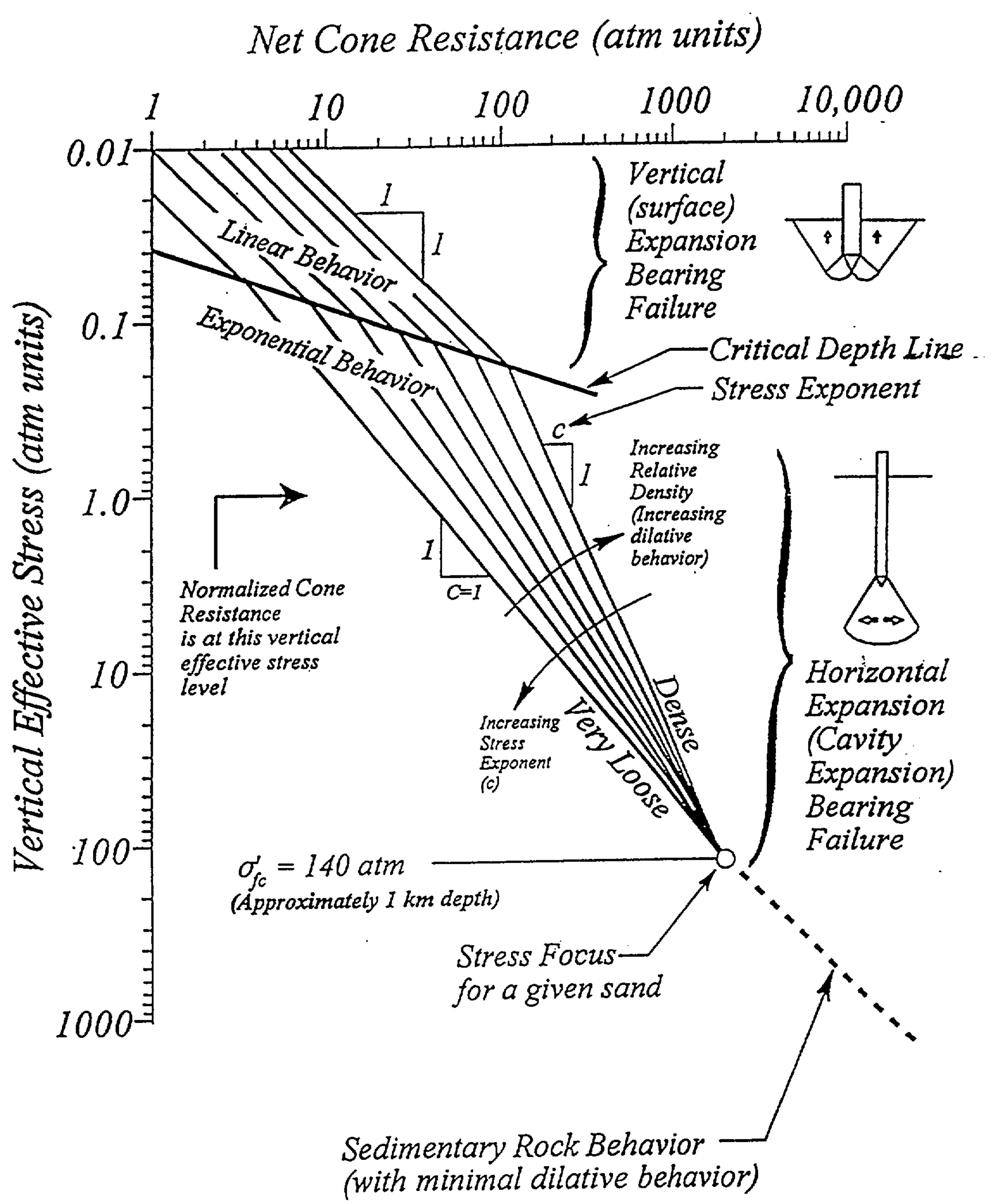

Figure 13. Depiction of cone resistance trends toward the stress focus for any relative density (Olsen, 1994).

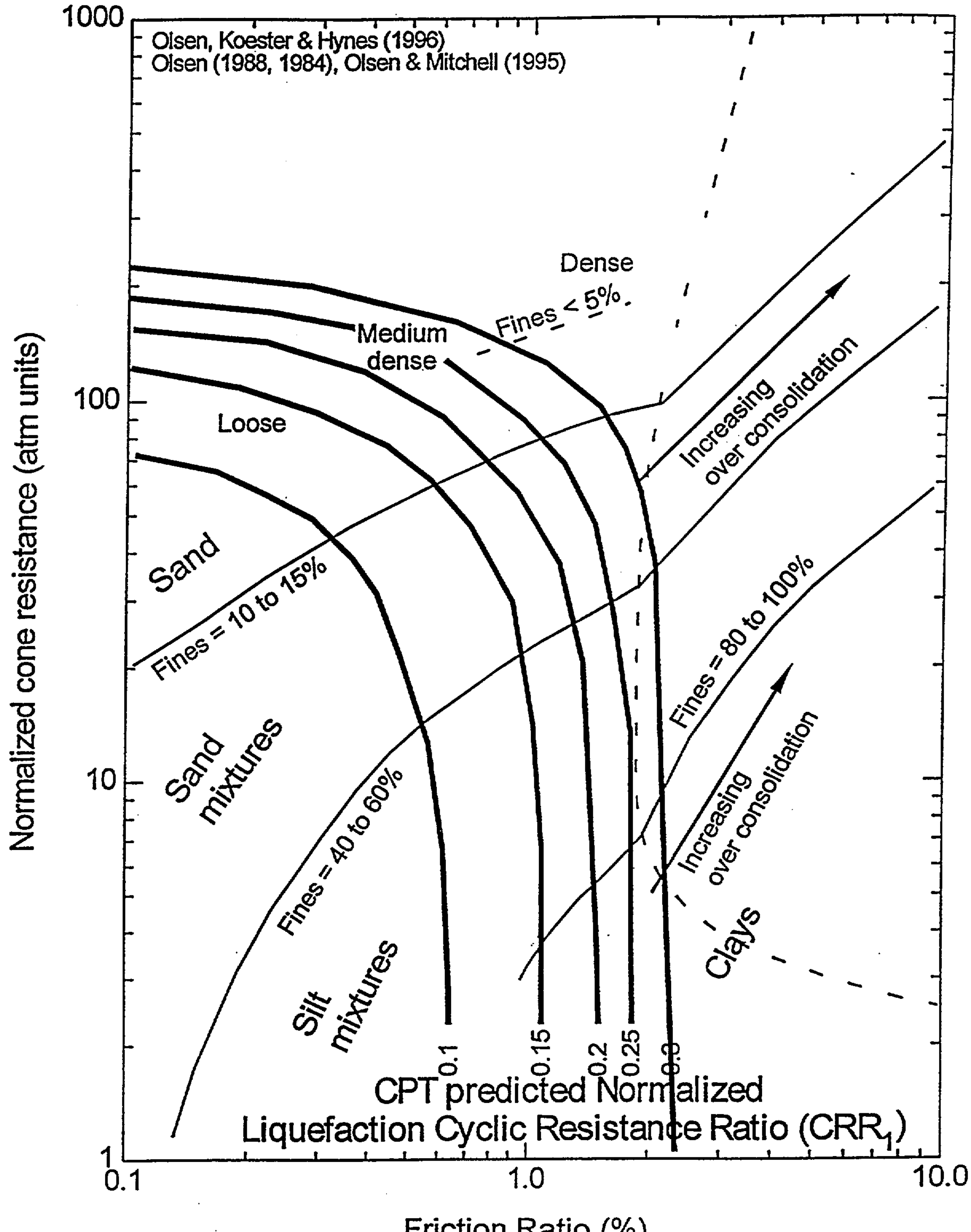

Figure 14. Estimation of the normalized liquefaction cyclic resistance ratio (CRR_1) using the CPT soil characterization techniques (Olsen, Koester, and Hynes, 1996)

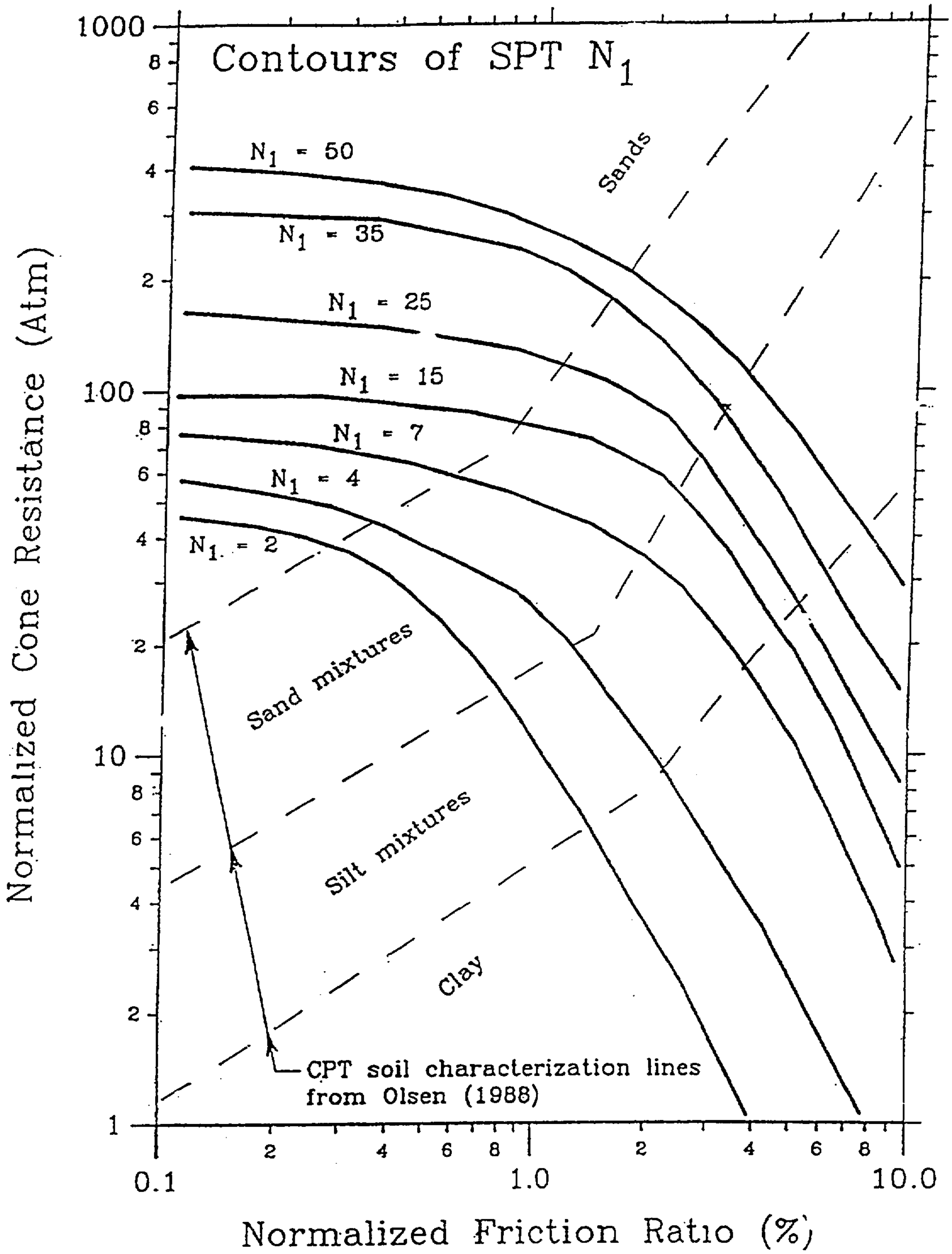

Figure 15. CPT estimation of SPT N_1 using both CPT measurements (Olsen 1994, 1988, 1986, 1984)

and De Alba (1986) used the q_c/N technique to establish a cone resistance-based technique for estimating CRR_1; however, this approach may result in unconservative estimates of CRR_1. The next step, after establishing SPT contours (Figure 15), was developing contours of CPT-estimated equivalent clean sand normalized blow counts, $(N_1)_{cs}$, using the procedure shown in Figure 16 (Olsen, 1988). Equivalent clean sand SPT contours were calculated based on the combination of SPT N_1 contours and CPT- estimated fines content together with the SPT-based silt correction relationship shown in Figure 17. CRR_1 contours were then approximated by converting the $(N_1)_{cs}$ contours to CRR_1 contours based on the Seed $(N_1)_{cs}$ to CRR_1 relationship (Figure 18). These SPT-estimated CRR_1 contours may serve as a framework for further refinements based on future cyclic laboratory and field performance data.

3.1.2.3 Becker Penetration Tests

Until relatively recently, coarse-grained soils were considered sufficiently free-draining to preclude development and retention of residual excess pore water pressures during earthquake shaking. The inherently strong frictional nature of granular materials containing particle sizes larger than sand is the basis for their selection in the construction of earth and rock fill embankments. In addition, the abundance of larger fractions of materials separated during borrow and fill placement makes their use for buttressing impervious compacted zones attractive.

Field observations of soil response during more recent moderate to strong earthquakes have revealed liquefaction and consequent post-earthquake instability in loose to medium dense gravels, both naturally deposited and placed by various artificial processes. Table 2 (Sy, Campanella, and Stewart, 1995) is a compilation of field occurrence data on liquefaction in gravels during earthquakes worldwide. Most of the observations recorded in the table are from events within the last 20 years; unless the gravels known to have liquefied were at or near the ground surface, there were no investigational tools available prior to the last two decades to confirm or deny the occurrence of liquefaction in gravels in the subsurface.

The Becker Hammer Drill is the tool of choice at present for in situ investigation of the density and, by inference, strength, of soils containing gravels or cobbles. Operation of the Becker Hammer Drill is depicted schematically in Figure 19. Liquefaction resistance and residual strength of gravelly soils are currently estimated by converting Becker Hammer Penetration Test (BPT) blowcounts to equivalent SPT blowcounts. BPT/SPT correlations employed to date for Corps of Engineers projects have considered deposit behavior to be largely a function of the operating efficiency of the Becker Hammer drill's double-acting diesel pile driver. Test procedures and data reduction techniques applied to use the BPT for estimating liquefaction resistance of gravelly or cobbly soils as described herein are excerpted from NCEER (1997).

Operating efficiency has been judged from measurements of the pressure acting within the bounce chamber of the pile driver apparatus, in the manner described by Harder and Seed (1986) and Harder (1988). Harder and Seed (1986) developed the relationship shown in Figure 20 to correct for combustion conditions within an ICE Model 180 diesel pile driver such as is used in Becker drill rigs, based on bounce chamber pressures. Once a combination of Becker blowcount, N_B, and bounce chamber pressure is plotted on this figure, the blowcount is adjusted by following the parallel correction curves for reduced efficiency down to the A-A' curve that bounds the curves to the lower right. The adjusted BPT blowcount, N_{bc}, was related by Harder and Seed (1986) to equivalent SPT N_{60} values as shown in Figure 21. The NCEER (1997) report suggests further that bounce chamber pressures be increased by 1.5 to 2 psi (10 to 14 kPa) for measurements made at approximately 2000 ft (610 m) above sea level, and by 4 to 6 psi (28 to 41 kPa) if measured at approximately 6000 ft (1829 m) above sea level.

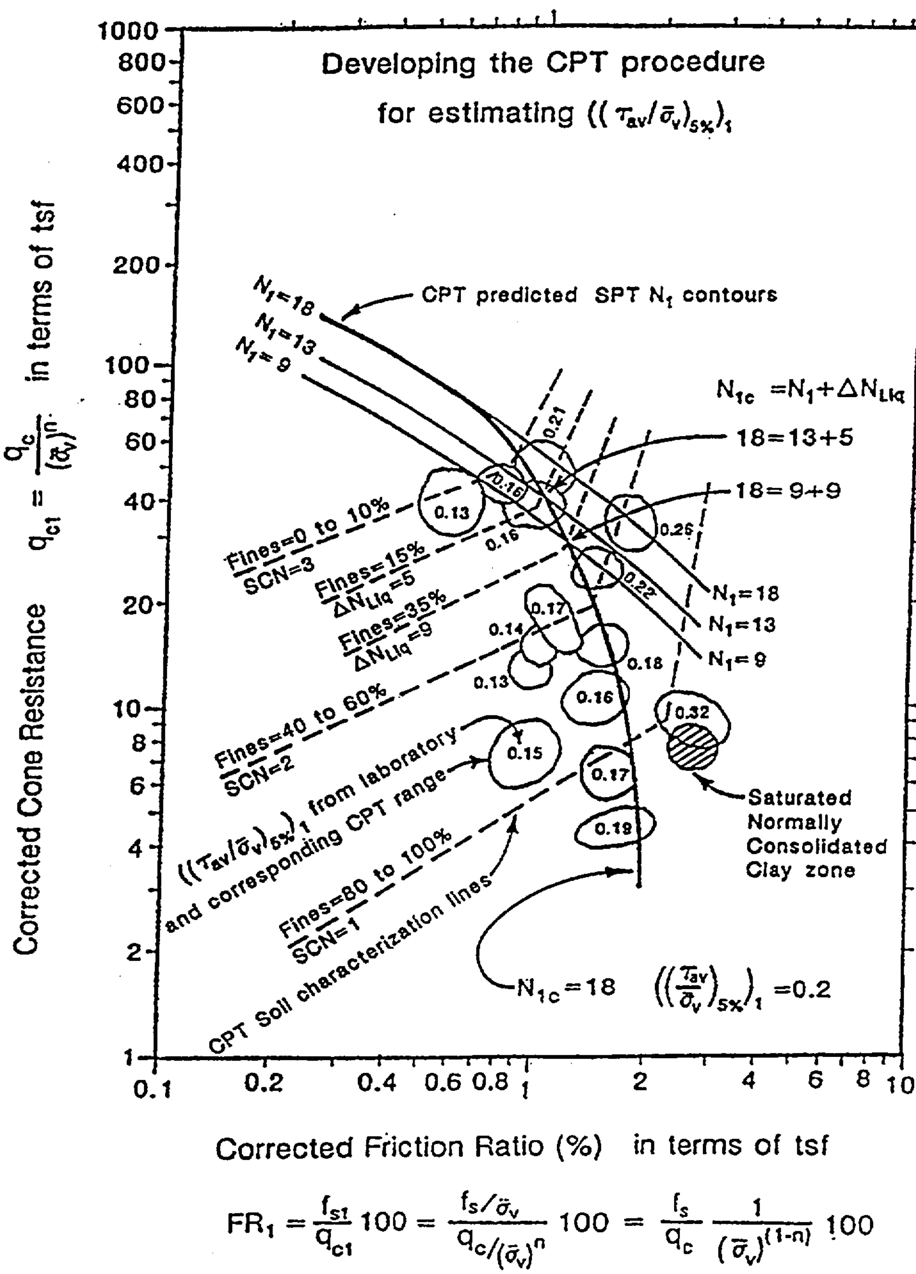

Figure 16. Graphical procedural steps for CPT-based determination of the SPT blowcount, fines content, equivalent clean sand SPT blowcount, and normalization liquefaction cyclic resistance ratio (CRR_1) (Olsen, 1988)

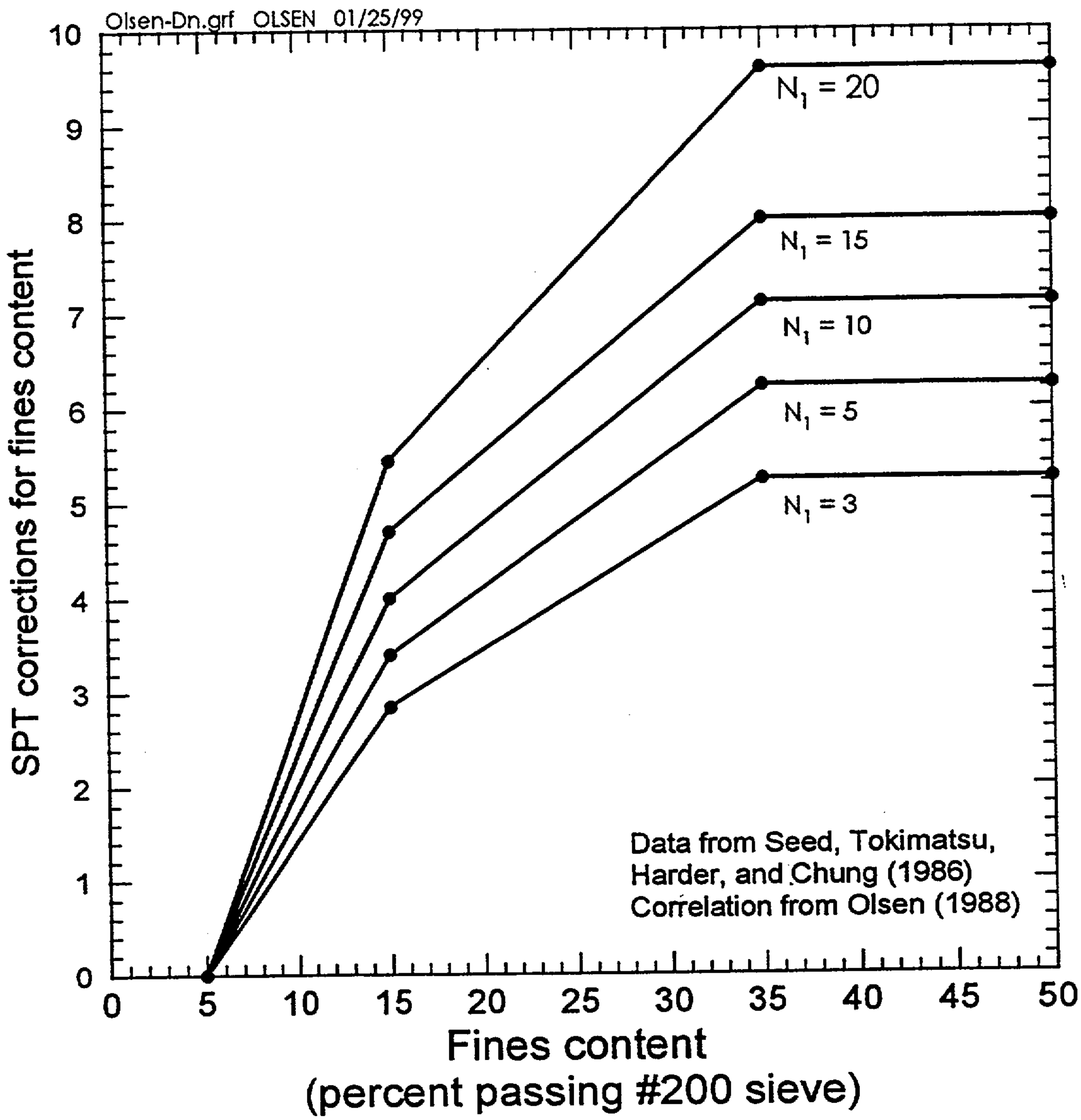

Figure 17. SPT blowcount fines content correction (Olsen, 1988)

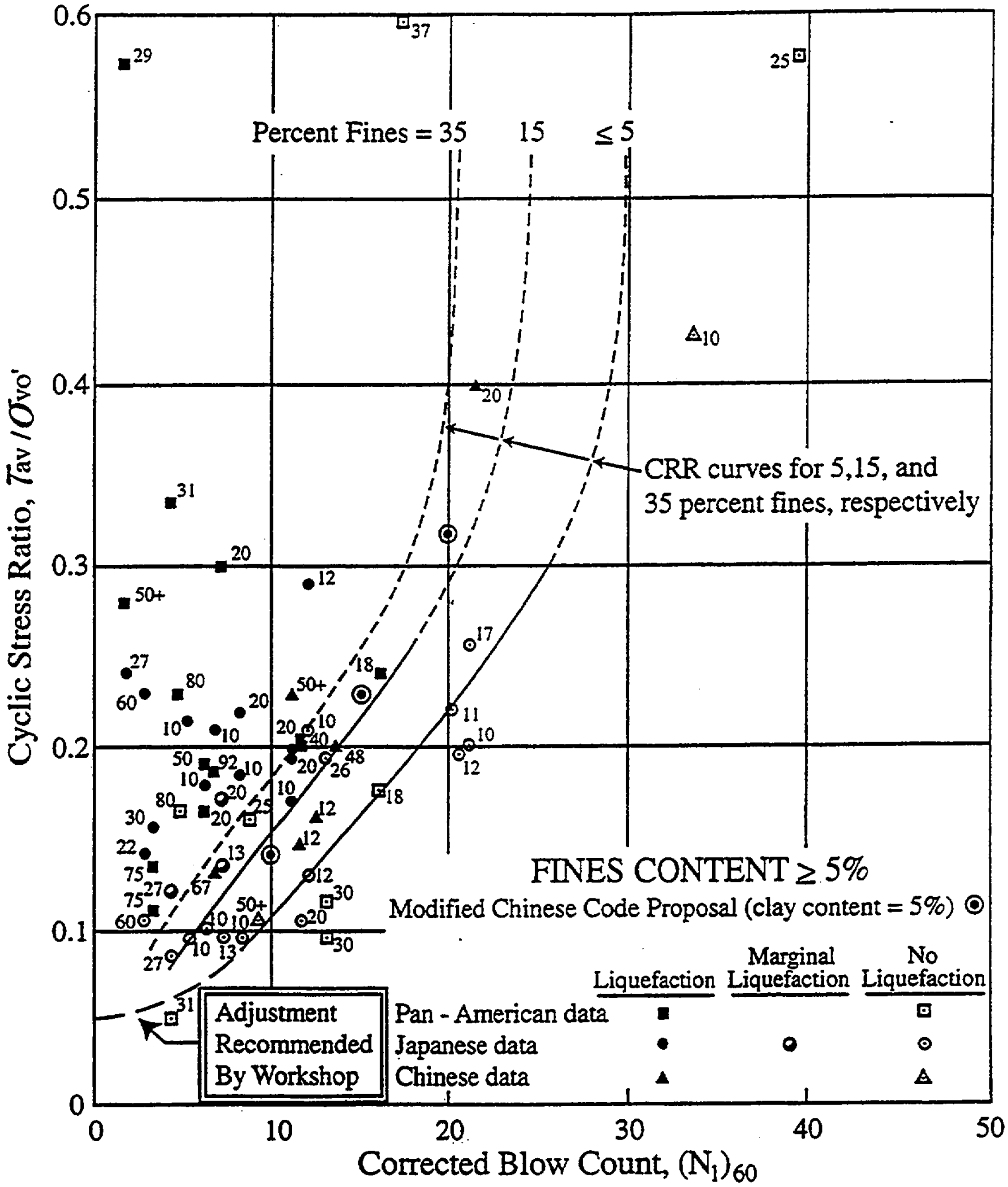

Figure 18. Curves recommended by NCEER workshop for calculation of CRR from SPT and fines content data (NCEER, 1997)

OBSERVED LIQUEFACTION IN GRAVELLY SOILS

YEAR	M	EARTHQUAKE	REFERENCE
1981	7.9	Mino-Owari, Japan	Tokimatsu and Yoshimi (1983)
1943	7.3	Fukui, Japan	Ishihara (1985)
1964	9.2	Valdez, Alaska	Coulter and Migliaccio (1966)
1975	7.3	Haicheng, PRC	Wang (1984)
1976	7.8	Tangshan, PRC	Wang (1984)
1978	7.4	Miyagiken-Oki, Japan	Tokimatsu and Yoshimi (1983)
1983	7.3	Borah Peak, Idaho	Youd, et al. (1985), Harder (1988)
1988	6.8	Armenia	Yegian, et al. (1994)
1992	5.8	Roermond, Netherlands	Maurenbrecher, et al. (1995)
1993	7.8	Hokkaido, Japan	Kokusho, et al. (1995)
1995	6.8	Kobe, Japan	Kokusho (1995)

Table 2. Summary of liquefaction occurrences in gravel deposits (after Sy, Campanella, and Stewart, 1995, supplemented by the author)

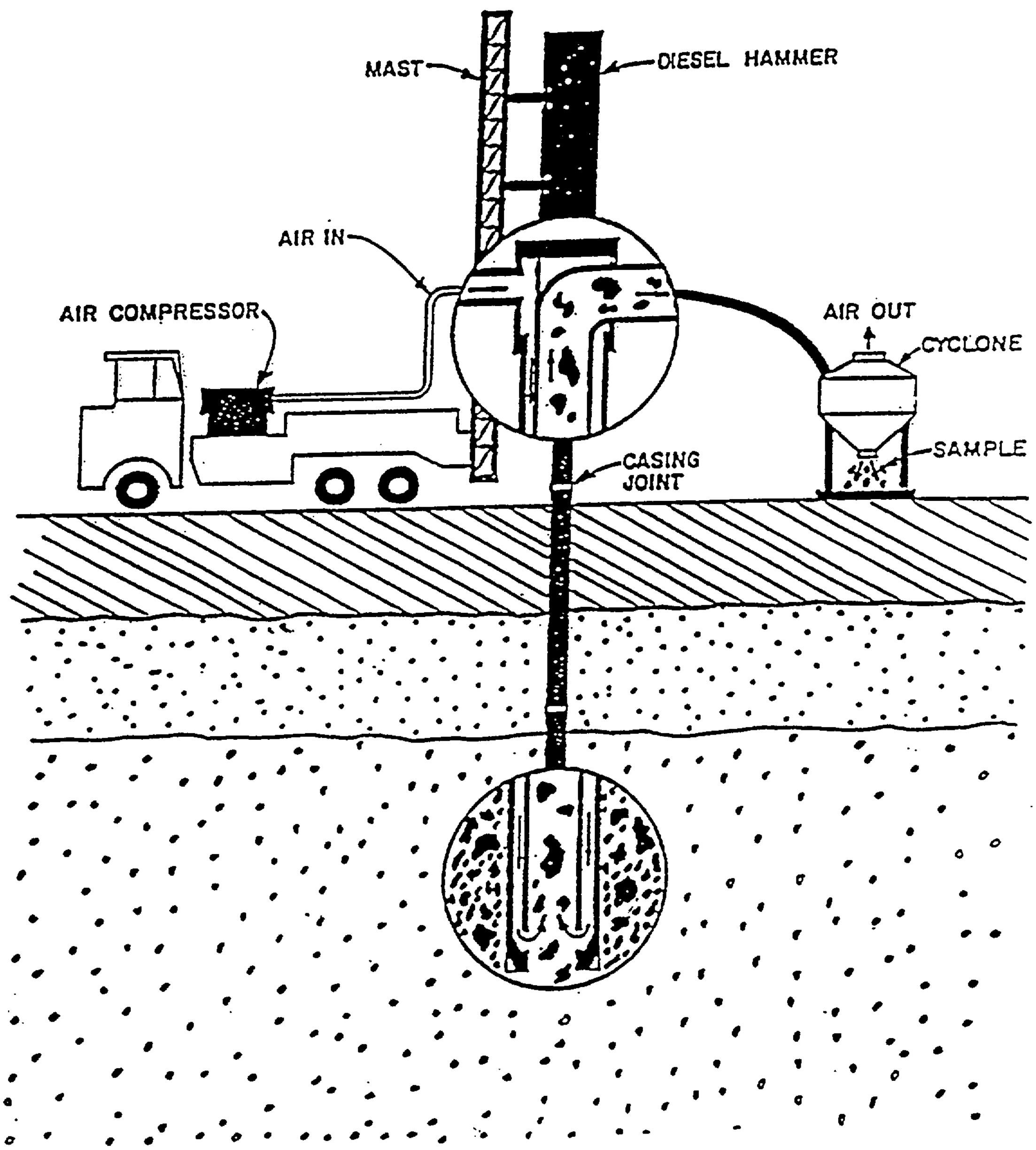

Figure 19. Schematic diagram of Becker Hammer sampling operation (Harder and Seed, 1986)

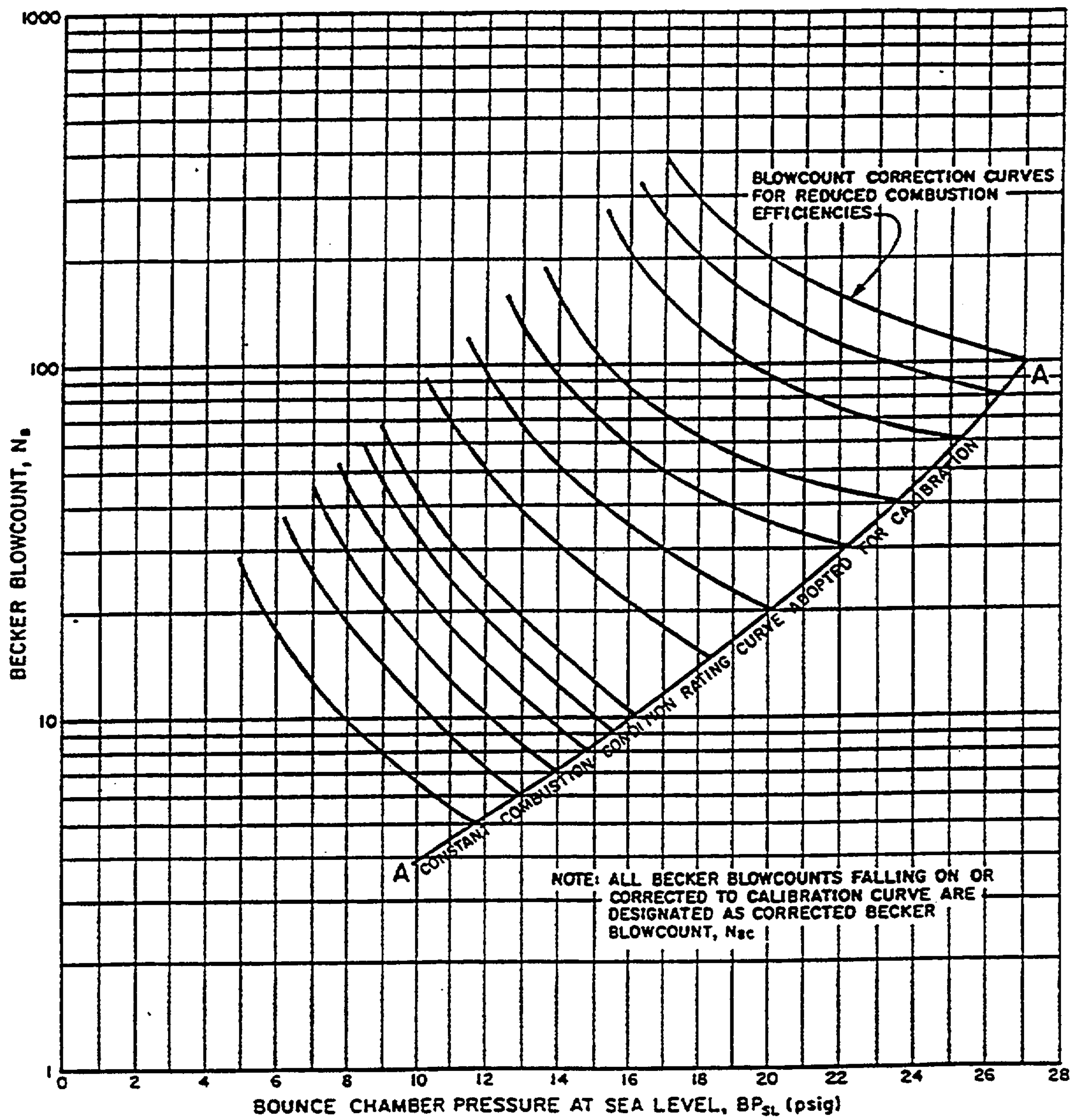

Figure 20. Correction curves adopted to correct Becker hammer blowcounts to constant combustion curve adopted for correction (from Harder and Seed, 1986)

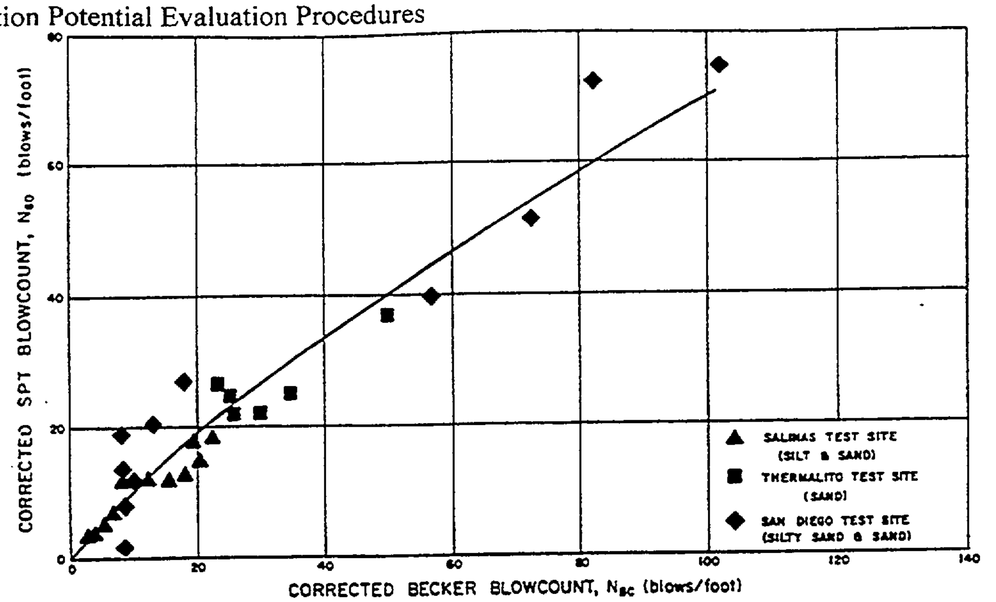

a. Original Harder and Seed (1986) Correlation

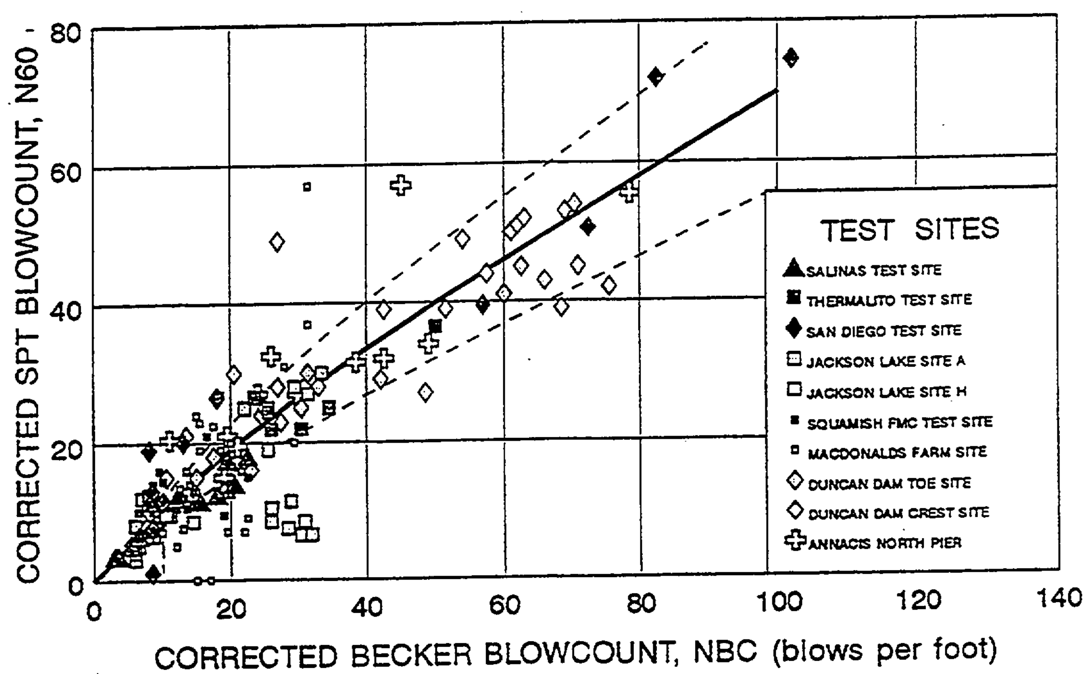

b. Harder and Seed (1986) Correlation Supplemented with Data from Additional Test Sites

Figure 21. Correlation between corrected Becker hammer and SPT blowcounts (from Harder and Seed, 1986)

The BPT is not standardized as yet, and interpretation of test results is subject to uncertainties. Selection of engineering properties inferred from BPT results is also an uncertain science in remediated soils, due to the altered lateral stress conditions in these deposits. Recent studies have concluded from field measurements using Pile Driving Analyzer (PDA) equipment that BPT efficiency is also strongly influenced by mechanical energy losses, including friction acting along the driven casing (Sy, 1993; Sy and Campanella, 1993; and Sy and Campanella, 1994). Uncertainties inherent in present BPT/SPT correlations considering only bounce chamber pressure may result in overconservative estimates of liquefaction resistance (more so with increasing depth). Additional detail on the application of PDA measurements and quantification of casing friction are found in the references just cited.

Ongoing research at the WES is directed toward minimizing accountable uncertainties in the in situ testing of gravelly soils; guidance will be published for Corps users as it is developed. For the present, the recommendations in NCEER (1997) should be followed with respect to BPT performance and results interpretation, adapted as follows:

1. The Becker Penetration Test should be performed with plugged-bit soundings in order to avoid an overly conservative evaluation of subsurface deposits.

2. In order to avoid the use of several correction factors, it is recommended that the Becker Penetration Test be performed with the following set of equipment:

   - AP-1000 Drill Rig (due to the establishment of much of the correlative data to date using this rig type; other rigs are acceptable, provided step 3, below, is followed to avoid equipment-specific variance of driving resistance).

   - Plugged 168-mm O.D. Drive Bit and Casing.

3. It is necessary to monitor the efficiency/performance of the diesel hammer during driving. This can be done using the bounce chamber pressure with the Harder and Seed method, or may be performed using more sophisticated instrumentation similar to that used by Sy and Campanella (1993). The Sy and Campanella approach provides insight on the tip and casing friction elements of Becker penetration resistance. However, for most investigations where depths are less than about 30 meters, the simpler Harder and Seed (1986) approach is probably warranted because of the greater data base together with its ease of implementation and lower cost.

4. Casing friction will remain a concern until either different equipment or approaches are developed to make the determined penetration resistance independent of casing length. For most investigations, the Harder and Seed (1986) approach with friction effects implicitly incorporated will probably be adequate. However, for depths greater than 30 meters and/or for sites with thick deposits of very dense material overlying much looser material, more sophisticated approaches involving wave equation techniques may be necessary. (*Note: as an interim recommendation, pending conclusive results from ongoing research at WES, total casing friction may be determined by intermittent measurement of the force required to pull the casing upward, by means of a load cell affixed to the drive head of the Becker drill rig. Friction correction may then be effected using the relationship reported by Sy and Campanella (1993).*) Unreasonably low penetration resistance will be determined with the Harder and Seed (1986) approach if Becker soundings are performed through cased boreholes to reduce friction effects.

5. For all projects involving the Becker Penetration Test to investigate gravelly deposits, it is recommended that a local correlation or check be performed either at the project site or nearby. This local check would consist of performing Becker soundings in sandy material near the depth of interest and to also perform high quality SPT's in the same layer. In this way, a check may be made on the applicability of the Becker equipment and correlations.

6. Several investigations have indicated that the Becker Penetration Test may not detect the presence of a very soft silt layer at depth. If such layers are thought to be present and of concern for the project, it is recommended that other investigative techniques (e.g., SPT) be carried out to explore and characterize such materials.

3.1.2.4 Large Penetrometer Tests

Gravel and larger particles in soil may impede the penetration of an SPT split spoon sampler and cause misleading high blowcounts and data scatter. Several sizes of split spoon drive samplers are available commercially and are often employed to sample soils containing coarse particles. Given the relatively recent emphasis on coarse soils in liquefaction potential evaluation, the data base is insufficient as yet to develop robust correlations of penetration resistance among various drive samplers. Most comparative research on larger penetrometers has been performed in Japan, where researchers have performed drive penetration tests using a Large Penetration Test (LPT) device, shown schematically in Figure 22 (Kokusho, 1989), that has a larger diameter and is driven by dropping a hammer that is 50 percent heavier from twice the height used for an SPT sampler. Figure 23 (Tanaka et al., 1989) compares profiles of penetration resistance blowcounts obtained using SPT and LPT equipment in natural gravelly soils. Figure 24 (Kokusho, 1989) illustrates penetration resistance comparisons from laboratory container experiments where gradation was controlled. Very close agreement was shown between SPT and LPT blowcounts in moderately dense uniform sand, in spite of the much larger driving energy involved in the LPT; in gravels, however, the LPT yields lower blowcounts. There is no standard practice for the performance of LPT's at present; ongoing research at WES is directed toward comparing results from various samplers and drive systems at a liquefiable gravel site to develop guidance for split spoon testing in coarse soils. In the interim, it is not considered sufficient to multiply blowcounts obtained using non-SPT samplers by a constant factor for evaluation of liquefaction potential.

3.1.2.5 Pressuremeter Applications

The use of the self-boring pressuremeter was proposed by Vaid, Byrne, and Hughes (1981) to evaluate liquefaction potential of sand through correlation with the dilation angle parameter. Dilation angle, defined as the inverse sine of the slope of a volume expansion-versus-shear strain curve, may be measured either from drained laboratory triaxial of simple shear tests or from in situ pressuremeter tests. Pilot tests on a hydraulic fill dam yielded reasonably similar estimation of liquefaction resistance from SPT blowcount-based and pressuremeter-based techniques.

3.1.2.6 Seismic Wave Velocity Measurements

Seismic wave velocities (P-wave and shear, or S-wave) are routinely determined through field geophysical surveys to obtain input for dynamic response analysis (Ballard and McLean, 1975 and Department of the Army, 1979). Dobry et al. (1981) describe the use of shear wave velocity to estimate a threshold earthquake acceleration for liquefaction.

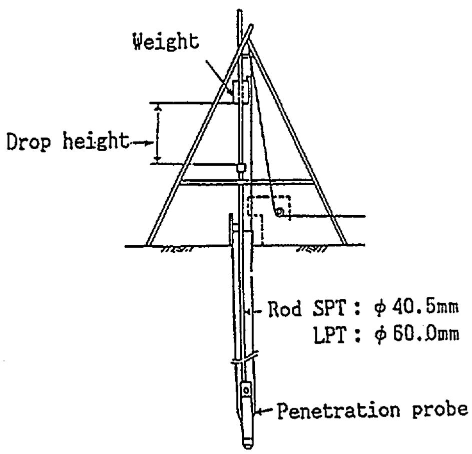

No.	(1)	(2)
Details of penetration probe	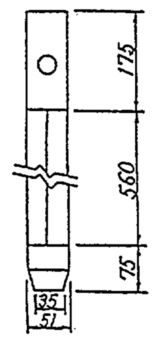	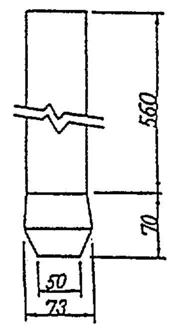
Test name	Standard Penetration Test	Large Penetration Test
Symbol	S.P.T	L.P.T
Drive method	Fall weight	Fall weight
Weight	622.3N	980N
Drop height	75 cm	150 cm
Drive length	30 cm	30 cm

Figure 22. Concept of dynamic penetration test (Kokusho, 1989)

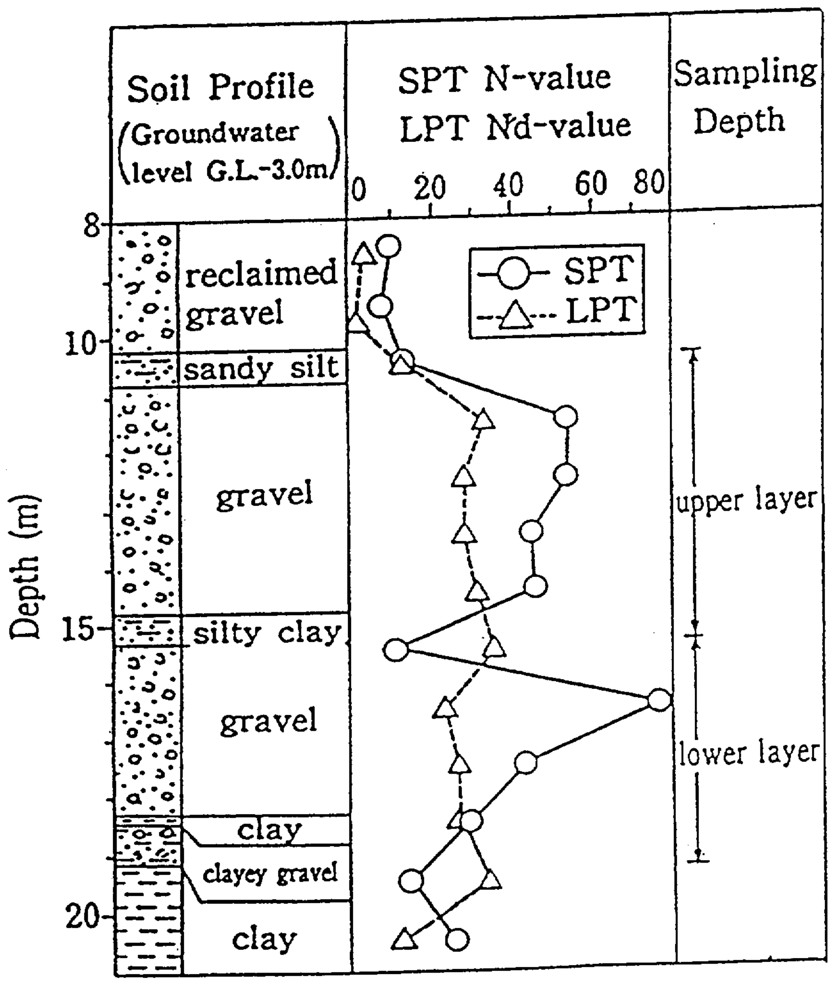

Figure 23. Soil profile at T-site (Tanaka, et al., 1989)

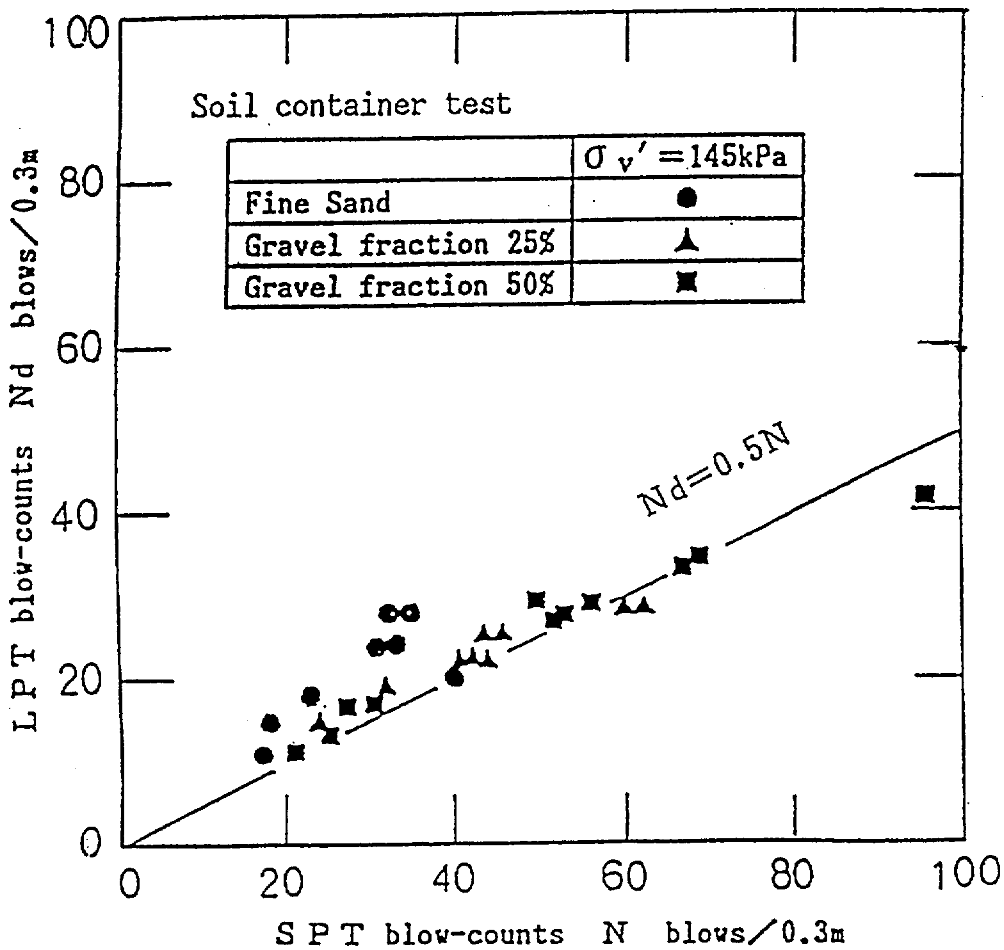

Figure 24. SPT vs. LPT relationship for gravelly soils (Kokusho, 1989)

Tokimatsu, Yoshimi, and Uchida (1988) proposed a method to evaluate in situ liquefaction resistance of dense sands that may eventually prove adaptable to other soils, wherein: (1) shear wave velocities are determined by geophysical survey; (2) high-quality samples are obtained by in situ freezing; (3) laboratory initial shear modulus, G_{max}, is determined by low amplitude cyclic shear testing (type of equipment unspecified) and compared to that calculated from field shear wave velocity; (4) laboratory G_{max} is adjusted (increased) by application of low amplitude (equipment again unspecified) preshearing until field and laboratory values match, and (5) cyclic triaxial tests are performed to measure liquefaction resistance of thawed specimens. Adjusted specimen liquefaction resistance is claimed to represent in situ behavior.

Stokoe et al. (1988) developed charts relating shear wave velocity to maximum surface acceleration, a_{max}, that predict liquefaction potential in clean sands (e.g., Figure 25). Applicability of the method to silty or clayey soils is not known; the method is attractive, due to the avoidance of sampling problems and its direct reliance on in situ stiffness of a deposit. Andrus and Stokoe (in NCEER, 1997) describe a shear wave velocity procedure based on field performance that is applied in the manner of penetration resistance methods; the resulting chart is shown in Figure 26. In this chart, shear wave velocity is adjusted for vertical effective confining stress to compute abscissa values, V_{S1}, from:

$$V_{S1} = V_S \left(\frac{P_a}{\sigma_v'} \right)^{0.25} \tag{5}$$

The chart is based on field performance in earthquakes with moment magnitude, M_w, equal to 7.5. Cyclic stress ratio causing liquefaction must be corrected for correspondence to other earthquake magnitudes as described in a later section. The authors recognized that additional study is required to extend the method to soils and conditions other than those represented in the data base used, particularly in deeper deposits (depth > 8 m) and denser soils (V_S > 200 m/s) shaken by stronger ground motions ($a_{max} \geq$ 0.4 g).

The Spectral Analysis of Surface Waves technique is widely applied to determine shear wave velocity profiles in a variety of applications (Stokoe and Nazarian, 1985 and Stokoe et al., 1988). This technique is also featured in the NCEER (1997) reference.

3.1.2.7 Other

A number of additional in situ testing techniques show promise as tools to assist in site characterization for liquefaction potential evaluation. None of the techniques mentioned in this section are yet substantiated by experience; their inclusion is for future reference.

Electrical resistivity and conductivity geophysical survey methods have been applied to characterize in situ properties using either surface or borehole sensor arrays (Department of the Army, 1979). Arulanandan and Kutter (1978) studied electrical anisotropy of soil deposits, developing a structural index that may correlate to liquefaction resistance. Erchul and Gularte (1982) investigated densification in liquefying sand deposits in the laboratory using electrical resistivity; they proposed extending the method to evaluate field deposits and monitor compaction efficiency.

Roe, DeAlba, and Celikkol (1981) determined the response of reconstituted laboratory soil specimens to a given low-amplitude P-wave excitation, demonstrating a relationship between acoustic signature so

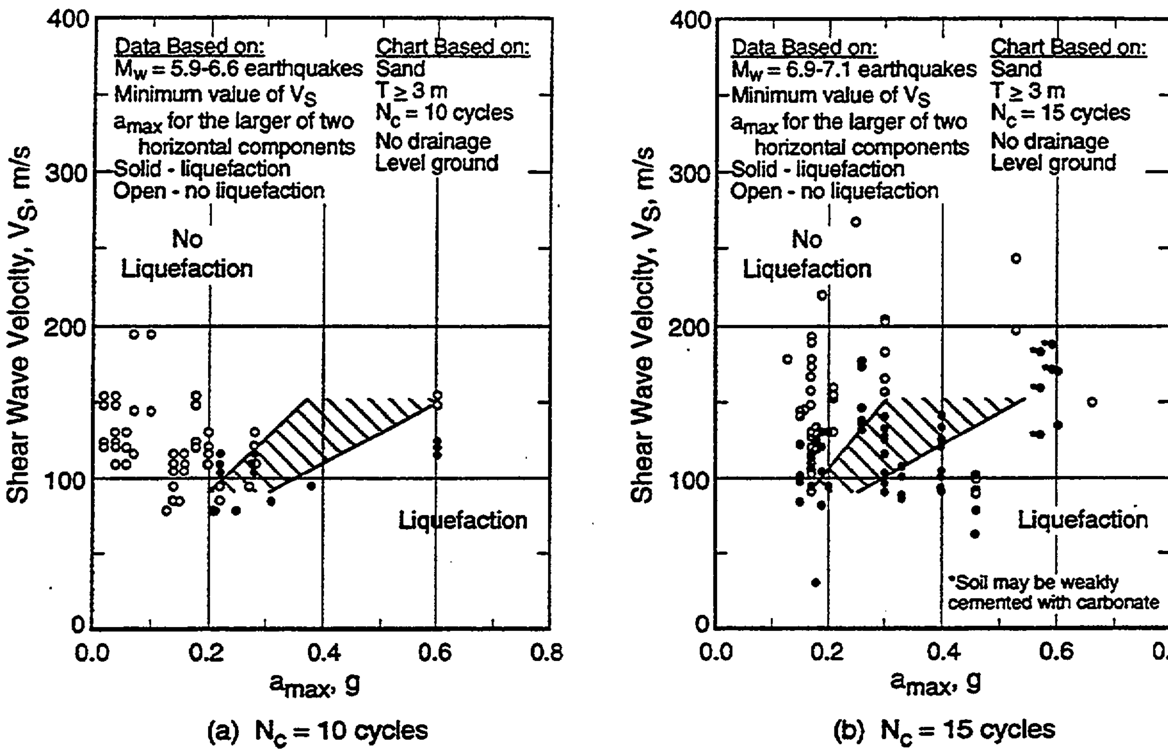

Figure 25. Chart to evaluate liquefaction potential based on shear wave velocity and maximum acceleration (NCEER, 1997, after Stokoe et al., 1988, and Andrus, 1994).

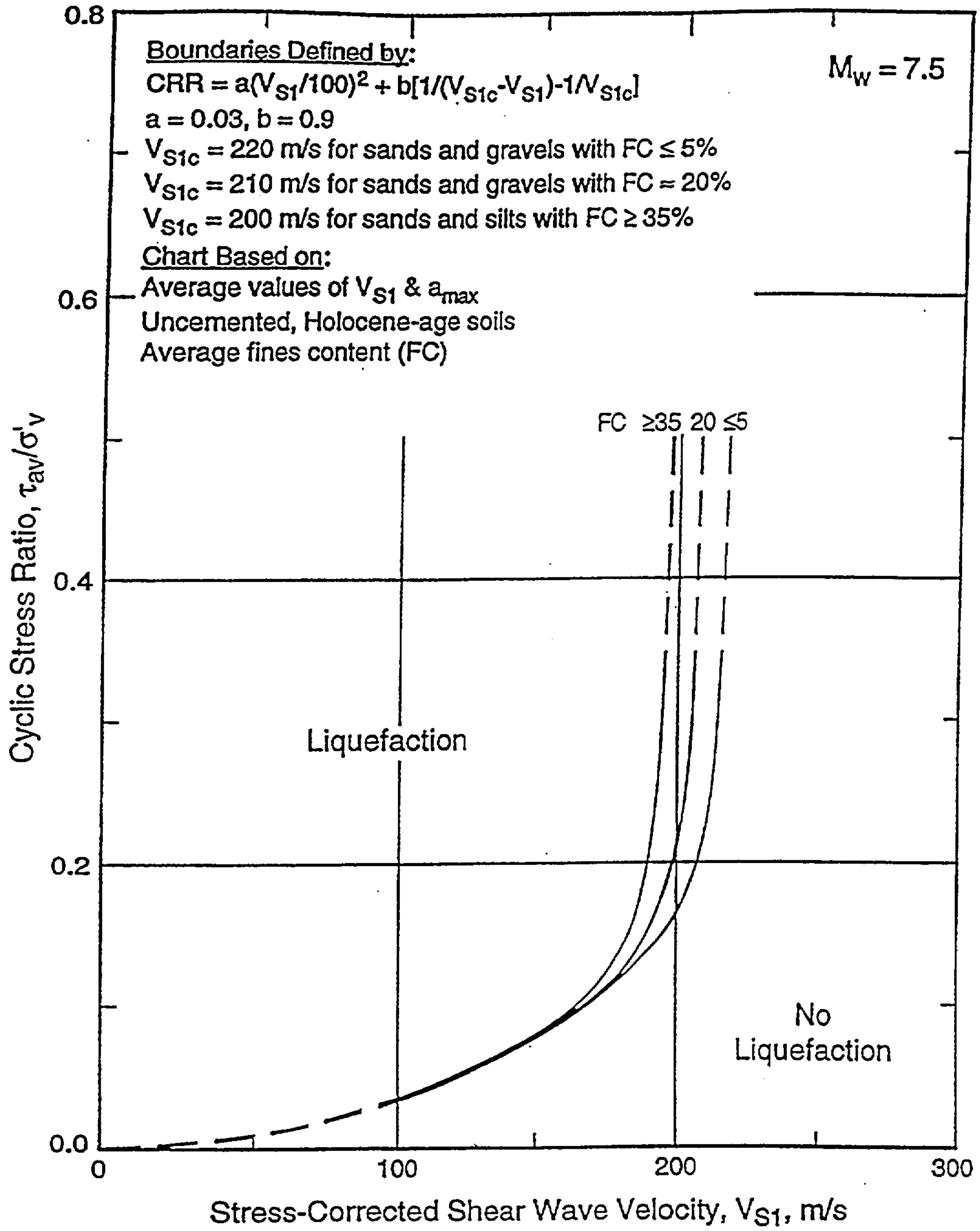

Figure 26. Recommended liquefaction assessment chart based on V_{S1} and CSR for magnitude 7.5 earthquake and uncemented soils of Holocene age (NCEER, 1997)

measured and liquefaction resistance. The study was aimed at evaluation of liquefaction potential in marine deposits where sampling is particularly difficult and a data base exists for acoustic response.

3.1.3 Undisturbed Sampling

Soil samples are disturbed both mechanically and by changes in their effective stress state on removal from a deposit in situ and transportation to testing facilities. The term "undisturbed" used in this report is liberally interpreted to imply sampling activities that minimize mechanical disturbance. As concerns liquefaction potential evaluation, Marcuson and Franklin (1979) reviewed techniques and apparatuses that are still commonly applied to sample granular soils. Significant conclusions reported in that reference include: (1) fixed-piston, thin-walled tube samplers used in boreholes supported by appropriately mixed drilling mud or fluid generally yield high quality samples of many sands; (2) the use of radiographs of samples within sampling tubes permits judgment of sampling disturbance for selection of representative specimens; (3) undisturbed gravel specimens can be successfully obtained only by hand carving larger block samples; and (4) in situ freezing of a larger-than-required volume of soil for subsequent trimming produces very high quality (with regard to mechanical disturbance) soil samples, as long as the freezing front is propagated in a manner that assures free drainage.

Marcuson and Franklin (1979) reported that fixed piston sampling operations tend to produce the best samples so obtained when used in medium dense sands. Tube sampling was observed to densify loose sands and dilate dense sands. The implication is that cyclic strength test results on tube sampled specimens, if interpreted directly, would be unconservative in the case of sands that were loose in situ, and overconservative in dense sands.

3.2 Screening Techniques

3.2.1 General

This section describes techniques for initial or screening evaluation of sites for liquefaction susceptibility of soils. The goal of these evaluations is to determine whether the site is clearly safe or if soils clearly will liquefy. Either determination will make further, more detailed, liquefaction potential evaluations unnecessary and work can proceed to the next phase (e.g., stability evaluation, design, etc). If the result of a screening evaluation is unclear, however, then a more detailed analysis will be needed, as described in subsequent sections.

The scope of the investigation required is dependent not only on the nature and complexity of geologic site conditions, but also on the economics of a project and on the level of risk acceptable for the proposed structure or development. Naturally, a more detailed liquefaction field study is necessary for critical structures and facilities (e.g., nuclear facilities, hospitals, large dams, power plants, air fields, critical harbor facilities, major bridge abutments, etc.) than for non-critical structures and facilities.

As discussed in earlier sections, most liquefaction hazards are associated with <u>sandy soils</u> and/or <u>silty soils of low plasticity</u>. Cohesive soils with fines contents of greater than 30 percent, and whose fines either (a) classify as clays based on the Unified Soil Classification System, or (b) have a Plasticity Index (PI) of greater than 30 percent, are not generally considered potentially susceptible to soil liquefaction. In the People's Republic of China, numerous instances of liquefaction have been observed in deposits of fine-grained silty, clayey soils, during recent strong earthquakes (Wang, 1979). Some soils with clay content (particles finer than 0.005 microns) less than 15 percent by weight, liquid limit less than 35 percent, and occurring at natural water contents greater than 90 percent of their liquid limit were found to have liquefied. There is, however, no available information (based on the observations in China) on the ground motion characteristics required to trigger this behavior, except that occurrences were reported for earthquakes ranging in Modified Mercalli Intensity from VII to IX (magnitude 5.5 to 7.4). These observances evolved into the criteria published in a definitive EERI monograph by Seed and Idriss (1982). Certain cohesive soils may be vulnerable to strength loss on remolding (e.g., sensitive clays and "quick" clays), and the hazard posed by the presence of these soils, though not classically defined as liquefaction and therefore not addressed by these guidelines, should also be assessed. Youd (1998) suggests that it is sufficiently conservative to assume, for screening purposes, that soils having dual Unified Soil Classification System designations, such as CL-ML, SM-SC, or GM-GC are potentially liquefiable; other designations involving the "C" descriptor exceed the clay content observed by Wang (1979) to bound liquefiable deposits.

In addition to sandy and silty soils, some gravelly soils are potentially vulnerable to liquefaction. Historically, geotechnical engineers have tended to consider gravelly soils safe with respect to potential liquefaction, and numerous references abound in which soil gradation plots indicate a boundary beyond which coarse (typically gravelly) soils will not liquefy. Considerable research since 1980 has shown, however, that gravelly soils can liquefy, and there are a number of well-documented field case histories confirming this (e.g., Coulter and Migliachio, 1966; Ishihara, 1984; Harder, 1988; Andrus and Youd, 1987; Andrus and Youd, 1989; Andrus, et al., 1992). Most coarse, gravelly soils drain relatively freely, but when (a) their voids are filled with finer particles, or (b) they are surrounded by less pervious soils, their drainage can be impeded and they may be vulnerable to cyclic pore pressure generation and/or liquefaction. Similarly, when they are of considerable thickness and lateral extent, deposits of coarse gravelly soils may not be capable of dissipating seismically-induced pore pressures and so may be vulnerable to potential liquefaction.

When gravelly soils are dense, and so are highly resistant to liquefaction, preliminary screening methods involving assessment of their density (and approximate relative density), shear wave velocity, and/or geologic age and depositional history may often suffice for evaluation of their liquefaction susceptibility. When these types of preliminary screening methods do not suffice, the best techniques currently available for detailed quantitative evaluation of the liquefaction resistance of coarse, gravelly soils are those described by Harder and Seed (1986), Sykora, Koester, and Hynes (1991), and NCEER (1997) involving the use of Becker Hammer penetration test resistance correlations. Given the uncertainties involved in the penetration resistance measured with the Becker Hammer, and in correlating BPT resistance to SPT resistance, it may be necessary to directly measure densities of gravelly materials in exploratory test pits. These pits can be expensive, since they may involve dewatering and excavation support by means of large casing.

3.2.2 Liquefaction Hazard Screening Evaluation

Liquefaction hazard at a site may be screened in two general steps: (1) a preliminary geologic/geotechnical site evaluation; and, if warranted, (2) a more detailed geotechnical evaluation of liquefaction potential and its potential consequences. In many instances, the early stages of such investigations will suffice to demonstrate the absence of liquefaction hazard at a proposed project site. Otherwise, it will be necessary to proceed with the types of studies described in the next section.

Preliminary geological/geotechnical site evaluation studies must address three basic questions:

(a) Are potentially liquefiable soil types present?

(b) If so, are they saturated and/or may they become saturated at some future date?

(c) If so, are they of sufficient thickness and/or lateral extent as to pose potential risk to the survival or function of the project?

If preliminary geologic investigations addressing these issues can clearly demonstrate the absence of liquefaction hazard at a site, then these preliminary investigations may, by themselves, be sufficient. If some uncertainty remains, however, then more comprehensive geotechnical studies should be undertaken.

3.2.2.1 Are Potentially Liquefiable Soil Types Present?

In assessing the potential presence of liquefiable soil types, investigations should extend to depths below which liquefiable soils cannot reasonably be expected to occur (e.g., to bedrock, or to hard competent soils of sufficient geologic age that possible underlying units could not reasonably be expected to pose a liquefaction hazard). At most sites where soil is present, such investigation will require either borings or trench/test pit excavation. Simple surface inspection will suffice only when bedrock is exposed over essentially the full site, or in very unusual cases when the local geology is sufficiently well-documented as to fully ensure the complete lack of possibility of occurrence of liquefiable soils (at depth) beneath the exposed surface soil unit(s).

Liquefaction resistance can be at least roughly correlated with geologic age, depositional environment and prior seismic history (see Table 1, introduced earlier). It should be noted that most liquefaction risk is associated with recent Holocene deposits and uncompacted fills, as progressively older units tend to have progressively higher resistance to liquefaction. There have, however, been a few observed cases of liquefaction of Pleistocene and even Pre-Pleistocene deposits, and particular caution should be used when dealing with very loose soils (e.g., dune sands, talus, etc.) and with extremely loose collapsible soils (e.g., loess).

3.2.2.2 Are They Saturated and/or May They Become Saturated?

If it can be demonstrated that any potentially liquefiable soil types present at a site (a) are currently unsaturated (e.g., are above the water table), (b) have not previously been saturated (e.g., are above the historic high water table), and (c) cannot reasonably be expected to become saturated, then such soils may be considered to pose no potential liquefaction hazard. Table 3 summarizes historical data relating water table depth to liquefaction susceptibility. It should be emphasized that project development, and/or changes in local or regional water management patterns, can significantly raise water table elevations. Extrapolation of data regarding water table elevations from adjacent sites will not, by itself, usually suffice to demonstrate the absence of liquefaction hazard in the absence of additional supporting data from the proposed project site itself, except in those unusual cases where a combination of uniformity of local geology and very low regional water tables permits very conservative assessment of water table depths. Preliminary geologic site evaluations should also address the possibility of local perched water tables or locally saturated soil units being present at a proposed project site.

3.2.2.3 Is the Geometry of Potentially Liquefiable Deposits Such that They Pose No Risk?

If the presence of potentially liquefiable soil types cannot be discounted, and if it cannot be shown that such soils are not and will not become saturated, then the absence of significant liquefaction hazard may still be demonstrated if it can be shown that potentially liquefiable soil deposits are of insufficient

Groundwater Table Depth	Relative Liquefaction Susceptibility
< 3 m	Very High
3 m to 6 m	High
6 m to 10 m	Moderate
10 m to 15 m	Low
> 15 m	Very Low

Table 3. Relative liquefaction susceptibility of natural deposits as a function of groundwater table depth (Youd, 1998)

thickness and/or lateral extent to pose any risk to the proposed structure(s) or facilities. It should be noted that relatively thin seams of liquefiable soils (on the order of only a few inches thick), if (a) very loose (and thus having very low or negligible residual undrained strength), and (b) laterally continuous over sufficient area, can represent potentially hazardous planes of weakness and sliding, and may thus pose hazard with respect to translational site instability and/or lateral spreading and related ground displacements. When suitably sound lateral containment is provided to eliminate potential sliding on liquefied layers, then potentially liquefiable zones of finite thickness occurring at depth may be deemed to pose no significant sliding risk. It must be considered, however, that buildings may settle (uniformly, or more likely, differentially) even if a liquefiable soil layer is contained, and sand boils can cause serious damage if they fill the floor of a critical facility.

3.2.3 Quantitative Evaluation of Liquefaction Resistance

If the preliminary geologic site evaluation indicates the presence of potentially liquefiable soils, either in a saturated condition or in a location which might subsequently become saturated, and of sufficient extent as to pose some level of risk, then the resistance of these soils to liquefaction and/or significant strength loss due to cyclic pore pressure generation under seismic loading should be evaluated. Similarly, if the preliminary geologic site evaluation does not conclusively eliminate the possibility of liquefaction hazard at the site, then more extensive analyses are required. Quantitative evaluation of liquefaction potential, addressed in the next section, is generally accomplished in two steps: (1) a quantitative evaluation of resistance to cyclic pore pressure generation or "triggering" of liquefaction, and (2) an evaluation of the undrained residual strength characteristics of the potentially liquefiable soils, leading to an assessment of post-earthquake stability and deformations.

3.3 Evaluation of Liquefaction Susceptibility - General

Liquefaction susceptibility at a site is commonly expressed in terms of a factor of safety against the occurrence of liquefaction. This factor is defined as the ratio between available soil resistance to liquefaction, expressed in terms of the cyclic stresses required to cause soil liquefaction and the cyclic stresses generated by the design earthquake. Both of these parameters are in turn commonly normalized with respect to the effective overburden stress at the depth in question, and are respectively represented by *CRR* and *CSR*:

$$\begin{aligned} FS_{against\ liquefaction} &= \frac{Available\ Soil\ Resistance}{Earthquake\ Induced\ Stresses} \\ &= FS_1 = \frac{CRR_1}{CSR} \end{aligned} \tag{6}$$

The following methods for calculating the factor of safety against liquefaction have been used to various extents:

3.3.1 Analytical Methods

These methods typically rely on laboratory test results to determine either liquefaction resistance or soil properties that can be used to predict the development of liquefaction. Various equivalent linear and nonlinear computer methods are used with the laboratory data to evaluate the potential for liquefaction.

Because of the considerable difficulty in obtaining undisturbed samples of loose granular (liquefiable) sediment for laboratory evaluation of constitutive soil properties, the use of analytical methods, which rely on accurate measurements of constitutive properties, are usually limited to critical projects or to research. If reliable screening procedures have not ruled out the possibility of liquefaction at a nuclear power facility, a comprehensive laboratory testing program may be justified. Laboratory methods are discussed in a subsequent section.

3.3.2 Physical Modeling

Physical modeling is a well-known approach to solving engineering problems so complex that they are not amenable to exact mathematical solution. Obviously, the state of stress in a small-scale model under normal self-weight (gravity) loading will be much different from the state of stress in a full size prototype. If the model materials have stress-dependent constitutive behavior and exhibit time dependent response phenomena, quantitative and even qualitative differences in behavior might be expected between a small-scale model and the corresponding full size prototype. Unless measures are taken in the small scale modeling process, not only will measurable parameters such as stress, deformation, pressure, and time for processes in the model be different from those in the prototype, but the observed response or failure mechanism may also be quite different in the model than in the prototype. However, if a small scale model could be subjected to an increased acceleration field, the stress level caused by self weight in the model would be the same as the corresponding stress level existing in the prototype. Many of the problems and limitations associated with testing a small-scale model would thus be removed. Acceleration above normal gravity (1 g) is achieved through the use of a centrifuge, and in the elevated gravity field, model behavior will theoretically be directly correlated with that of the full sized prototype if the experiment has been designed properly.

The primary advantages of a centrifuge test are that model stresses and strains can be made equal to those of the prototype, and extrapolation of model results to predict prototype behavior are simpler and more reliable than in 1 g models for most cases (due to the effects of self weight stress states). For models that involve nonlinear material behavior, the stresses in the model will be equal to those in the corresponding prototype. If the same materials in a prototype are used for a model and if the model experiences the same stresses as the prototype, the strains will be the same at corresponding points within the model and prototype, and the patterns of deformation will be identical. This is the main principle in centrifuge modeling, that a 1/N model accelerated to a gravitational force of Ng will be subjected at comparable points in the soil mass to the same stresses as the prototype, where N is the scaling factor and g is the acceleration of gravity.

In recent years, no application in centrifuge modeling has received more attention than seismic simulation, especially in the United States and Japan, where earthquakes are common occurrences and earthquake hazard mitigation is a major challenge to the engineering profession. This is especially true in the geotechnical engineering community. Considerable advances have been made in developing an understanding of the pertinent dynamic soil properties that influence the performance of soil deposits and soil structures under seismic loading. Numerous analytical procedures have been proposed to explain and correlate the observed earthquake induced phenomena. Some procedures are empirical, while others are based on coupled theories of soil/water interaction incorporating elasto-plastic constitutive models. However, due to a lack of quality field data, there remains a considerable gap in our understanding of the phenomena of permanent deformations, especially those occurring during liquefaction. Because of this and the inherent difficulties in orchestrating full-scale seismic events, physical modeling in the centrifuge has become a popular alternative for studying the seismic performance of earth structures. Scale models can be prepared with prescribed soil property profiles and shaken in the simulated gravity environment in a centrifuge with controllable base input motion. The model response may be studied qualitatively, and also produces quantitative data for calibrating numerical procedures and validating specific prototype designs.

Numerous studies by many researchers have demonstrated the benefits of centrifuge modeling (Whitman, Lambe, and Kutter, 1981; Schofield, 1981; Scott, 1983; Arulanandan, Anandarajah, and Abghari, 1983; Steedman, 1984; Coe, Prevost, and Scanlan, 1985; Hushmand, Scott, and Crouse, 1988; and Ketcham, Ko, and Sture, 1991). In addition, a cooperative research project called VELACS (Verification of Earthquake Liquefaction Analysis by Centrifuge Studies) sponsored by the National Science Foundation verified the use of centrifuge studies for seismic simulation capabilities. Arulanandan and Scott (1993) have reported results of these centrifuge experiments and their predictions. Centrifuge modeling may prove to be very cost-effective, given the amount of data obtainable from each test.

The primary disadvantage to centrifuge testing involves the improper modeling of particle size. When an experiment is conducted in the laboratory or in a field environment, the soil particle size is correct but the stresses and strains can not be accurately duplicated. Centrifuge testing permits correct modeling of the stresses and strains through the increased gravity field. However, models are constructed with small particle size material to compensate for the scaling effects that occur in the increased gravity environment. Therefore, the particle size is incorrect and the relationships such as interlocking, etc. are lost. A second disadvantage involves the replication of in situ soil conditions and the in situ loading history. This is typically not a problem in applications such as verification of theories, parametric studies, verification of numerical analysis, or study of soil response phenomena. However, it is a problem if the objective of the test is to realistically model an existing facility and judge it's response to external stimuli such as a dam shaken by an earthquake. It will not be possible to build a centrifuge model and incorporate the soils in situ conditions and loading history. Modeling and interpretation problems arise if the stress-strain behavior of a material is strain-rate dependent. For true similitude, the time scales would need to be the same in the model and prototype.

3.3.3 Empirical Procedures

Because of difficulties in analytically or physically modeling soil conditions at liquefiable sites, the use of empirical methods has become widely adopted in routine engineering practice. Procedures for carrying out a liquefaction assessment using the empirical method are summarized in following sections. More detail on development of the methods is given by (Seed, 1983), National Research Council (NRC, 1985), NEHRP Recommended Provisions for the Development of Seismic Regulations for New Buildings (BSSC, 1991). The most recent information on empirical methods is found in the proceedings of the 1996 NCEER workshop on the subject, held at Salt Lake City, Utah (NCEER, 1997). Subsequent discussions on various methods reflect consensus achieved among the geotechnical engineering community during and consequent to that workshop.

3.3.4 Laboratory Cyclic Strength Testing

Ideally, the best cyclic test to evaluate response of soils to earthquake shaking would be one that correctly simulates the loading to which the soil would be subjected in situ. Cyclic simple shear tests may best reproduce the straining in a soil specimen caused by upwardly propagating earthquake waves. Various configurations of cyclic simple shear, cyclic triaxial, large-scale shake table, and cyclic torsional shear (on solid or hollow specimens) apparatuses have been employed to study liquefaction resistance. Elemental laboratory cyclic test techniques and their relative applicabilities are surveyed by Woods (1981) and Wood (1982).

Historically, the most common cyclic loading technique for investigating liquefaction resistance involves the performance of the cyclic triaxial test, as a consequence of such factors as availability of equipment and relative ease of preparing undisturbed specimens. This is in spite of wide recognition of the inability of the test to accurately represent field earthquake stresses and boundary conditions (Seed and Idriss, 1982). Figures 27 and 28 are a schematic drawing of the cyclic triaxial test apparatus and a sample recording of load, deformation, and pore pressure response, respectively. Cyclic strength curves such as are typically generated from cyclic triaxial data are shown in Figure 29. Instructions for performance of cyclic triaxial tests may be found in Engineer Manual 1110-2-1906 (Department of the Army, 1986).

Previous studies have demonstrated that cyclic triaxial strengths (in fact, strengths determined from any unidirectional loading test) are higher than those expected to produce equivalent effects in the field (Seed, 1976). Reduction factors were developed to adjust laboratory cyclic test strengths to estimate field liquefaction resistance (e.g., multiplication of cyclic triaxial strengths by factors ranging from 0.57 to 1 for soils where the lateral earth pressure coefficient, K_o, ranges from 0.4 to 1, respectively, described by Seed and Idriss, 1982). Estimation of field liquefaction resistance from laboratory cyclic test results may not be possible by universal application of simple factors; recent research has shown that the comparison between cyclic triaxial and cyclic simple shear strengths depends on gradation, density, and soil type (Koester, 1992). Furthermore, boundary conditions have been shown to cause water migration within the test specimens subjected to cyclic loading (Castro, 1969, Casagrande and Rendon, 1978), leading to unreliable results. Thus the use of cyclic load tests for evaluating seismically induced pore pressures in sandy soils in situ is very rare in the U.S.; laboratory cyclic tests are more often used to establish parametric effects on cyclic strength behavior.

3.4 Procedures for Empirical Evaluation of Liquefaction Susceptibility

3.4.1 Evaluation of Earthquake-Induced Cyclic Stress Ratios

This step consists of evaluating the equivalent uniform cyclic stress ratio (CSR_{eq}) induced by the design earthquake. CSR_{eq} is a measure of the intensity of earthquake-induced cyclic loading, normalized with respect to vertical effective stress. For relatively level ground conditions (surface slopes or grades of less than about 15 degrees), this can be done by either of two basic methods as follows:

3.4.1.1 Method 1. Simple, Empirical Evaluation Based on Prior Analyses

This is the most widely used method of evaluating CSR_{eq} for liquefaction studies for structural foundations. The first step is to evaluate the peak (maximum, transient) horizontal acceleration occurring at the surface of the site (the peak ground surface acceleration; a_{max}). This may differ significantly from the peak ground acceleration value selected from the seismological study, as local site conditions can significantly modify a_{max}. It should be noted that soft alluvial deposits may amplify levels of ground surface acceleration relative to the acceleration levels which might be expected if the site conditions consisted of either stiff, shallow soils or rock. Evaluation of a_{max} to account for local site conditions may either be done empirically, or may involve performing dynamic site response analyses.

Having developed an estimate of a_{max} at the ground surface, corresponding estimates of the maximum horizontal acceleration at various depths (at points of interest within potentially liquefiable soil deposits) can be developed as

$$a_{max,z} = (a_{max})\ (r_d) \tag{7}$$

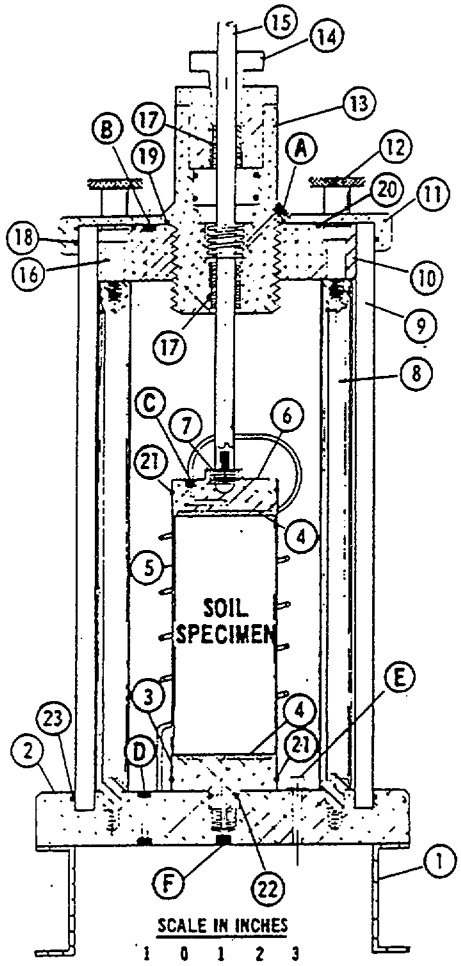

TRIAXIAL COMPRESSION CHAMBER

A. HYDROSTATIC SEAL AIR SUPPLY PORT
B. VENT
C. TOP DRAINAGE PORT
D. CHAMBER FLUID DRAIN
E. TRANSDUCER CABLE CONNECTOR
F. BOTTOM DRAINAGE PORT

PART NO.	NAME	MATERIAL	QUANTITY
1	CHAMBER FOOT	ALUMINUM CHANNEL	2
2	CHAMBER BASE	ALUMINUM PLATE	1
3	SPECIMEN BASE	ALUMINUM	1
4	POROUS PLATE	STAINLESS STEEL	2
5	SPECIMEN MEMBRANE	RUBBER	1
6	SPECIMEN CAP	ALUMINUM	1
7	SPECIMEN CAP CONNECTOR	BRASS	1
8	BEARING SUPPORT ROD	STAINLESS STEEL	2
9	CYLINDER	CLEAR ACRYLIC	1
10	CHAMBER CAP	ALUMINUM	1
11	CYLINDER SEALING RING	ALUMINUM	1
12	LOCKING KNOBS	STEEL	3
13	AIR BEARING ASSEMBLY	ALUMINUM	1
14	PISTON LOCK	BRASS	1
15	LOADING PISTON	STAINLESS STEEL	1
16	SHOULDER SCREW	STEEL	2
17	BALL BUSHING	STAINLESS STEEL	2
18	O-RING	RUBBER	1
19	O-RING	RUBBER	1
20	O-RING	RUBBER	1
21	O-RING	RUBBER	2
22	O-RING	RUBBER	1
23	O-RING	RUBBER	1

Figure 27. Schematic of cyclic triaxial test equipment (Department of the Army, 1986)

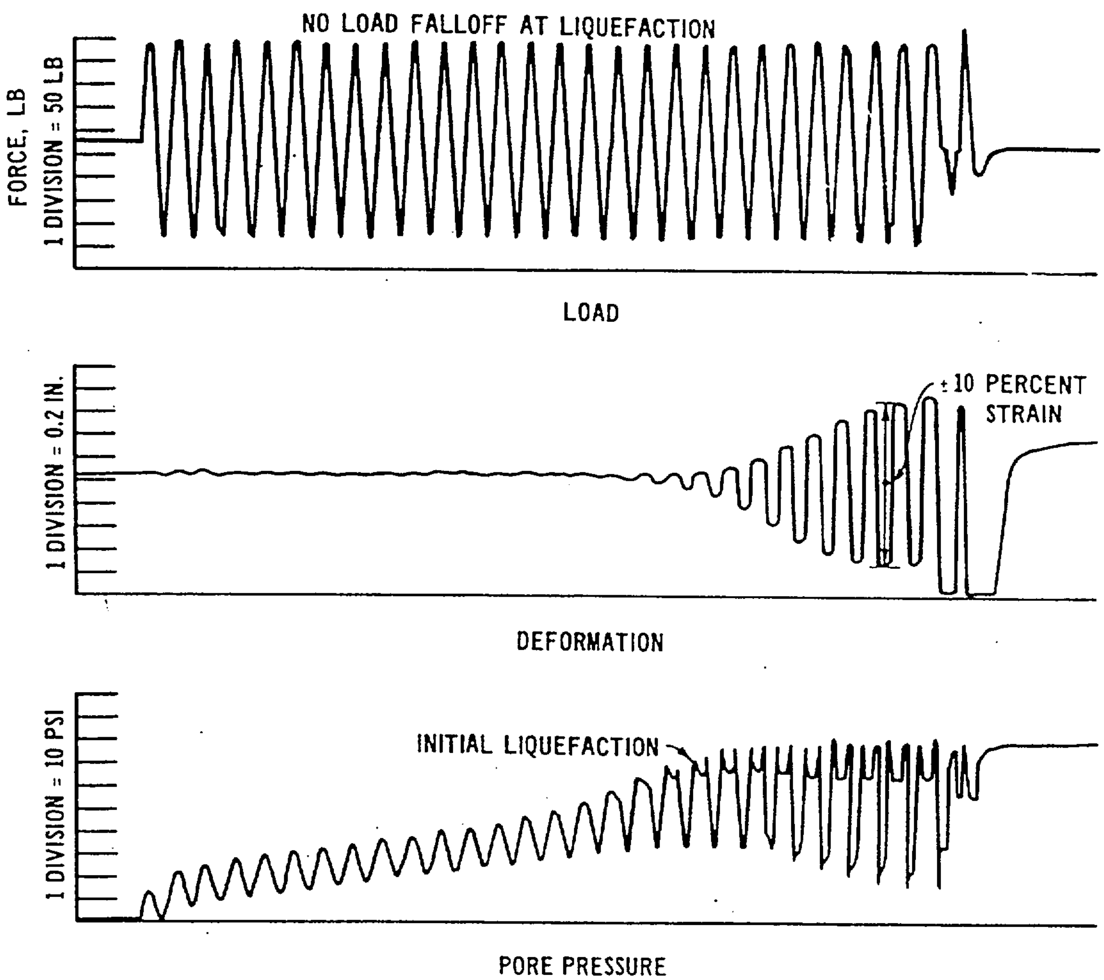

Figure 28. Typical analog recordings of load, deformation, and pore pressures during a cyclic triaxial test (Department of the Army, 1986)

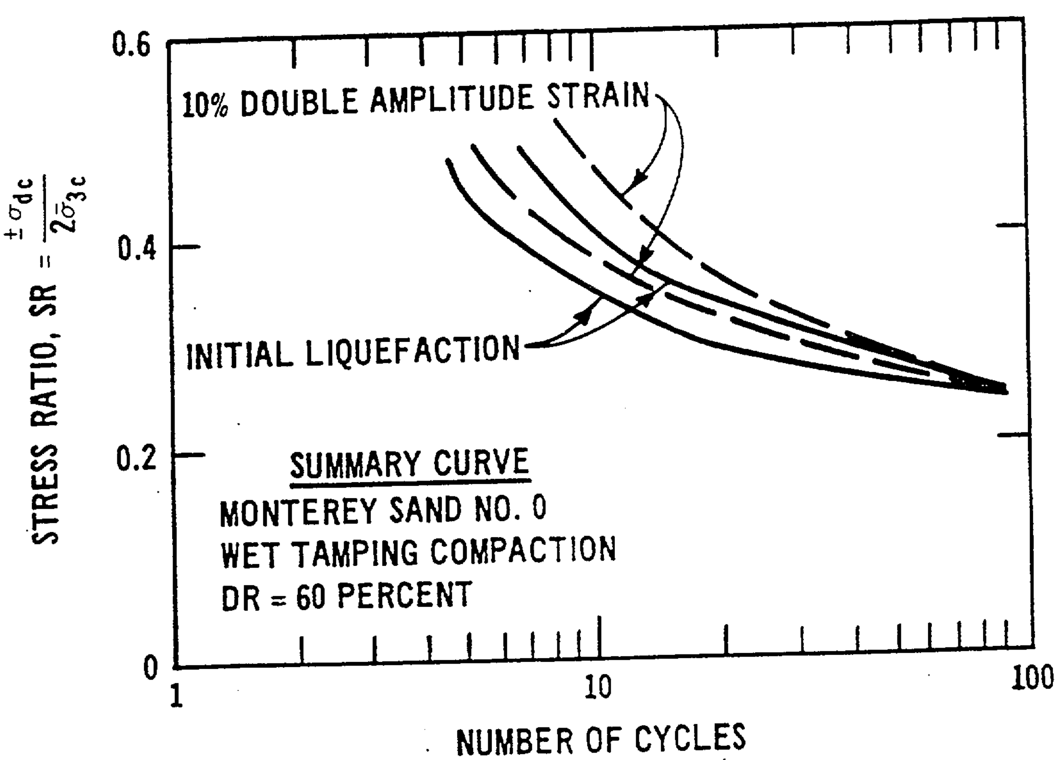

Figure 29. Cyclic triaxial strength curves for Monterey No. 0 sand (Department of the Army, 1986).

where

a_{max} = Peak ground surface acceleration [g]
$a_{max,z}$ = Peak horizontal acceleration at depth = z
r_d = Empirical reduction factor from Figure 30

The results of numerous response analyses were summarized by Seed and Idriss (1971), and the results are presented in Figure 30 (NCEER, 1997), which shows the peak acceleration reduction factor (r_d) as a function of depth for analyses of level and nearly level sites. It should be noted that r_d is fairly well-defined to depths of up to about 40 feet, but is highly variable at greater depths (so that conservative selection of upper-bound or near upper-bound r_d values is recommended here). Similarly, the r_d values shown in Figure 30 are directly applicable to level sites with relatively horizontal subsurface soil layering. These r_d values should be applied with caution to significantly sloping sites and/or to sites with complex subsurface geometry: in such cases, it may be advisable to perform two-dimensional or even three-dimensional seismic response analyses to evaluate cyclic shear stresses directly, as described in Method 2 below.

Having developed estimates of the maximum horizontal acceleration at each point of interest, the equivalent uniform cyclic stress ratio (CSR_{eq}) at each point can then be taken as

$$CSR_{eq} = 0.65\left(\frac{a_{max,z}}{g}\right)\left(\frac{\sigma_o}{\sigma_o'}\right) \qquad (8)$$

where

σ_o = Total (vertical overburden stress at point of interest
σ_o' = Effective vertical overburden stress at point of interest
$a_{max,z}$ = Maximum horizontal acceleration at the point of interest
g = acceleration of gravity.

As computed by Eq. 10 above, CSR_{eq} is taken to be equal to 65 percent of the peak (transient, non-repeating) cyclic stress ratio at the point of interest. This is a consequence of analyses reported by Seed and Idriss (1971) that determined the average equivalent uniform shear stress to be about 65 percent of the maximum shear stress developed by a typical irregular stress history.

3.4.1.2 Method 2. Direct Calculation of $\tau_{hv,cyclic,max}$ or $a_{max,z}$ at Each Point of Interest

A second approach is to directly calculate the peak (transient, non-repeating) cyclic shear stress acting on a horizontal plane ($\tau_{hv,cyclic,max}$) or the peak (transient, non-repeating) horizontal acceleration ($a_{max,z}$) at each point of interest. This is accomplished through a dynamic site response analyses. If $a_{max,z}$ values are calculated, then CSR_{eq} can be derived using Eq. 10. If values of $\tau_{hv,cyclic,max}$ are calculated at each point of interest, then the associated values of CSR_{eq} can be calculated as

$$CSR_{eq} = 0.65\left(\frac{\tau_{hv,cyclic,max}}{\sigma_o'}\right) \qquad (9)$$

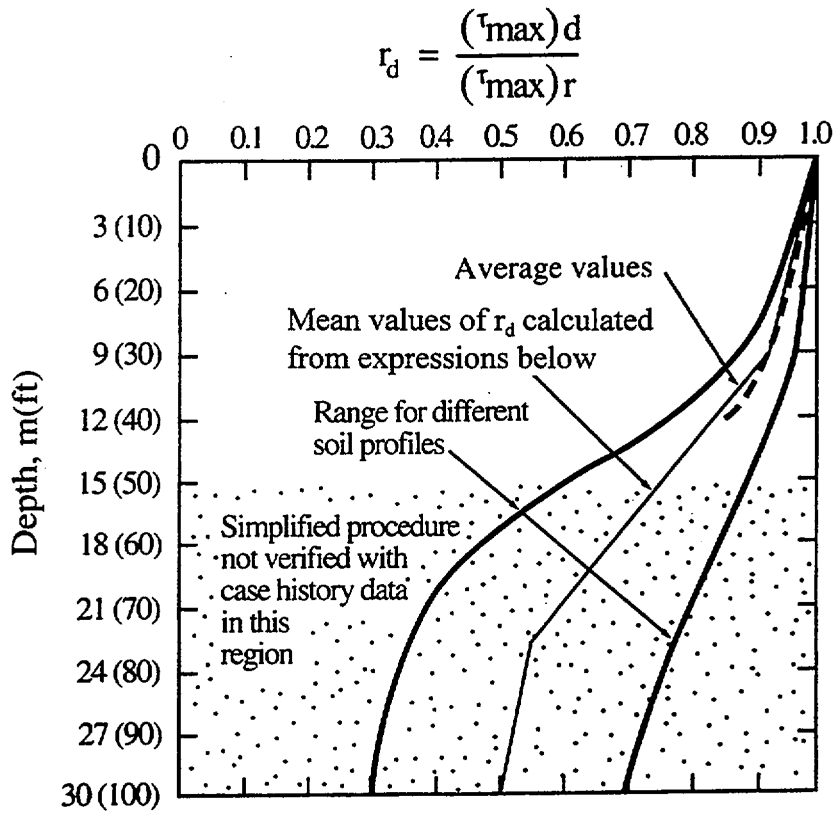

$r_d = 1.0 - 0.00765z$ for $z \leq 9.15$ m
$r_d = 1.174 - 0.0267z$ for $9.15 < z \leq 23$ m
$r_d = 0.744 - 0.008z$ for $23 < z \leq 30$ m
$r_d = 0.50$ for $z > 30$ m

Figure 30. Variations of the parameter r_d with depth (NCEER, 1997)

where

$\tau_{hv,cyclic,max}$ = the peak horizontal cyclic shear stress at the point of interest, and
σ_o' = the effective (vertical) overburden stress at the point of interest.

It should be noted that for non-level ground conditions (e.g., slopes, embankments, dams, etc.) it is generally necessary to incorporate consideration of the overall problem geometry (and stratigraphy) in evaluation of either $\tau_{hv,cyclic,max}$ or $a_{max,z}$ at each point within the slope or the underlying foundation soils. This often requires the use of either two-dimensional or three-dimensional finite element analyses of dynamic response, as described by Marcuson, Hynes, and Franklin (1990).

3.4.2 Evaluation of In Situ Liquefaction Resistance

Having calculated the equivalent uniform cyclic shear stress ratios resulting from the earthquake loading at each point of interest, the next step is to evaluate the resistance of the in situ materials to cyclic pore pressure generation or accumulation of cyclic shear strain. This constitutes evaluation of the resistance to "triggering" or initiation of liquefaction, defined as in Section 2.1. The evaluation of in situ liquefaction resistance of soils not containing significant amounts of gravel can be accomplished using either Standard Penetration Test (SPT) or Cone Penetration Test (CPT) penetration resistance data; Becker Penetration Tests (BPTs) may be used to determine penetration resistance analogous to SPT or CPT data in gravelly soils. The following discussions emphasize the SPT-based approach, due to its extensive worldwide data base and practice; Section 3.1.2.2 detailed liquefaction potential evaluation using the CPT.

Figure 18 shows a recommended relationship between corrected SPT penetration resistance $(N_1)_{60}$ and the equivalent uniform cyclic stress ratio required to "trigger" liquefaction during an earthquake with a duration (or number of loading cycles) representative of a typical earthquake with a magnitude of M = 7-1/2 (NCEER, 1997, based on the data of Seed et al., 1985). In this relationship, cyclic resistance ratio (CRR) is defined as the ratio of the cyclic shear stress acting on a horizontal plane ($\tau_{hv,cyclic}$) to the initial (pre-earthquake) effective vertical or overburden stress (σ_o') for the boundary lines in the figure. The relationships presented in Figure 18: (a) directly account for the influence of fines content on the relationship between penetration resistance and liquefaction resistance, and (b) are based on a corrected or "standardized" SPT penetration resistance. Figure 18 summarizes a very large data base of field (case history) performance, and presents the most reliable basis currently available for assessment of in situ liquefaction resistance based on SPT penetration resistance. The relationships described earlier in this report for CPT assessment of liquefaction resistance are also considered reliable in current practice. Additional field data from seismic events occurring between 1984 and 1991 have upheld the relationships presented in this figure.

3.4.2.1 "Standardized" SPT criteria

The following commentary and guidance is given with respect to the standard penetration test in recognition of the variety of equipment and procedures used to conduct standard penetration tests, and because the measured blow count, N_m, is sensitive to equipment and operational procedures. Special attention must be given to the determination of normalized blow count, $(N_1)_{60}$, used in Figure 18. When developing the empirical relation between blow count and liquefaction resistance, it was recognized that the blow count from the SPT is influenced by factors such as the method of drilling, the type of hammer, the sampler design, and type of mechanism for lifting and dropping the hammer. The magnitude of these variations are shown by the data in Table 4. The following procedures and specifications for SPT tests,

Country		Hammer Type	Hammer Release	ER: Energy Ratio or Estimated Rod Energy	Correction Factor for 60% Rod Energy
I.	JAPAN**				
	A.	Donut	Free-Fall	78%	78/60 = 1.30
*	B.	Donut	Rope & Pulley with special throw release	67% (55%)**	67/60 = 1.12 (55/60 = <u>0.89</u>)**
II.	USA				
*	A.	Safety	Rope & Pulley	60%	60/60 = 1.00
	B.	Donut	Rope & Pulley	45%	45/60 = 0.75
	C.	Pilcon-type "free-fall"	Mechanical	70%	70/60 = 1.16
III.	ARGENTINA				
*	A.	Donut	Rope & Pulley	45%	45/60 = 0.75
IV.	CHINA				
*	A.	Donut	Free-Fall***	60%	60/60 = 1.00
	B.	Donut	Rope & Pulley	50%	50/60 = 0.83

* Most prevalent method in this country today.

** Japanese SPT results require additional corrections for borehole diameter and blow frequency effects, and the <u>cumulative</u> effect of both hammer type and hammer release along with these additional corrections is equivalent to an overall "effective energy ratio" of <u>ER 55%</u>.

*** Plem-Type hammers develop an energy ratio of about 60%.

Table 4. Summary of energy ratios (ER) for some common SPT procedures (after Seed, et al., 1984, 1986)

excerpted from Seed, et al. (1985), were developed in order to reduce variability in N_m for liquefaction investigations:

(a) The impact should be delivered by a rope and drum system with two turns of the a rope around the rotating drum (cathead winch) to lift a hammer weighing 140 lb; ideally, a drive system should be used for which the energy ratio (ER) has been measured or can be reliably estimated.

(b) The hole should be approximately 4 in.. (100 mm) diameter and drilled with a tricone or baffled drag bit that produces upward deflection of the drilling fluid to prevent erosion of soil below the cutting edge of the bit. Bentonitic drilling mud should be used for borehole stability, and special care is required to assure that the drilling fluid level in the hole never drops below the ground water table.

(c) A or AW rod should be used in holes less than 50 ft deep. N or NW rod should be used in deeper holes.

(d) The split spoon sampling tube should be equipped with liners or otherwise have a constant internal diameter of 1-3/8 in.

(e) Application of blows should be at a rate of 30 to 40 blows per minute. (Some engineers suggest that a slower rate of 20 to 30 blows per minute is easier to achieve and control and gives comparable results.) The blow count, N_m, is determined by counting the blows required to drive the penetrometer the last 12 in. of an 18-in. depth interval, i.e., from 6-in. to 18 in. below the bottom of the hole.

The consensus of current practice toward standardized procedures and adjustments for SPT blowcounts measured in evaluations of liquefaction resistance is reflected in the following expression for calculation of $(N_1)_{60}$ (NCEER, 1997).

$$(N_1)_{60} = N C_N C_E C_B C_R C_S \tag{10}$$

Table 5 (NCEER 1997, after Skempton, 1986) provides values for the correction factors in this expression, which are described in more detail in the following sections.

3.4.2.2 Corrections to SPT N_m Values to Yield $(N_1)_{60}$ Values

3.4.2.2.1 Corrections for Hammer Type and Release System

Blowcounts (N-values) obtained using hammer-types and/or hammer release mechanisms other than those listed in Table 4 must be corrected to generate "standardized" blowcounts (N_{60}-values) as:

$$N_{60} = N_m \left(\frac{ER}{60\%} \right) \tag{11}$$

where *ER* is an energy ratio, expressed as the percent of theoretical maximum free fall energy delivered to the top of the drill stem by the hammer system actually used. This can be determined directly, using a dynamic energy measurement system, or can be estimated (for the most common alternate systems in

Factor	Equipment Variable	Term	Correction
Overburden Pressure		C_N	$(P_a/\sigma'_{vo})^{0.5}$ $C_N \leq 2$
Energy ratio	Donut Hammer Safety Hammer Automatic-Trip Donut-Type Hammer	C_E	0.5 to 1.0 0.7 to 1.2 0.8 to 1.3
Borehole diameter	65 mm to 115 mm 150 mm 200 mm	C_B	1.0 1.05 1.15
Rod length	3 m to 4 m 4 m to 6 m 6m to 10 m 10 to 30 m >30 m	C_R	0.75 0.85 0.95 1.0 <1.0
Sampling method	Standard sampler Sampler without liners	C_S	1.0 1.1 to 1.3

Table 5. Corrections to SPT N-values (NCEER, 1997, modified from Skempton, 1986)

widespread use) based on correlations and data summarized by Seed et al. (1985) and presented in Table 4. For most applications, the choice is simplified by using the values available in Table 5. It should also be noted that automatic trip hammers are becoming more commonly used in practice and are generally less variable with regard to energy delivery.

3.4.2.2.2 Correction for Sampler Configuration

An additional correction, increasing the measured N-value by between 10 percent and 30 percent, can be necessitated by the use of an ASTM standard sampler configured to accommodate an internal sample liner (tube), but with the liner omitted, so that the inside diameter of the sampler is larger than the 1.375 in. specified by ASTM. The use of such an unlined sampler is actually by far the most common practice in the U.S., and it causes a reduction in frictional drag inside the sampler, lowering the measured blowcounts by about 10 percent to 30 percent (increasing percentage change with increased blowcount). Accordingly, when an unlined sampler with space for a liner is used, the resulting blowcounts must be corrected using the C_S factor given in Table 5. It is further recommended that C_S be varied from 1.1 to 1.25 for $N \leq 5$ to $N > 30$ blows/ft.

3.4.2.2.3 Correction for Short Rod Lengths

It is recommended to use the correction factors C_R given in Table 5 to adjust N-values measured at the given depth ranges for dynamic inefficiencies inherent in short rod driving systems.

3.4.2.2.4 Correction for Overburden Stresses

Penetration resistance, once adjusted for energy input as described above, must then be further corrected to account for effective overburden stress to develop the final, standardized and corrected penetration resistance at a hypothetical overburden stress of $\sigma_o' = 1$ ton/ft^2 (1 kg/cm^2). Dr. H. B. Seed and his colleagues have long recommended a pair of relationships between σ_o' and C_N: one for sandy soils at $D_R \approx$ 40 percent to 60 percent and one for $D_R \approx$ 60 percent to 80 percent, as shown in Figure 31. An alternate relationship, proposed by Liao and Whitman (1985), is

$$C_N = \frac{1}{\sqrt{\sigma_o'}} \tag{12}$$

where σ_o' is expressed in units of [tons/ft^2]. The value given in Table 5 reflects this relationship, adapted to account for other units of pressure, and constrains the value to be not greater than 2.

This provides a relationship intermediate between the two suggested relationships shown in Figure 31, and so eliminates the need to estimate D_R. If D_R must be estimated, then for in situ, clean sandy soils not placed recently, the approximate relationships presented in Figure 32 (Torrey, Dunbar, and Peterson, 1988) can be used as a guide. This relationship should not be used for freshly placed soils, or for coarser materials than fine to medium sands. (Additional proposed relationships between penetration resistance and relative density are presented in Figure 32). It should also be noted that these overburden corrections are applicable only to silty and sandy soils; the overburden corrections for coarser gravelly soils differ significantly.

It should be noted in Figure 18 that varying levels of CRR vs. $(N_1)_{60}$, are shown for fines contents of ≤ 5 percent, 15 percent, and ≥ 35 percent. In sandy soils, increased fines contents results in an increase

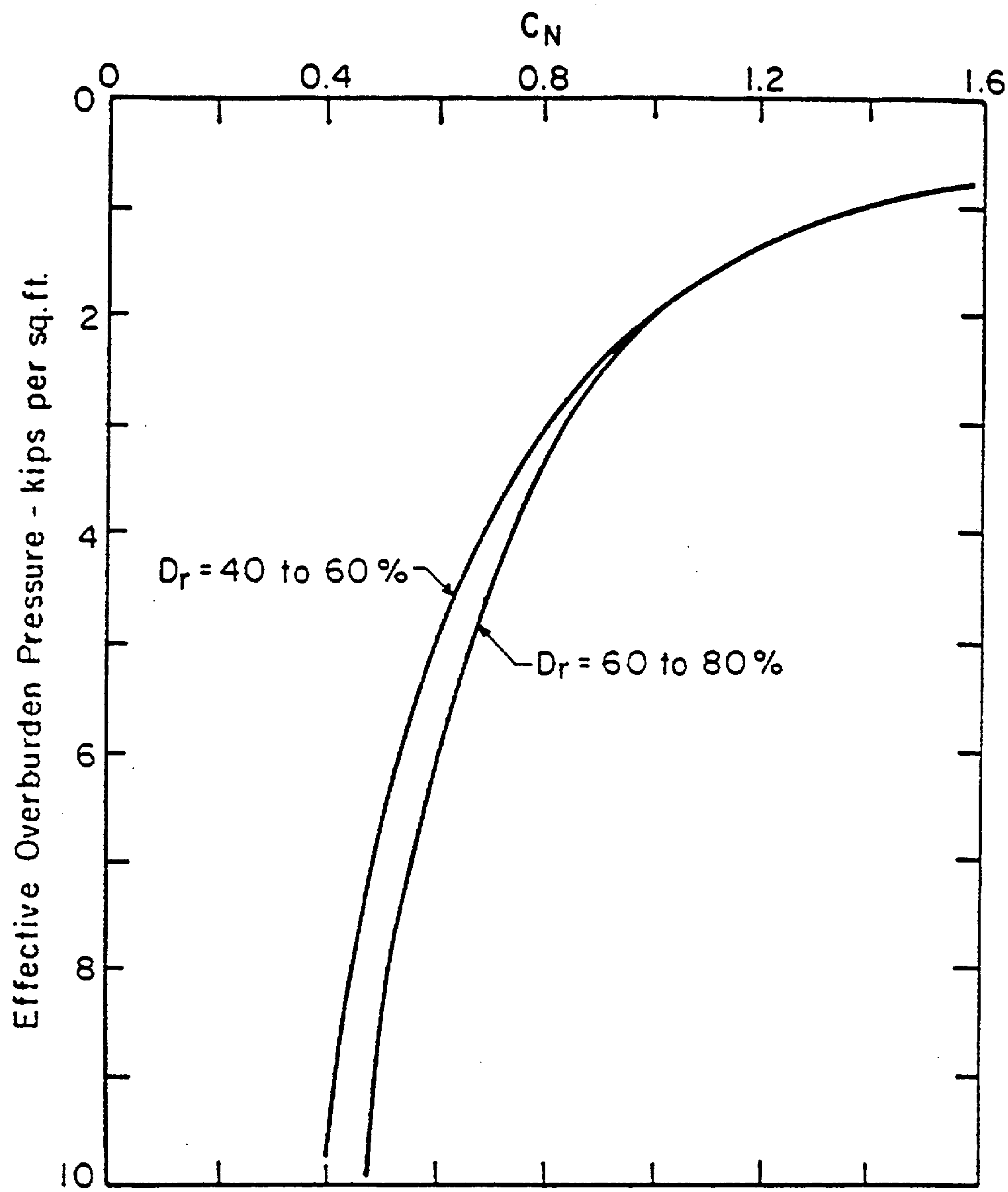

Figure 31. Correlation between correction factor C_N and effective overburden pressure (based on data from Marcuson and Bieganousky, 1977)

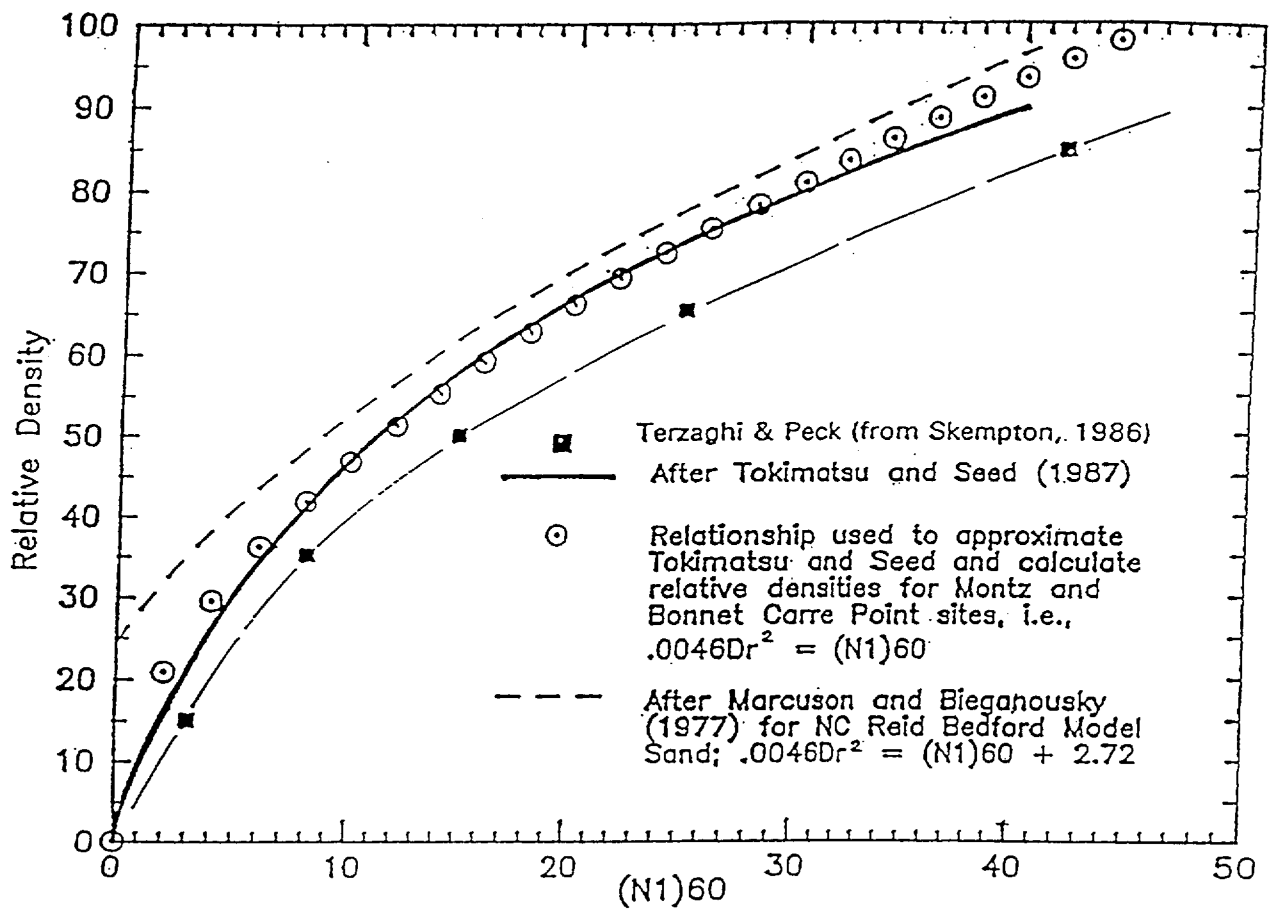

Figure 32. Several proposed relationships between SPT penetration resistance and relative density (Torrey, Dunbar, and Peterson, 1988)

in the ratio of liquefaction resistance (or CRR) to penetration resistance (or $(N_1)_{60}$). It was recognized by participants in the NCEER (1997) workshop that the reason for this increase is unclear; it is not well understood whether it results from greater liquefaction resistance or lesser penetration resistance consequential to increased compressibility and reduced permeability of soils containing fines. The consensus of workshop participants was that any correction for fines content should be related to penetration resistance *and* fines content, and the following relationship was produced to facilitate spreadsheets and other automated computational schemes in the determination of the equivalent clean sand corrected blowcount, $(N_1)_{60cs}$:

$$(N_1)_{60cs} = \alpha + \beta\ (N_1)_{60} \tag{13}$$

where coefficients α and β are given by the following equations:

$\alpha = 0$ for FC $\leq$ 5 percent (14a)
$\alpha = \exp\{1.76 - (190/FC^2)]$ for FC < FC < 35 percent (14b)
$\alpha = 5.0$ for FC $\geq$ 35 percent (14c)

$\beta = 1.0$ for FC $\leq$ 5 percent (15a)
$\beta = [0.99 + (FC^{1.5}/1000)]$ for FC < FC < 35 percent (15b)
$\beta = 1.2$ for FC $\geq$ 35 percent (15c)

and where FC is the fines content measured from laboratory gradation tests on recovered soil samples.

3.4.3 Correction for Earthquake Magnitudes other than M = 7-1/2

The relationships between $(N_1)_{60}$ and the equivalent uniform cyclic stress ratio necessary to cause liquefaction (CRR) in Figure 18 can be extended to earthquakes of magnitude other than M ≈ 7-1/2 by noting that earthquakes of larger magnitude tend to produce a longer duration of shaking and thus more cycles of loading. Seed, Arango, and Chan (1975) and Seed and Idriss (1982) introduced procedures for converting a typical, irregular earthquake-induced cyclic load history to an equivalent number of uniform loading cycles with an amplitude equal to 65 percent of the peak or maximum amplitude of the irregular load history. A number of relationships have been developed to adjust liquefaction resistance for magnitudes other than M ≈ 7-1/2; the NCEER (1997) recommended range for a magnitude scaling factor, MSF, is depicted in Figure 33. The hashed section for earthquakes with magnitudes less than 7.5 allows designers to choose levels of conservatism appropriate to their application. The curve labeled "Idriss" is recommended for earthquakes of magnitudes larger than 7.5. In any event, for earthquakes of M ≠ 7-1/2, the value of CRR determined from Figure 18 can be corrected as follows:

$$CRR_{1(M=M)} = CRR_{1(M=7-1/2)} \cdot MSF \tag{16}$$

It should be noted that this scaling of CRR, for magnitude (or duration) effects using MSF, is equivalent to a vertical shifting of the relationships shown in Figure 18. The "limiting" values of $(N_1)_{60}$ shown in Figure 18 (e.g., $(N_1)_{60}$ ≈ 30 blows/ft for clean sands with less than 5 percent fines) are penetration resistances corresponding to sufficiently high densities (or relative densities) that the soils in question are strongly dilative and thus not vulnerable to liquefaction. These cut-off values are not magnitude-dependent (or duration-dependent). Similarly, the factor of safety with respect to liquefaction (FS_l) formulated in terms of CRR and CSR will have no meaning to the right of the relationships shown in

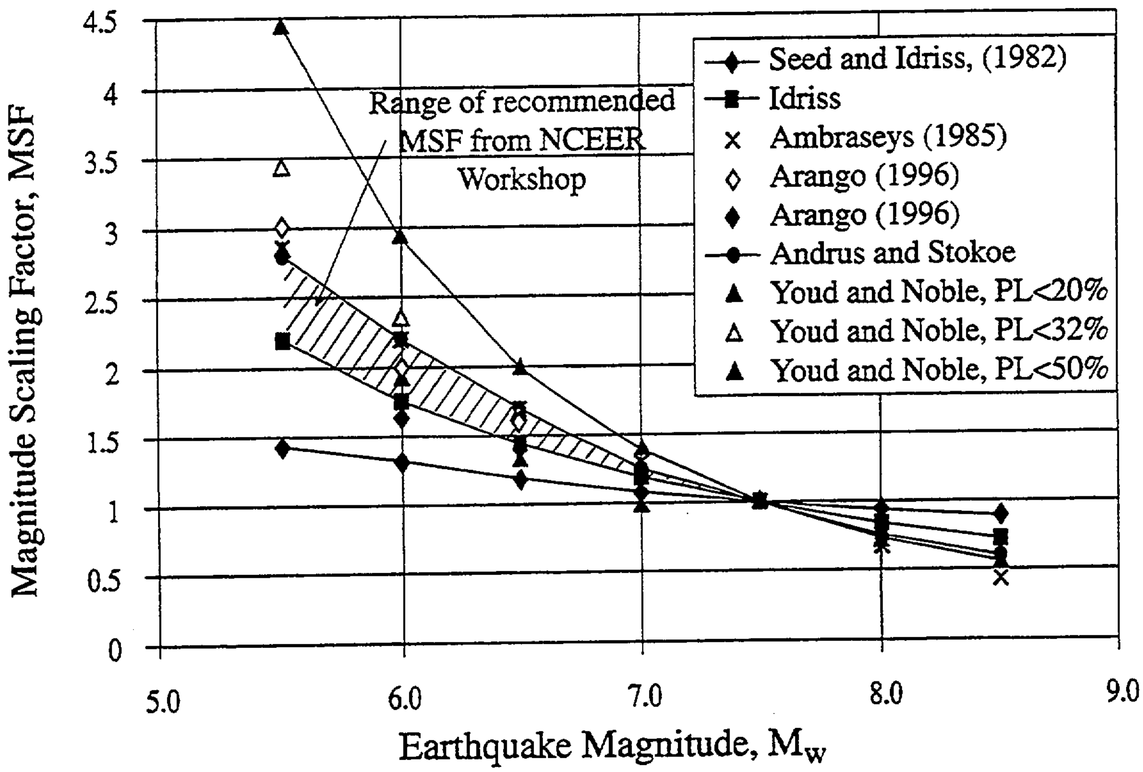

M < 7.5

Lower bound, Idriss, MSF = $10^{2.24}/M^{2.56}$

Upper bound, Andrus and Stokoe (NCEER, 1997), MSF = $(M_w/7.5)^{-3.3}$

M > 7.5

Idriss, MSF = $10^{2.24}/M^{2.56}$

Figure 33. Relationship between K_M and magnitude (NCEER, 1997)

Figure 18: any meaningful discussion of uncertainty or factor of safety at these high $(N_1)_{60}$-values should more correctly revolve around the uncertainties in (a) determining the position of these cut-offs, and (b) uncertainties in evaluation of in situ $(N_1)_{60}$ for the soil deposits in question.

3.4.4 Correction of CRR for Effective Overburden Stress

Virtually all of the field (case history) data represented in Figure 18 (and in similar collections of data for other magnitude ranges) are for level ground conditions and relatively shallow soils with relatively small initial effective overburden stresses. Laboratory measurements typically indicate that for a given soil, consistency (relative density for sands and gravels) and stress history, there is a non-linear relationship between liquefaction resistance and confining stress (Seed and Idriss, 1981; Seed, 1983; Vaid and Thomas, 1995; Hynes, 1988; Harder, 1988; Seed and Harder, 1990; Pillai and Byrne, 1994; and NCEER, 1997). Consequently, if liquefaction resistance, either from laboratory measurements performed at a confining stress of 1 atm or estimated from correlations to in situ measurements such as Standard Penetration Tests (SPT), are linearly extrapolated to higher effective confining stress levels, the calculated liquefaction resistance may be too high. The effect of confining stress on liquefaction resistance is further complicated by soil compressibility and stress history.

The state-of-the-practice approach to account for the non-linear relationship between liquefaction resistance and vertical effective stress is to use published charts derived from existing laboratory data on similar materials or to determine a site specific relationship with a comprehensive laboratory testing program. For a given soil at a given consistency and stress history, the CRR generally decreases with increasing vertical effective stress. This decrease is described by the factor K_σ, defined as the ratio of CRR for a given σ_v' to the CRR at a vertical effective stress of 1 atm, CRR_1 (compared at the same relative density). Values of CRR from Figure 18 can be used for in situ conditions where $\sigma_o' \leq 1$ ton/ft^2 (1 kg/cm^2), but must be corrected for conditions with initial effective overburden stresses greater than 1 ton/ft^2 as:

$$CRR_{1(\sigma_o' = \sigma_o')} = CRR_{1(\sigma_o' = 1\ tsf)} \cdot K_\sigma \tag{17}$$

Hynes and Olsen (1998) determined from a study of the available lab data base that method of deposition, aging, stress history and density strongly influence K_σ. These effects are emphasized at low confining stresses, such as 1 atm, and are de-emphasized as confining stresses increase, and ultimately converge at the stress focus. Within the stress range of interest for most critical structures, typically less than 10 atm, K_σ is not strongly influenced by soil type. Specimens pluviated in the laboratory may represent recently deposited materials such as dredged and liquefied materials. Hynes and Olsen (1998) concluded, however, that for water-laid foundation deposits (typical for dams and many facilities on alluvial ground), high quality undisturbed specimens are necessary to determine field-relevant values of K_σ. Figure 34 presents a series of relationships for K_σ; the "clean sand" curve may be used for most applications.

3.4.5 Correction of CRR for Initial Static Shear Stress

All of the above corrections have been based on level ground conditions, that is, conditions in which no pre-earthquake static shear stresses act on horizontal planes within the soil. Generation of pore pressures and accumulation of shear strains under cyclic loading can be significantly affected by the presence of a static (non-cyclic) shear stress, and this too must be accounted for in analysis of liquefaction resistance within dams and embankments. Early relationships suggested to account for this suggested that the presence of initial static shear stress on a horizontal plane was strongly beneficial, and that it significantly increased the soil's resistance to liquefaction. This remains true for relatively dense soils, or soils which

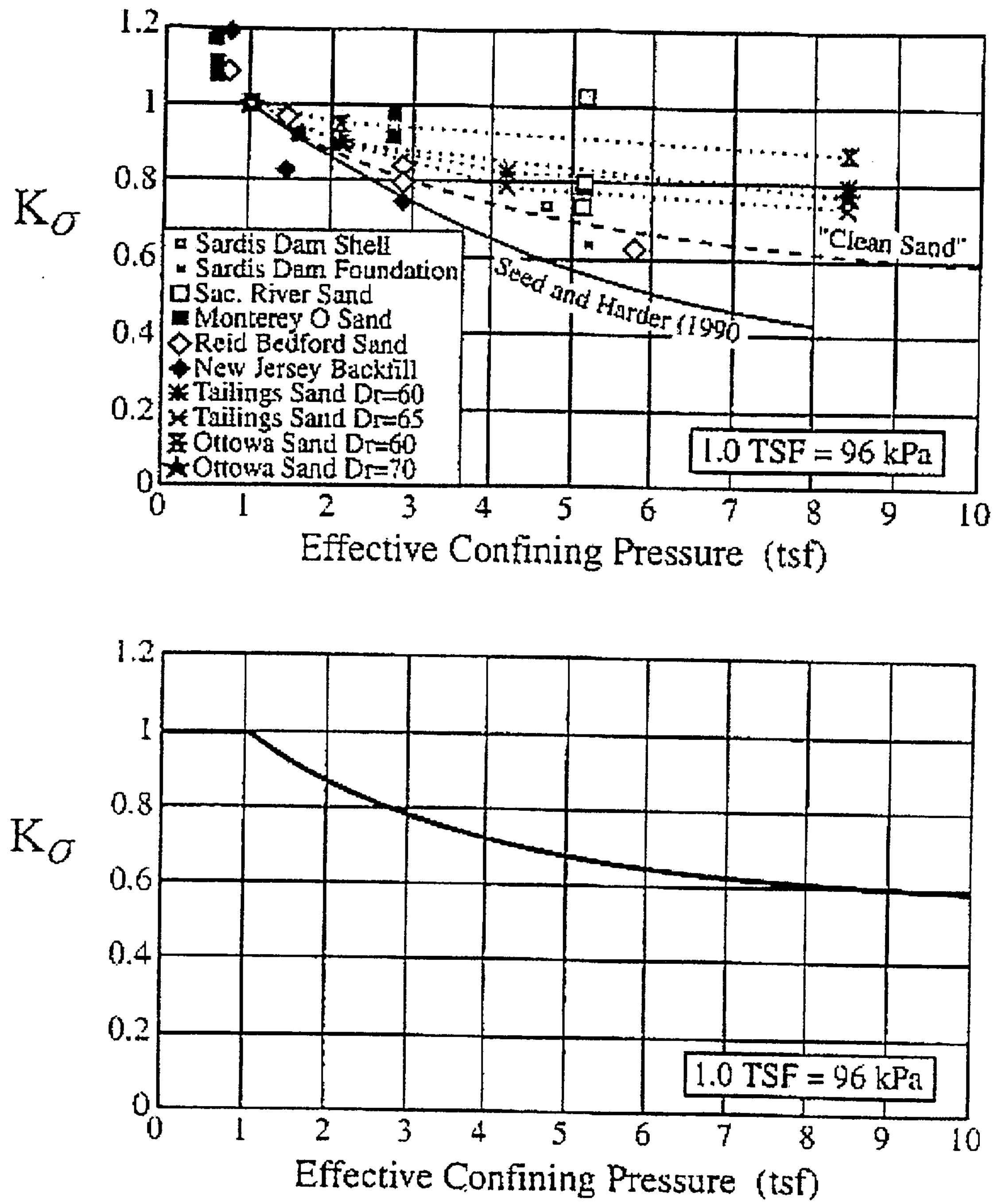

$K_\sigma = -(1.106E\text{-}9 * \sigma'^{3}_{vo}) + (2.552E\text{-}6 * \sigma'^{2}_{vo}) - (2.053E\text{-}3 * \sigma'_{vo}) + 1.1893$

NOTE: this equation is for σ'_{vo} in kPa

Figure 34. K_σ recommendations from NCEER (1997) workshop

would tend to dilate under uni-directional shearing. Studies have shown, however, have shown that for very loose soils (soils which are less dilative or more contractive under uni-directional shearing), the presence of initial static shear stress can actually decrease the resistance of the soil to the initiation of liquefaction (e.g., Castro, 1969; Seed and Harder, 1990). The original method proposed by Seed (1983) to account for the effects of initial static shear stresses employed the following equation:

$$CRR_{1(\alpha=\alpha)} = CRR_{1(\alpha=0)} \cdot K_\alpha \tag{18}$$

where α is defined as the ratio of initial static shear stress on a horizontal plane to the initial effective overburden stress as $\alpha = \tau_{hv}/\sigma_o')$. Relationships between α and K_α are presented in Figure 35 (Seed and Harder, 1990), based on data available at this time. These are based on data for conditions where $\sigma_o' \leq$ 3 tons/ft^2 (3 kg/cm^2), and are appropriate only for these conditions. At higher initial effective overburden stresses, soils will be less dilative or more contractive, and K_α values will decrease.

3.5 Energy Approach

An empirical procedure has been recently developed that delineates field occurrence data for liquefaction based on consideration of the seismic energy to which sites were subjected. The methods described above consider the maximum cyclic stress ratio, which has been shown to be a function of peak acceleration, and a later correction is necessary to adjust liquefaction resistance for various earthquake magnitudes. Kayen (1993) correlated liquefaction occurrence data with seismic energy, characterized by the Arias intensity associated with site motions where recordings were available or could be reliably estimated. Arias intensity is defined by the total energy of the undamped response spectrum of a motion, that is, the energy absorbed by a series of single-degree-of-freedom oscillators when excited by an earthquake's motion history. This total energy may be calculated from the following expression:

$$I_h = I_{xx} + I_{yy} = \frac{\pi}{2g}\int_0^t \cdot a_x^2(t)\,dt + \frac{\pi}{2g}\int_0^t \cdot a_y^2(t)\,dt \tag{19}$$

where I_h is total Arias intensity, I_{xx} and I_{yy} are components of Arias intensity in orthogonal horizontal directions, respectively, $a_x(t)$ and $a_y(t)$ are acceleration histories from accelerograms in the x and y directions, and g is the acceleration of gravity. Dimensional units of Arias intensity are length divided by time, or velocity. Figure 36 is a plot of Arias intensity versus $(N_1)_{60}$ developed by Kayen (1993) after adjusting for depths of the data set's deposits and incorporating the corrections for fines contents used to develop Figure 18. This method has the advantage that corrections to liquefaction resistance for earthquake magnitude are unnecessary, and ties the evaluation of liquefaction potential to a measure of the entire motion history. This procedure has not yet been sufficiently verified for immediate use in practice, but many feel that it is fundamentally attractive and will see more use in the future as additional ground motion records become available.

3.6 Evaluation of Factor of Safety and Residual Excess Pore Pressure Generation

Comparing the calculated equivalent, uniform, earthquake-induced cyclic stress ratios (CSR_{eq}) with the uniform cyclic stress ratios necessary to fully trigger liquefaction (CRR), the factor of safety against

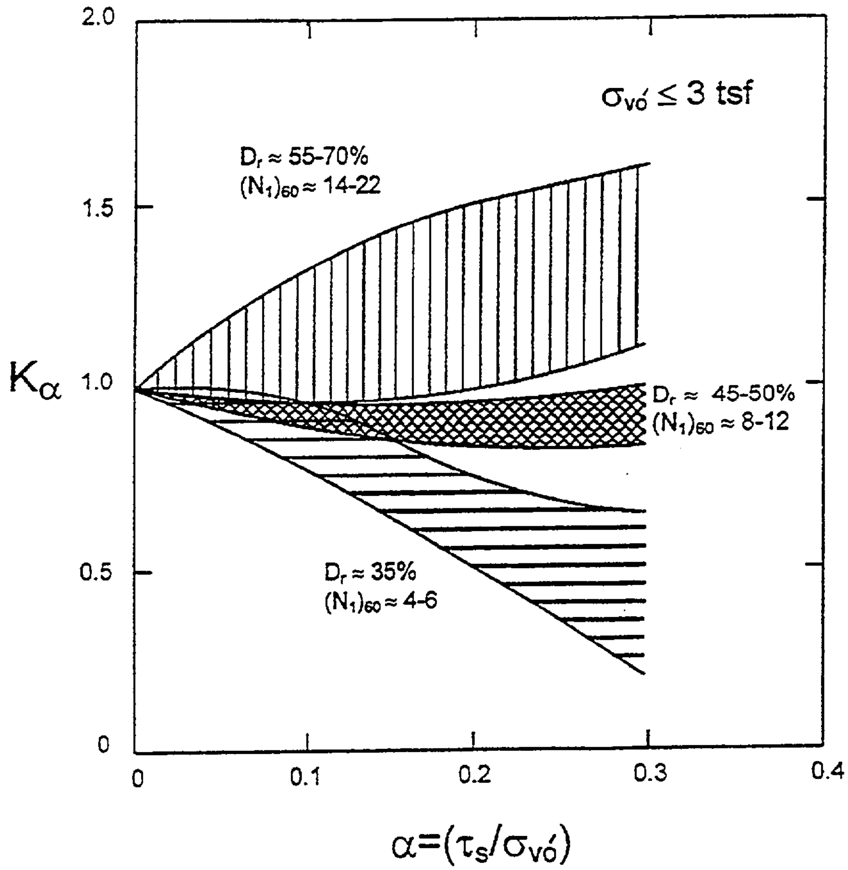

Figure 35. K_α recommendations from NCEER (1997) workshop

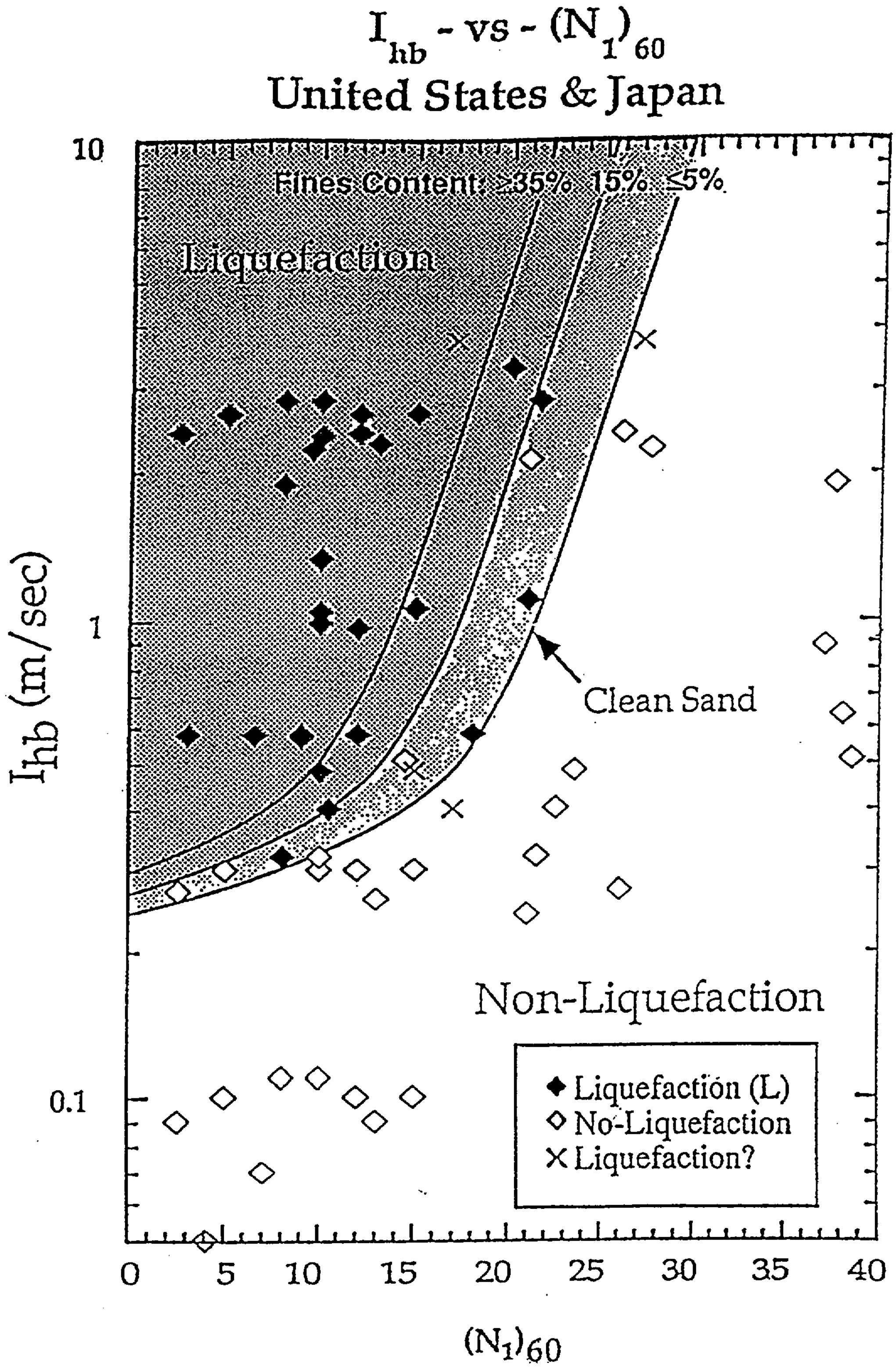

Figure 36. Observed liquefaction data plotted as a function of fines content and Arias Intensity I_{hb} (Kayen and Mitchell, 1997, after Kayen, 1993, reprinted with permission from ASCE)

"triggering" of liquefaction can be calculated as shown in Eq. 5. This factor of safety, FS_l, can be interpreted in a number of ways. Figure 37 (Marcuson, Hynes, and Franklin, 1990) shows a plot of residual excess pore pressure ratio ($r_u = \Delta u_e/\sigma_o'$) based on laboratory test data for level ground conditions ($\alpha = 0$) as summarized by Tokimatsu and Yoshimi (1983) for sandy soils, and Evans (1987) and Hynes (1988) for gravelly soils. For non-level ground conditions ($\alpha \neq 0$), the effective vertical stress need not necessarily be fully balanced by pore pressure increases to initiate large deformations in the presence of combined cyclic and static shear stresses. Accordingly, when $\alpha \neq 0$, the residual excess pore pressure ratio is best defined as the ratio of cyclically-generated pore pressures (Δu_e) to the excess pore pressure necessary to initiate large deformations (Δu_{lim}) as

$$r_{u,\alpha} = \left(\frac{\Delta u_e}{\Delta u_{\lim}} \right) \tag{20}$$

Considerable judgment should be used in interpreting the ramifications of these levels of pore pressure generation. Nonetheless, it appears that a reliable analysis can be performed by considering that:

1. Soil elements with low factors of safety ($FS_l \leq 1.1$) would achieve conditions wherein soil liquefaction should be considered to have been "triggered," and undrained residual strengths (S_r) should be assigned to these zones for further stability and deformation analyses.

2. Soil elements with a high factor of safety ($FS_l \geq 1.4$) would suffer relatively minor cyclic pore pressure generation, and should be assigned some large fraction of their (drained) static strength for further stability and deformation analyses.

3. Soil elements with intermediate factors of safety ($FS_l \approx 1.1$ to 1.4) should be assigned strength values somewhere between (though in some cases including) the values appropriate to conditions 1 and 2 above. Whether the values assigned should be nearer to the initial static strength or to the residual undrained strength is a function of FS_l whether or not the soil is judged to be strongly contractive in unidirectional shearing (and thus potentially vulnerable to progressive failure), and levels of uncertainty involved in various steps of the analysis up to this point (for any specific case). When soils are strongly contractive (e.g., when residual undrained strengths are low relative to the initial static shear stresses acting to promote failure), then the possibility of progressive failure/deformation should be considered; it is prudent in such cases to assume mobilization of undrained residual strengths within the contractive soil units.

3.7 Example Calculations

3.7.1 Given

It is proposed to construct a 3-story reinforced concrete office building on a site near to a harbor. The approximately level site consists of 90 feet of fine to medium sands and silty sands (fines content varies randomly from about 5 percent to 30 percent), underlain by 75 ft of very stiff, overconsolidated silty clay. Bedrock occurs at a depth of about 165 ft. The groundwater table occurs at a depth of about 20 ft, and varies little with seasonal changes. Two borings with SPT have been performed at the site, and Figure 38 shows the resulting measured SPT N-values. SPT were performed using a safety hammer, with a mechanical trip-hammer release system. The SPT sampler was of constant 1.375-inch inside diameter (there was no space for a liner within the sampler barrel).

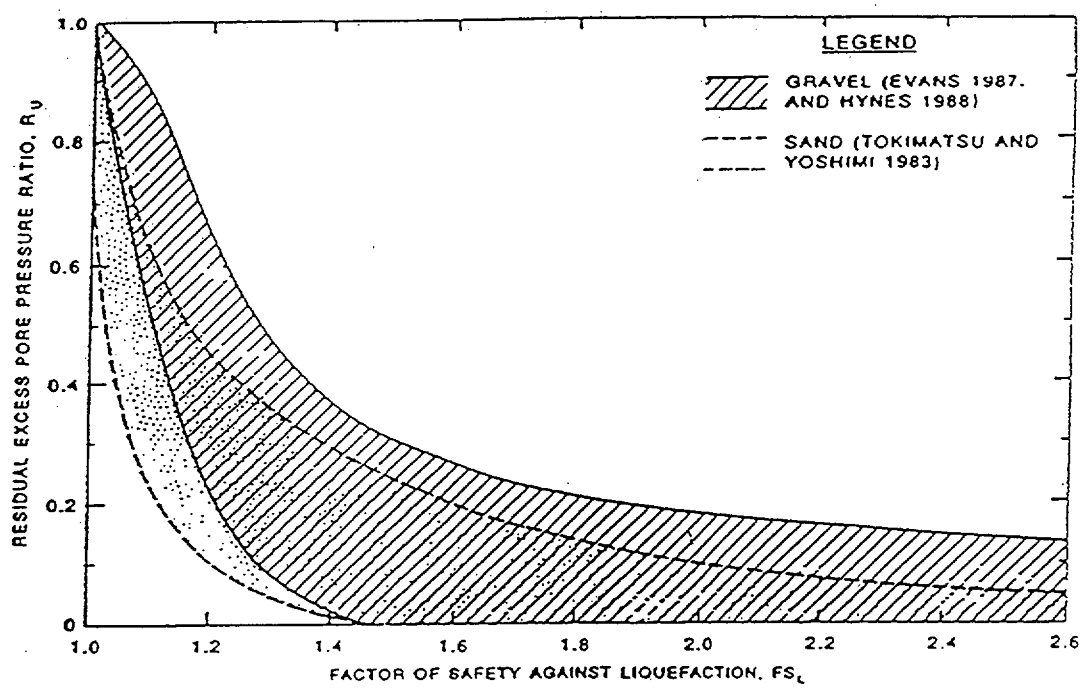

Figure 37. Relationship between residual excess pore water pressure ratio and factor of safety against liquefaction, from laboratory data (Marcuson, Hynes, and Franklin, 1990, reprinted with permission from EERI)

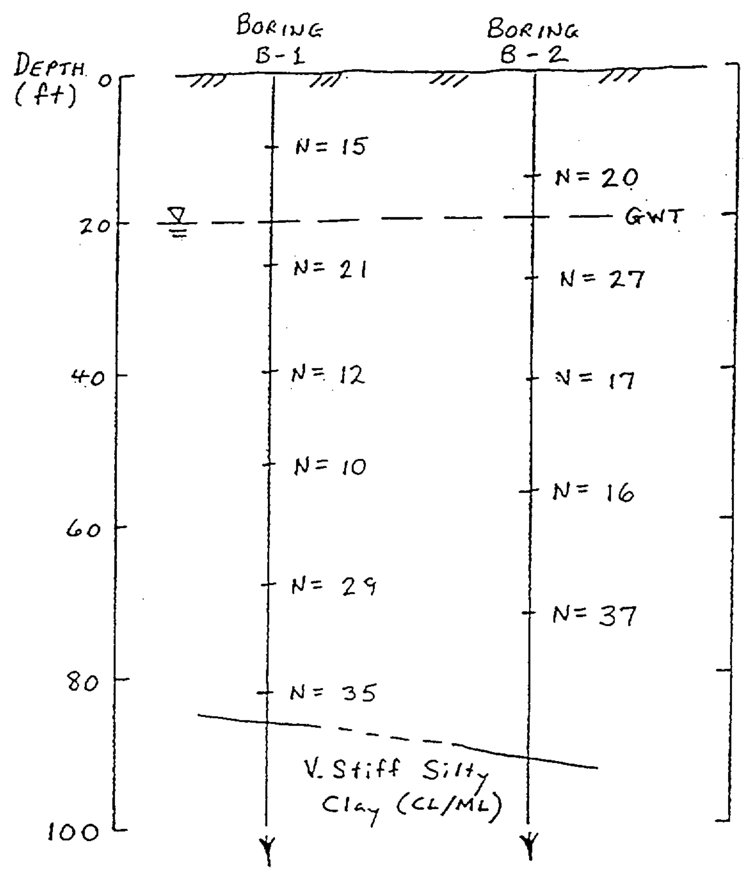

Figure 38. Example problem soil profile with raw SPT blowcounts

Seismicity studies indicate that the level of peak acceleration on rock at the site, $a_{max,\,rock} = 0.19$ g, and this has been selected as the design-level seismic event. These studies have also resulted in selection of a magnitude of $M_s = 7$ as characterizing the design-level event.

3.7.2 Problem

Evaluate resistance to liquefaction, and develop estimates of pore pressure generation (in terms of cyclically-induced pore pressure ratio: Δr_u) for the design-level seismic event. Finally, determine values for undrained residual strength, $S_{u,r}$ for liquefied soils to use in post-earthquake stability analysis.

Step 1: The SPT N-values must be corrected for equipment and procedural effects to develop $(N_1)_{60}$ values:

There was no measurement of actual hammer energy made, so the safety hammer with mechanical trip-release will be based on use of Table 4 for Type II.C having an efficiency or energy ratio of ER ≈ 70 percent. Accordingly, all N-values will be multiplied by (70 percent/60 percent).

No correction for sampler configuration is required in this case.

The first SPT N-value in Boring B-1 could be multiplied by 0.75 to account for short rod lengths, but as it is at the margin of the range recommended for correction, this will not be done.

As the only equipment and procedural corrections required are the energy ratio corrections, N_{60} values will be calculated (using Equation 14) as

$$N_{60} = (N)(70/60) = (1.16)N$$

The resulting N_{60}-values are presented in the fourth column of Table 6.

Step 2: The N_{60}-values must be corrected for overburden effects to develop $(N_1)_{60}$-values. Estimates of effective overburden stress will be made based on the following assumed soil unit weights:

γ_m (above W.T.) = 120 lb/ft^3
γ_s (below W.T.) = 125 lb/ft^3

Overburden correction factors will be calculated as

$$C_N = 1/\sqrt{\sigma_o'}$$

where σ_o' = effective vertical stress in units of tons/ft^2. The resulting calculated values of σ_o', C_N, and $(N_1)_{60}$ are presented in the last three columns of Table 6.

Step 3: Based on inspection of Table 6, it now appears that a somewhat looser zone of sands exists at depths of between about 35 ft to 65 ft. Accordingly, the sand stratum will be subdivided into four sub-strata as indicated in Table 7.

The depth ranges and representative $(N_1)_{60}$-values used for analyses of each of these four substrata are presented in the first two columns of Table 7. It should be noted that the representative $(N_1)_{60}$-values

Table 6 Corrections to N-values for Example Problem

Boring No.	Depth (ft)	N (blows/ft)	N_{60} (blows/ft)	σ_o' (tons/ft^2)	C_N	$(N_1)_{60}$ (blows/ft)	
B-1	10.0	15	17.4	0.60	1.29	22.5	$(N_1)_{60} \approx 22$ blows/ft
B-2	15.5	20	23.2	0.93	1.04	24.1	
B-1	25.5	21	24.4	1.37	0.85	20.7	
B-2	28.0	27	31.3	1.45	0.83	26.0	
B-3	40.0	12	13.9	1.83	0.74	10.3	$(N_1)_{60} \approx 10$ blows/ft
B-2	41.5	17	19.7	1.87	0.73	14.4	
B-1	52.0	10	11.6	2.20	0.67	7.8	
B-2	56.0	16	18.6	2.33	0.66	12.2	
B-3	68.0	29	33.7	2.70	0.61	20.5	$(N_1)_{60} \approx 22$ blows/ft
B-2	72.0	37	42.9	2.82	0.59	25.5	
B-1	82.0	35	40.6	3.14	0.56	22.7	

Table 7 Calculation of Factor of Safety and Residual Excess Pore Pressure Ratio

Sublayer No.	Depth Range (ft)	Representative $(N_1)_{60}$ (blows/ft)	σ_o (tons/ft^2)	σ_o' (tons/ft^2)	r_d	CSR_{eq}	CRR (M=7.0)	FS_1	Δr_u (%)
1	0 to 20	22	0.60	0.60	0.98	0.20	NA	NA	0
2	20 to 36	22	1.70	1.45	0.93	0.22	0.38	1.73	20% (0 to 30%)
3	36 to 62	10	3.01	2.11	0.77	0.22	0.16	0.73	Liquefies Fully
4	62 to 85	22	4.51	2.85	0.57	0.18	0.34	1.21	45% (15 to 50%)

selected are not exact numerical averages within each depth range, but are instead conservatively selected values corresponding more nearly to lower-33-percentile values.

Step 4: Within each sub-layer, estimate CSR_{eq}:

As the upper sub-layer is not saturated, it is not necessary to evaluate CSR_{eq} within this sub-stratum for the purpose of determining liquefaction potential. It has been estimated here to be used in a later example to develop estimates of seismically-induced settlements.

If sub-strata are relatively thick, it can be necessary to develop estimates of CSR_{eq}, at more than one depth within each stratum. Similarly, for non-level ground conditions, it can be necessary to develop estimates of CSR_{eq} at multiple points within each soil unit. For this example problem as site conditions correspond to level ground conditions ($\alpha = 0$) and as the sub-layers are of manageable thickness, it will suffice to simply evaluate CSR_{eq} at the mid-point of each sub-stratum.

Site response analyses have been performed, and it has been found that local site conditions (the soil profile present) can amplify acceleration levels relative to those which would occur "on rock." For the levels of acceleration considered here, these analyses suggested that the value of the $a_{max} = 0.19$ g be increased to a peak ground surface acceleration of $a_{max} = 0.31$ g. Values of CSR_{eq} will then be calculated using Equation 11, and this calculation is presented in the third through seventh columns of Table 7. Values of r_d for depths of more than 40 ft are "near-upper-bound" values from Figure 30. Effective and total overburden stresses, as well as CSR_{eq}, are calculated at the mid-point of each layer. Note: It is often desirable to subdivide into smaller sublayers to better discretize the system for analysis. The resulting calculated CSR_{eq} values for the magnitude 7 design-level event are presented in Table 7, Column 7.

Step 5: Evaluate the CRR, required to "trigger" liquefaction:

Values of CRR (M = 7.5) for each sub-layer can be obtained from Figure 18. For the sands at this example site, an average fines content of 15 percent will be used. The resulting values must then be scaled for both overburden pressure and magnitude effects (Equations 20 and 19, respectively). Overburden corrections for sub-layers 2 through 4 range from 0.93 to 0.80 (from Figure 34), and the magnitude scaling factor was $C_M = 1.26$ (from the upper bound of the recommended range in Figure 33, for M = 7.0). Note: If τ_{hv} was not equal to zero (as it is in this example), then α would not be equal to zero, and a K_α-correction would also have been required.

Step 6: Divide Column 8 by Column 7 to estimate FS_l and then estimate Δr_u using Figure 37:

The last two columns of Table 7 present the results of this step. As the upper sub-layer is above the water table, no calculation is necessary for Sub-layer No. 1. Sub-layer No. 2 has a high FS_l and will experience only minor cyclic pore pressure increase. Sub-layer No. 3 has a low FS_l: liquefaction would occur here. The deepest layer, Sub-layer No. 4, has a relatively low FS_l and can be expected to experience significant cyclic pore pressure generation.

Step 7: Evaluation of undrained residual (steady state) strength, $S_{u,r}$ (S_{us}).

Now develop estimates of the in situ undrained residual strengths of the sandy (silty sand) foundation soils.

First, based on an average or representative fines content of approximately 15 percent, correct the $(N_1)_{60}$ values for each sub-layer (from Table 7) using N_{corr} = 1.5 blows/ft (see Eq. 1). The resulting corrected penetration resistances are then as shown in the fourth column of Table 8. Second, using the $(N_1)_{60\text{-}cs}$ values from Table 8, and the relationship in Figure 8, evaluate $S_{u,r}$. The resulting values are shown in the last column of Table 8. For Sub-layer No. 1, which is above the water table, fully-drained (C-D) effective stress shear strengths should be employed in seismic stability, displacement and bearing capacity analyses. For Sub-layers No. 2 and 4, the $S_{u,r}$-values shown represent a conservative extrapolation of the relationship in Figure 8. The actual strengths modeled in these layers should not, however, be greater than their fully-drained (C-D) effective stress shear strengths. The value of $S_{u,r} \approx 250$ psf is appropriate for Sub-layer No. 3 for all subsequent seismic stability, displacement, and bearing capacity analyses.

4 ANALYSIS OF DISPLACEMENTS ACCOMPANYING LIQUEFACTION

4.1 Background

Several techniques have been proposed for estimating lateral ground displacement at sites where liquefaction is anticipated consequent to design earthquake shaking, including analytical models, physical models, and empirical correlations. The two most popular analytical approaches include finite element analysis and sliding block analysis. Non-linear finite element analyses have been proposed for evaluation of ground deformation at liquefaction sites (such as TARA-3FL (Finn and Yogendrakumar, 1989)). These analyses require constitutive stress-strain relationships and/or undrained steady state strength data. Because of difficulties inherent in sampling and testing to define these properties for field sites, applications of these procedures are usually limited to critical projects or to research. Final design of nuclear facilities would be best served by rigorous analysis; the techniques discussed here will assist preliminary evaluations of deformation potential and consequences.

Empirical procedures have become a standard procedure for determining liquefaction susceptibility and are now available for estimating lateral spread displacement. These empirical procedures have the advantage of using standard field tests and soil classification properties. For general engineering applications, where a high degree of accuracy is not required, empirical analyses are adequate and can be conservatively applied for basic engineering design. Where additional accuracy is required, the empirical estimates may be improved by the more sophisticated finite element or mechanistic sliding block analyses. This report does not address distinction of deformations as to whether their levels are acceptable or tolerable; neither are forces exerted on structures by deforming ground addressed. Both aspects must be considered in design of critical structure foundations.

4.2 Inertial Deformations (Newmark Sliding Block Analogy)

The potential magnitude of seismically-induced down slope permanent deformations in earth dams and embankments that are not directly associated with pervasive liquefaction are often estimated using a "sliding block" analogy first used in the 1950's to this purpose (Taylor and Whitman 1952) that was later formalized as a procedure by Newmark (1960, 1965). In this method of analysis, the part of the slope displaced by earthquake shaking is idealized as a rigid block sliding on an inclined plane with a pseudo-static horizontal acceleration (expressed as a fraction of gravity) applied to the center of the gravity of the sliding mass (Figure 39). The value of pseudo-static horizontal acceleration that causes the factor of

Table 8 Evaluation of Residual Strength of Liquefied Soil for Example Problem

Sub-Layer No.	Depth Range (ft)	Representative $(N_1)_{60}$ (blows/ft)	Fines-Corrected $(N_1)_{60\text{-}cs}$ (blows/ft)	$S_{u,r}$
1	0 to 20	22	23.5	NA
2	20 to 36	22	23.5	1,400 psf
3	36 to 62	10	11.5	250 psf
4	62 to 85	22	23.5	1,400 psf

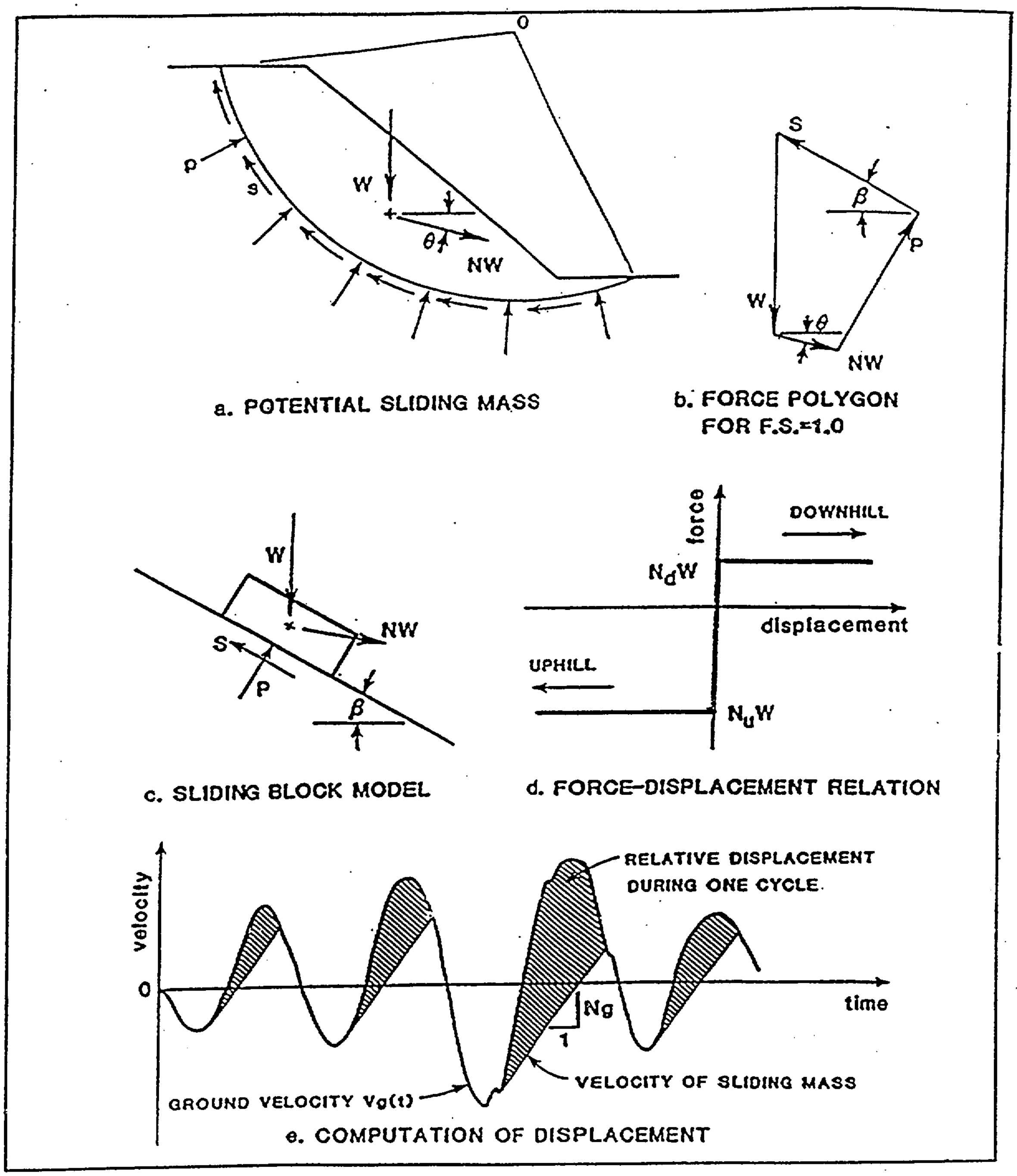

Figure 39. Principal components of the sliding block analysis (Franklin and Chang, 1977)

safety against sliding of the slope to equal unity is called the yield acceleration. During the course of an earthquake, the acceleration applied to the base fluctuates. Displacement begins when the earthquake-induced accelerations of the base exceed the yield acceleration between the block and the base. Displacement stops when the relative velocity between the block and the base returns to zero. Several variations of this method have been subsequently published including: Ambraseys (1960); Ambraseys and Sarma (1967); Sarma (1975); Nadim and Whitman (1983); Chang et al. (1984); Constantinou et al. (1984); Constantinou and Gazetas (1984); Hynes-Griffin and Franklin (1984); Dakoulas and Gazetas (1986); Lin and Whitman (1986); Stamatopoulos and Whitman (1987); Ambraseys and Menu (1988); Yan (1991); Yegian et al. (1992); Marcuson et al. (1992); and Gazetas and Uddin (1994).

Franklin and Chang (1977), Makdisi and Seed (1978), and Hynes-Griffin and Franklin (1984) present displacement calculations for a large data base of ground motions (more than three hundred records). Generalized charts were developed from Makdisi and Seed (1978) to be used as described below. The method is applicable where a well-defined shear plane/shear zone develops as a sliding surface. Other assumptions include: (1) no displacement occurs at accelerations below the yield acceleration, (2) deformation occurs plastically along a discrete basal shear surface when the yield acceleration is exceeded, (3) the shear surface is inclined and planar, (4) there is no up slope movement, and (5) the yield acceleration is not displacement dependent, and thus remains constant throughout the analysis.

Calculations of yield acceleration of the potential sliding mass, maximum average acceleration over a specified depth and maximum crest acceleration (for a trapezoidal embankment, such as a dam) are required inputs for this analysis. Yield accelerations of potential sliding masses in the embankment may be determined using a slope stability computer program, such as UTEXAS3 (developed by Stephen G. Wright at the University of Texas at Austin) adapted for microcomputer use as documented by Edris and Wright (1992). In this computer program, a pseudo-static horizontal force is applied to the center of gravity of each slice of the potential sliding mass to simulate earthquake loading. A seismic coefficient by which the weight of each slice is multiplied to obtain the pseudo-static horizontal force is required as an input parameter. A reduction of 20 percent in the static strength of the embankment material is typically initially assumed to result from earthquake loading in this analysis, as recommended by Makdisi and Seed (1978) and Hynes-Griffin and Franklin (1984). UTEXAS3 or similar codes are used to search for sliding surfaces having minimum factors of safety against sliding for a given seismic coefficient. Seismic coefficients are then varied as input parameters; the seismic coefficient producing a factor of safety against sliding of unity for a particular sliding mass is its yield acceleration.

The Makdisi and Seed procedure involves three steps: determining the yield acceleration K_y, as just described; determining the maximum averaged cyclic load expressed as acceleration K_{max} induced by the earthquake; and determining the displacement u resulting from the motions. The average cyclic load K_{max} varies with the volume and location of material involved in the sliding mass. In the case of dams, a number of case histories have produced the relationship accounting for geometric amplification effects between base and crest acceleration, $\ddot{u}_{max}$, shown in Figure 40 (modified by W. I. Cameron, U.S. Army Engineer Waterways Experiment Station, 1996, after Harder, 1991). The chart is entered with a peak ground acceleration selected for the site. Figure 41 shows how K_{max}, normalized by the crest acceleration $\ddot{u}_{max}$, varies with depth of the sliding surface. For full-depth surfaces, the ratio of K_{max} to $\ddot{u}_{max}$ is about 0.35. These full depth surfaces are generally the most important for dams, since movement along them could involve disruption of internal drainage and water barrier features. Figure 42 shows the variation of displacement with yield acceleration for various magnitudes; the ratio of K_y to K_{max} may then be used to estimate displacement of the sliding mass in question.

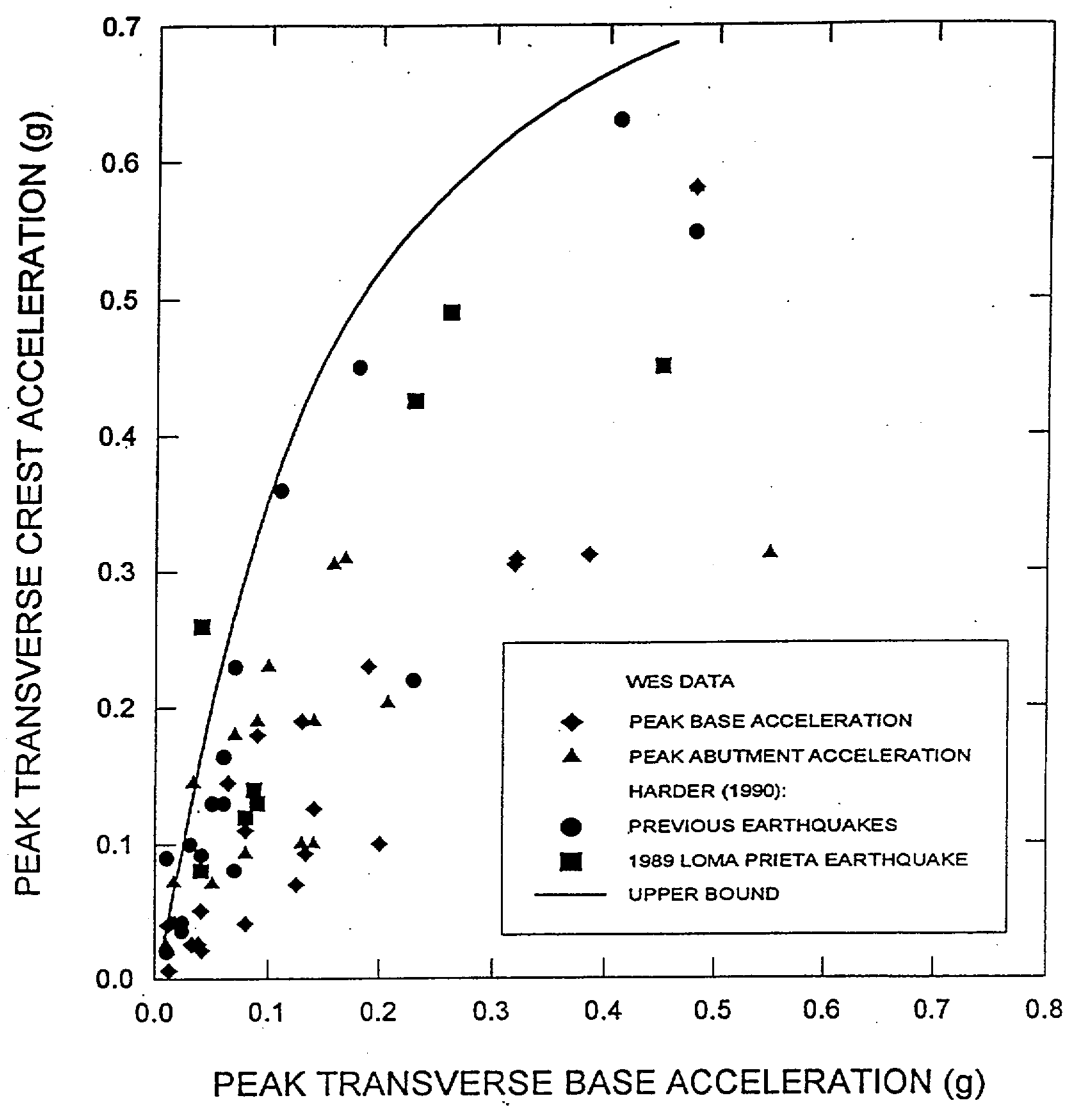

Figure 40. Comparison of peak base and crest transverse accelerations measured at earth dams (from Harder, et al. 1990, as modified by Cameron, 1996)

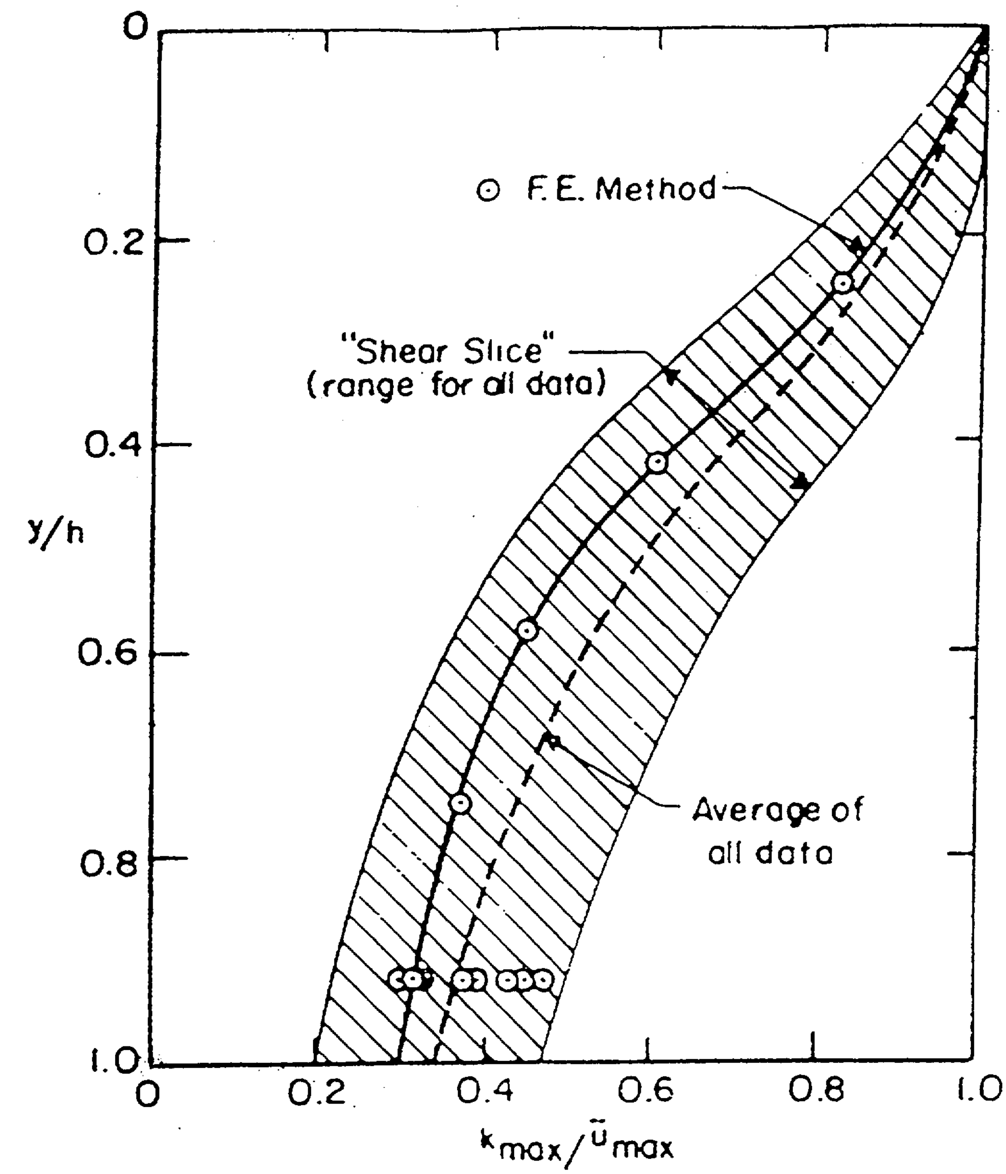

Figure 41. Relationship of the variation of maximum acceleration ratio with depth of sliding mass (Makdisi and Seed, 1978, reprinted with permission from ASCE)

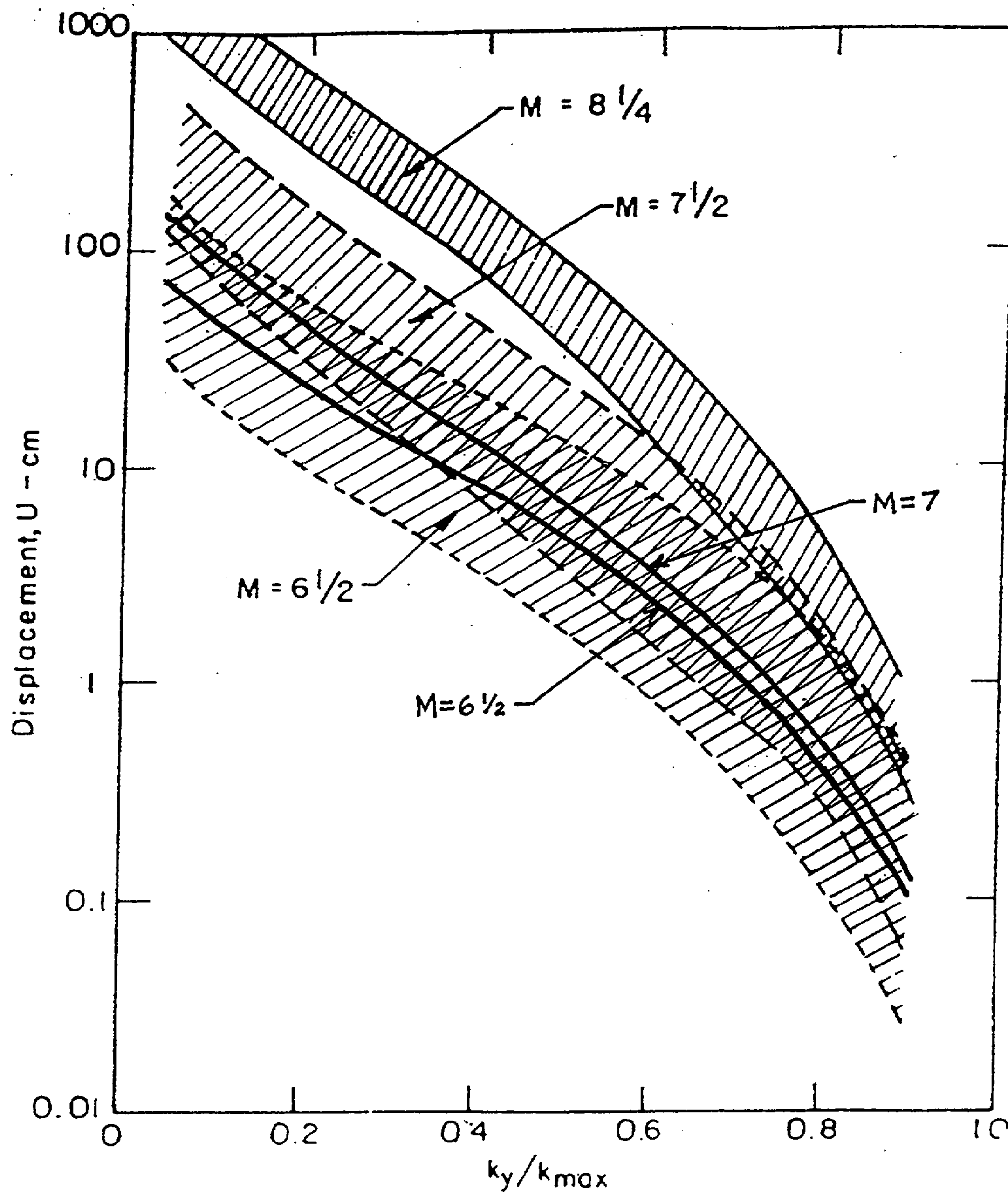

Figure 42. Variation of displacement with yield acceleration for various earthquake magnitudes (Makdisi and Seed, 1978, reprinted with permission from ASCE)

The Newmark sliding block analogy was developed primarily to estimate inertial displacements for earth dams and embankments. However, the Newmark method has also been applied to a number of different design and remediation problems involving not only earth dams and embankments, but also natural and man-made slopes and waste containment facilities. A recent study sponsored by the U.S. Corps of Engineers examined case histories of earthquake-induced deformations in a variety of earthen structures and concluded that the Newmark method of analysis appears to be suitable for estimation of earthquake-induced permanent deformations in those structures. However, the method appears to be most reliable in the range of permanent deformations from about 0.3 m to 1.0 m for maximum accelerations ranging from 0.1 g to 0.5 g, respectively. Selection of shear strengths to use in the aforementioned slope stability calculations is a function of the deformation estimate; studies by Stark and Contreras (1996a, b) of landslides caused during the 1964 Alaska Earthquake produced the recommendation that a shear strength equal to 80 percent of the peak undrained shear strength is appropriate for cohesive soils when deformations are estimated to be 0.1 m or less. If deformations are estimated to be 1.0 m or greater in cohesive soils, analysis should be repeated using no more than about 20 percent of the peak undrained shear strength. In saturated cohesionless soils, strength may be adjusted to account for increase in residual pore water pressures developed during shaking; if these soils are less than 80 percent saturated, it is appropriate to use drained shear strength for seismic loading conditions.

4.3 Lateral Spreading Estimation

Another mode of lateral deformation to consider, once the potential for complete slope failure or unacceptably large inertial deformations accompanying sliding of substantially intact masses of ground during or after earthquake shaking are evaluated, is liquefaction-induced lateral spread. Gently sloping ground may displace down slope or toward free faces (such as incised river channels or excavations), generating earth pressures against any obstacles to the deformation, such as retaining walls, abutments, or foundations. A screening guide produced by Youd (1998) notes that this mode of deformation has been responsible for most liquefaction-induced damage to bridges during past earthquakes. Several empirical lateral spread estimation methods have been proposed, as published by Hamada et al. (1987); Towhata et al. (1991); Yasuda et al. (1991); and Bartlett and Youd (1995). The first three methods use elastic models to predict lateral spread displacements. Although these elastic beam procedures have yielded results comparable to measured displacements, some assumptions create uncertainty in the results. These include the elastic moduli of the soil beam and shear moduli for the liquefied soil. Also, the assumption of a continuous elastic soil beam seems to be contrary to the fissured and fractured ground surface observed to be created by many lateral spreads.

The procedure by Bartlett and Youd (1995) was selected to be explained in further detail in this report. This empirical procedure has the advantage of using standard field tests, commonly determined soil textural properties, and easily obtained topographical information for estimating lateral displacement.

The Bartlett and Youd (1995) approach is based on lateral spread case history data collected and evaluated from eight earthquakes and numerous lateral spreads. All information pertaining to these earthquakes and lateral spreads can be found in the Bartlett and Youd (1995) reference. The procedure is derived in recognition of a number of factors associated with liquefaction and by applying the technique of stepwise multiple linear regression to first define the factors that most influence ground displacements and then to construct a regression model incorporating those factors. To incorporate the influences of geometric factors, two independent models are required: a free-face model (areas near steep slopes) and a ground-slope model (areas with gently sloping terrain). The respective empirical expressions follow:

For free-face conditions:

$$LOG\,D_H = -16.3658 + 1.1782\,M - 0.9275\,LOG\,R - 0.0133\,R + 0.6572\,LOG\,W + 0.3483\,LOG\,T_{15} + 4.5270\,LOG(100 - F_{15} - 0.9224\,(D_{50}))_{15} \tag{21}$$

For ground-slope conditions:

$$LOG\,D_H = -15.7870 + 1.1782\,M - 0.9275\,LOG\,R - 0.0133\,R + 0.4293\,LOG\,S + 0.3483\,LOG\,T_{15} + 4.5270\,LOG(100 - F_{15} - 0.9224\,(D_{50}))_{15} \tag{22}$$

where

D_H = estimated lateral ground displacement in meters
$(D_{50})_{15}$ = average mean grain size in granular layers included in T_{15}, in mm
F_{15} = average fines content (fraction of sediment sample passing No. 200 sieve) for granular layers included in T_{15}, in percent
M = earthquake magnitude (moment magnitude)
R = Horizontal distance from the seismic energy source, in kilometers
S = ground slope, in percent
T_{15} = cumulative thickness of saturated granular layers with corrected blow counts, $(N_1)_{60}$, less than 15, in meters
W = Ratio of the height of the free face to the distance from the base of the free face to the point in question, in percent

The reader is strongly encouraged to review the Bartlett and Youd (1995) paper before utilizing the method, in order to fully understand the applications and limitations of the procedure. In particular, the method was developed from lateral spread data on gently sloping ground; it should not be applied to engineered slopes of larger embankments or excavations.

4.4 Settlements Consequent to Liquefaction

One consequence of liquefaction is some degree of densification in saturated soils, leading to often substantial ground settlement. The time necessary for complete pore water pressure dissipation is, of course, a function of permeability, which is, in turn, strongly dependent on fines content and gradation in general. A procedure developed by Tokimatsu and Seed (1987) is appropriate for hazard screening purposes and is summarized below for estimation of settlement due to liquefaction of granular soils. Fully nonlinear analytical modeling of earthquake-induced soil deformations is a subject of much contemporary research, as discussed earlier.

Tokimatsu and Seed (1987) demonstrated the dependence of volumetric strains produced by dissipation of excess pore water pressures on cyclic shear strain amplitude and initial relative density of the deposit. Cyclic shear strains are themselves a function of cyclic shear stress ratio (CSR), relative density, and earthquake magnitude. The relationship shown in Figure 43 may be used to estimate volumetric strain in a given layer, if the SPT blowcount (adjusted for fines contents effects if necessary) and the earthquake-induced cyclic shear stress ratio (divided by the correction factor described in earlier sections on liquefaction resistance for magnitudes other than 7.5 on which the supportive data were based) are known. The change in layer thickness is then determined by multiplying the volumetric strain by layer thickness. Changes in discrete layer thicknesses may be summed over total depth in a profile to estimate total settlement induced by liquefaction.

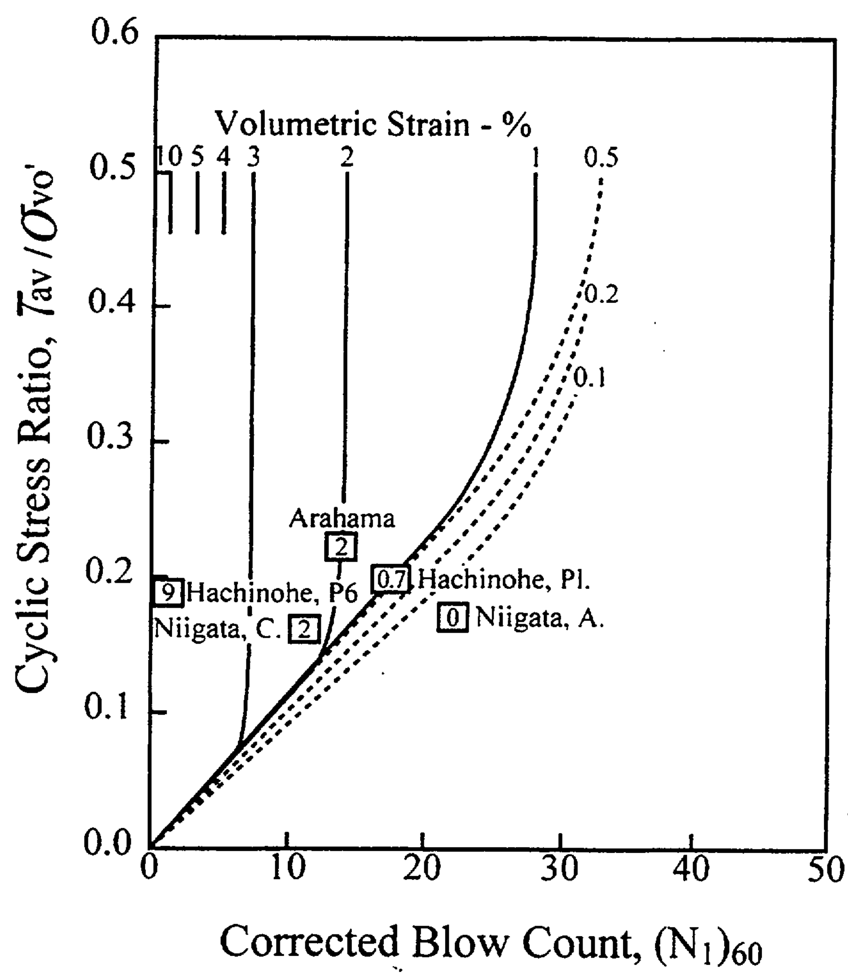

Figure 43. Curves for estimating volumetric strain at liquefiable sites (Youd, 1998, after Tokimatsu and Seed, 1987)

5 CONCLUSIONS

This report was prepared in response to a request by the U.S. Nuclear Regulatory Commission for development of new guidelines design basis evaluation of liquefaction potential and post-earthquake stability of soils as a consequence of recent developments in geotechnical earthquake engineering research and practice. This report provides technical bases for subsequent development of regulatory guidance that reflects both current practice and the state-of-the-art for evaluation of seismic stability of soils, with emphasis on the potential for and consequences of seismically-induced liquefaction of soils beneath foundations. Substantial changes have taken place during the last three decades, particularly in the performance of in situ investigations and the interpretation and application of test results to evaluate seismic stability of foundation soils.

The report describes deterministic procedures and criteria that are currently applied to assess the liquefaction potential of soils ranging in gradation from gravels to clays, and provides guidance for simplified analysis of the consequences of liquefaction, i.e., lateral spreading of level or gently sloping deposits. Approaches to estimate earthquake-induced deformation of slopes are also discussed, with emphasis on the applicability of simplified techniques and the informed selection of strengths to use in these estimates. Probabilistic approaches are presented in a separate report, in view of the NRC's concern over seismic margin issues.

This document is a comprehensive compilation of the state of the art in geotechnical earthquake engineering applied to liquefaction potential evaluation. It begins with historical background information and definitions to establish a convention for analysis. The determination and use of residual of strength of liquefied soils is described, to allow informed selection of shear resistance parameters for post-earthquake stability analysis on earthen structures or foundations. Screening procedures are detailed that can be readily performed in a preliminary site assessment for liquefaction hazard; more complex analysis schemes are presented for cases where liquefaction cannot be reliably precluded by screening studies and for which a larger, site specific investigation effort is justified. In situ testing procedures are emphasized throughout, as representative of the prevalent practice. An Appendix presents guidance for a sampling-and-testing method for steady state strength determination; the use of multiple techniques for assessing liquefaction hazard at critical sites is encouraged.

Procedures are described for estimation of earthquake-induced permanent deformations that occur during shaking, including down slope sliding of slopes and lateral spreading of essentially level ground deposits toward an open face. Gross flow sliding displacements within soils that experience pervasive liquefaction are beyond the scope of this report and are the subject of great controversy and research. This document is not intended to serve as a step-by-step manual; some specific recommendations are offered, however, it was the purpose of the authors to allow for engineering judgment, thus it is more comprehensive as a reference document. An example problem is included to illustrate the evaluation of liquefaction triggering and estimation of residual strength of liquefied soils.

REFERENCES

Ambraseys, N. N., "On the behavior of Earth Dams," *Proceedings of the Second World Conference on Earthquake Engineering*, Tokyo and Kyoto, Japan, Vol. 1, pp. 331-356, 1960.

References

Ambraseys, N. N. and Sarma, S. K., "The response of Earth Dams to Strong Earthquakes," *Geotechnique*, Vol. 17, pp. 181-213, 1967.

Ambraseys, N. N. and Menu, J. M., "Earthquake-Induced Ground Displacements," *Earthquake Engineering and Structural Dynamics,* Vol. 16, pp. 985-1006, 1988.

American Society for Testing and Materials, "Standard Method of Penetration Test and Split-Barrel Sampling of Soils," ASTM D1586-67, Annual Book of Standards, 1967.

Andrus, R. D., "In Situ Characterization of Gravelly Soils that Liquefied in the 1983 Borah Peak Earthquake," Ph.D. Dissertation, University of Texas at Austin, 533 p.

Andrus, R. D. and Youd, T. L. "Subsurface Investigation of a Liquefaction-Induced Lateral Spread, Thousand Springs Valley, Idaho," Miscellaneous Paper GL-87-8, U.S.A.E. Waterways Experiment Station, Vicksburg, MS, 1987.

Andrus, R. D. and Youd, T. L. "Penetration Tests in Liquefiable Gravel," *Proceedings*, 12th Int. Conf. on Soil Mech. and Found. Engineering, Rio De Janiero, Brazil, Vol. 1, pp. 679-682, 1989.

Andrus, R. D., Stokoe, K. H., Bay, J. A., and Youd, T. L., "In Situ V_s of Gravelly Soils Which Liquefied," *Proceedings*, 10th World Conf. on Earthquake Engineering, Madrid, Spain, 19-25 July, pp. 1447-1452, 1992.

Arulanandan, K., Anandarajah, A., and Abghari, A., "Centrifugal Modeling of Soil Liquefaction Susceptibility," *American Society of Civil Engineers, Journal of Geotechnical Engineering* 109(3), pp. 281-300, March 1983.

Arulanandan, K. and Kutter, B, "A Directional Structure Index Related to Sand Liquefaction," *Proceedings, Earthquake Engineering and Soil Dynamics*, American Society of Civil Engineers Specialty Conference, Pasadena, CA, Vol. II, pp. 213-230, 19-21 June 1978.

Arulanandan, K. and Scott, R. F., "Project VELACS – Control Test Results," *American Society of Civil Engineers, Journal of Geotechnical Engineering*, Vol. 119, pp. 1276-1292, 1993.

Ballard, R. F., Jr. and McLean, F. G., "Seismic Field Methods for In Situ Moduli," *Proceedings, Conference on In Situ Measurements of Soil Properties*, American Society of Civil Engineers, Raleigh, North Carolina, Vol. I, pp. 121-150, 1975.

Bartlett, S. F. and Youd, T.L., "Empirical Prediction of Liquefaction Induced Lateral Spread," *American Society of Civil Engineers, Journal of the Geotechnical Engineering Division*, Vol. 121(4), pp. 316-329, 1995.

Baziar, M. H., and Dobry, R., "Residual Strength and Large-Deformation Potential of Loose Silty Sands," *American Society of Civil Engineers, Journal of the Geotechnical Engineering Division,* Vol. 121, No. 12, pp. 896-906, 1995.

Bromhead, E. N., "A simple ring shear apparatus," *Ground Engineering*, Vol. 12(5), pp. 40-44, 1979.

BSSC, "NEHRP Recommended Provisions for the Development of Seismic Regulations for New Buildings," Building Seismic Safety Council, Chapter 7 Commentary, pp. 151-163, 1991.

Byrne, P. M., Jitno, H., and Salgado, F., "Earthquake Induced Displacement of Soil-Structures Systems," *Proceedings, 10th World Conference on Earthquake Engineering*, Madrid, Spain, pp. 1407-1412, 1992.

Campanella, R. G. and Lim, B. S., "Liquefaction Characteristics of Undisturbed Soils," *Proceedings, International Conference on Recent Advances in Geotechnical Earthquake Engineering and Soil Dynamics*, St. Louis, Vol. I, pp. 227-230, 1981.

Carter, D. P., and Seed, H. B., "Liquefaction Potential of Sand Deposits under Low Levels of Excitation," Report No. EERC 88-11, Earthquake Engineering Research Center, Berkeley, CA, 1988.

Casagrande, A., "Characteristics of Cohesionless Soils Affecting the Stability of Slopes and Earth Fills," *Journal of Boston Society of Civil Engineers*, January, 1936 (Reprinted in Contributions to Soil Mechanics, Boston Society of Civil Engineers, October 1940).

Casagrande, A. and Rendon, F., "Gyratory Shear Apparatus Design, Testing Procedures, and Test Results on Undrained Sand," Technical Report, U.S. Army Engineer Waterways Experiment Station, Vicksburg, Mississippi, 1978.

Castro, G., "Liquefaction of Sands," Harvard Soil Mechanics Series No. 81, Harvard University, Cambridge, MA, January, 1969.

Castro, G., "Liquefaction and Cyclic Mobility of Saturated Sands," *American Society of Civil Engineers, Journal of the Geotechnical Engineering Division,* Vol. 101(GT6), pp. 551-569, 1975.

Castro, G., Keller, T. O., and Boynton, S. S., "Re-evaluation of the Lower San Fernando Dam - Report 1: An Investigation of the February 9, 1971 Slide," Contract Report GL-89-2, U.S. Army Engineer Waterways Experiment Station, Vicksburg, MS, September, 1989.

Castro, G. and Poulos, S. J., "Factors Affecting Liquefaction and Cyclic Mobility," *American Society of Civil Engineers, Journal of the Geotechnical Engineering Division,* Vol. 103(GT6), pp. 501-506, 1977.

Castro, G., Poulos, S. J., France, J. W., and Enos, J. L., "Liquefaction Induced by Cyclic Loading," Report by Geotechnical Engineers, Inc., to the National Science Foundation, Washington, D.C., March, 1982.

Chang, C-J., Chen, W. and Yao, J. T. P., "Seismic Displacements in Slopes by Limit Analysis," *American Society of Civil Engineers, Journal of Geotechnical Engineering,* Vol. 110, No. GT7, pp. 860-874, 1984.

Coe, C.J., Prevost, J. H., and Scanlan, R. H., "Dynamic Stress Wave Reflections/Attenuation: Earthquake Simulation in Centrifuge Models," *Earthquake Engineering and Structural Dynamics*, Vol. 13(1), pp. 109-128, 1985.

Constantinou, M.C. and Gazetas, G., "Probabilistic Seismic Sliding Deformations of Earth Dams and Slopes," *American Society of Civil Engineers, Proceedings of the Specialty Conference on Probabilistic Methods and Structural Reliability*, New York, NY, pp. 318-321, 1984.

References

Constantinou, M.C., Gazetas, G. and Tadjdakhsh, "Stochastic Sliding of Rigid Mass against Asymmetric Coulomb Friction," *Earthquake Engineering and Structural Dynamics*, No. 12, pp. 777-793, 1984.

Coulter, H. W., and Migliaccio, R. R., "Effects of the Earthquake of March 27, 1964, at Valdez, Alaska," U.S. Geological Survey Professional Paper 542-C, U.S. Department of the Interior, 1966.

Dakoulas, P. and Gazetas, G., "Seismic Shear Strains and Seismic Coefficients in Dams & Embankments," *Soil Dynamics and Earthquake Engineering*, Vol. 5, No. 2, pp. 75-83, 1986.

DeAlba, P., Seed, H. B., and Chan, C. K., "Sand Liquefaction in Large-Scale Simple Shear Tests," *American Society of Civil Engineers, Journal of the Geotechnical Engineering Division,* Vol. 102(GT9), pp. 909-927, 1976.

Department of the Army, "Geophysical Exploration," Engineer Manual 1110-1-1802, Office, Chief of Engineers, Washington, D.C., 1979.

Department of the Army, "Laboratory Soils Testing," Engineer Manual 1110-2-1906, Office, Chief of Engineers, Washington, D.C., 1986.

Dobry, R., Stokoe, K. H., Ladd, R. S., and Youd, T. L., "Liquefaction Susceptibility from S-Wave Velocity," In situ Testing to Evaluate Liquefaction Susceptibility, Session No. 24, Preprint No. 81-544, American Society of Civil Engineers National Convention, St. Louis, Missouri, 1981.

Edris, E. V., Jr., and Wright, S. G., "User 's Guide: UTEXAS3 Slope Stability Package," Technical Report GL-87-1, Vol. IV, U.S. Army Engineer Waterways Experiment Station, Vicksburg, Mississippi, 1992.

Erchul, R. A. and Gularte, R. C., "Electrical Resistivity used to Measure Liquefaction of Sand," *American Society of Civil Engineers, Journal of the Geotechnical Engineering Division,* Vol. 108(GT5), pp. 778-782, 1982.

Evans, M., "Undrained Cyclic Triaxial Testing of Gravels--The Effects of Membrane Compliance," Ph.D. Dissertation, University of California, Berkeley, CA, 1987.

Fairless, G. J., "Liquefaction Case Histories in New Zealand," Research Report 84/18, University of Canterbury, Christchurch, New Zealand, 1984.

Farrar, J. A., "Study of In situ Testing for Evaluation of Liquefaction Resistance and Occurrence," *Proceedings, 19th Joint Meeting of the U.S.-Japan Cooperative Program in Natural Resources Panel on Wind and Seismic Effects*, National Bureau of Standards, Gaithersburg, MD, pp. 239-280, 1988.

Federal Highway Administration, "Guidelines for Cone Penetration Test Performance and Design," Report No. FHWA-TS-78-209, Prepared for the U.S. Department of Transportation by Dr. John H. Schmertmann, University of Florida, 1978.

Finn, W. D. L., "Liquefaction Potential: Developments Since 1976," *Proceedings, International Conference on Recent Advances in Geotechnical Earthquake Engineering and Soil Dynamics*, St. Louis, Vol. II, pp. 655-682, 1981.

Finn, W. D. L. and Martin, G. R., "Fundamentals of Liquefaction under Cyclic Loading," *American Society of Civil Engineers, Journal of the Geotechnical Engineering Division,* Vol. 101(GT5), pp. 81-92, 1975.

Finn, W. D. L. and Yogendrakumar, M., "TARA-3FL: Program for Analysis of Liquefaction Induced Flow Deformations," Department of Civil Engineering, University of British Columbia, Vancouver, Canada, 1992.

Franklin, A. G. and Chang, F. K., "Earthquake Resistance of Earth and Rockfill Dams; Permanent Displacements of Earth Embankments by Newmark-Sliding Block Analysis," Miscellaneous Paper S-71-17, Report 5, U.S. Army Engineer Waterways Experiment Station, Vicksburg, Mississippi, 1977.

Gazetas, G. and Uddin, N., "Permanent Deformation on Preexisting Sliding Surfaces in Dams," *American Society of Civil Engineers, Journal of Geotechnical Engineering*, Vol. 120, No. 11, pp. 2041-2061, 1994.

Hamada, M., Towhata, I., Yasuda, S., Isoyama, R., "Study of Permanent Ground Displacement Induced by Seismic Liquefaction," *Computers and Geotechnics*, Elsevier Applied Science Publishers, Vol. 4(4), pp. 197-220, 1987.

Harder, L. F., Jr., "Use of Penetration Tests to Determine the Cyclic Loading Resistance of Gravelly Soils During Earthquake Shaking," Ph.D. Dissertation, University of California, Berkeley, CA, 1988.

Harder, L.F. Jr., "Performance of Earth Dams during Loma Prieta Earthquake," *Proceedings 2nd International Conference on Recent Advances in Geotechnical Earthquake Engineering and Soil Dynamics*, St. Louis, MO, pp. 1673-1690, 1991.

Harder, L. F., Jr., and Seed, H. B., "Determination of Penetration Resistance for Coarse-Grained Soils Using the Becker Hammer Drill," Report No. UCB/EERC-86/06, University of California, Berkeley, CA, 1986.

Hushmand, B., Scott, R. K., and Crouse, C. B., "Centrifuge Liquefaction Tests in a Laminar Box," *Geotechnique*, Vol. 38(2), pp. 253-262, 1988.

Hvorslev, M. J., "Subsurface Exploration and Sampling of Soils for Civil Engineering Purposes," American Society of Civil Engineers, Engineering Foundation, November, 1949.

Hynes, M. E., "Pore Pressure Generation Characteristics of Gravels under Undrained Cyclic Loading," Ph.D. Thesis, University of California, Berkeley, CA, 1988.

Hynes, M. E. and Olsen, R. S., "Influence of Confining Stress on Liquefaction Resistance," *Proceedings, International Symposium on the Physics and Mechanics of Liquefaction, Johns Hopkins University*, sponsored by the National Science Foundation, Baltimore, MD 10-11 September 1998, A. A. Balkema publishers (in press), 1998.

Hynes-Griffin, M.E. and Franklin, A.G., "Rationalizing the Seismic Coefficient Methods," Miscellaneous Paper GL-84-13, U.S. Army Engineer Waterway Experiment Station, Vicksburg, MS, 1984.

References

Ishihara, K., "Post-Earthquake Failure of a Tailings Dam Due to Liquefaction of the Pond Deposit," *Proceedings, International Conference on Case Histories in Geotechnical Engineering*, St Louis, MO, May 6-11, 1984, Vol. III, pp. 1129-1146, 1984.

Ishihara, K., "Stability of natural slopes during earthquakes," *Proceedings, 11th International Conference on Soil Mechanics and Foundation Engineering,* San Francisco, CA, Vol. 1, 321-376, 1985.

Ishihara, K. and Nagase, H., "Multi-Directional Irregular Loading Tests on Sand," Advances in the Art of Testing Soils under Cyclic Conditions, Proceedings of a session sponsored by the Geotechnical Engineering Division in conjunction with the American Society of Civil Engineers Convention in Detroit, MI, October, 1985, (ed. Khosla, V.), pp. 99-119, 1985.

Ishihara, K. and Takatsu, H., "Effects of Overconsolidation and K_o Conditions on the Liquefaction Characteristics of Sands," *Japanese Society of Soil Mechanics and Foundation Engineering, Soils and Foundations*, Vol. 19(4), pp. 60-68, 1979.

Kaufman, L. P., "Percentage Silt Content in Sands and its Effects on Liquefaction Potential," M.S. Thesis, University of Colorado, Denver, CO, 1981.

Kayen, R. E, "Accelerogram-Energy Approach for Prediction of Earthquake-Induced Ground Liquefaction," unpublished PhD dissertation, University of California, Berkeley, CA, 1993.

Kayen, R. E., and Mitchell, J. K., "Assessment of Liquefaction Potential During Earthquakes by Arias Intensity," *Journal of Geotechnical Engineering,* ASCE, 123(12), pp. 1162-1174, 1997.

Ketcham, S., Ko, H. Y., and Sture, S., "Performance of an Earthquake Motion Simulator for a Small Geotechnical Centrifuge," *Proceedings, Centrifuge 91*, A. A. Balkema, Rotterdam, The Netherlands, pp. 361-368, 1991.

Koester, J. P., "Cyclic Strength and Pore Pressure Generation Characteristics of Fine-Grained Soils," thesis submitted in partial fulfillment of the requirements for Doctor of Philosophy, College of Engineering, University of Colorado, Boulder, CO, 1992.

Koester, J. P. and Franklin, A. G., "Current Methodologies for Assessing the Potential for Earthquake-Induced Liquefaction in Soils," Research Report No. NUREG/CR-4430 prepared by Geotechnical Laboratory, U.S. Army Engineer Waterways Experiment Station for the U.S. Nuclear Regulatory Commission, 1985.

Kokusho, T., "Earthquake Geotechnical Studies for Gravelly Ground," *Proceedings, International Seminar on Dynamic Behavior of Clays, Sands, and Gravels*, Kitakyushu, Japan, November, 24-25, 1989, pp. 228-266, 1989.

Kokusho, T., Tanaka, Y., Kudo, K. And Kawai, T., "Liquefaction case study of volcanic gravel layer during 1993 Hokkaido-Nansei-Oki earthquake," *Proceedings, 3rd International Conference on Recent Advances in Geotechnical Earthquake Engineering and Soil Dynamics,* St. Louis, MO, 235-242, 1995.

Kovacs, W. D., Salomone, L. A., and Yokel, F. Y., "Energy Measurement in the Standard Penetration Test," NBS Building Science Series 135, National Bureau of Standards, Washington, D.C., 1981.

Kuribayashi, E. and Tatsuoka, F., "Brief Review of Liquefaction During Earthquakes in Japan," *Japanese Society of Soil Mechanics and Foundation Engineering, Soils and Foundations*, Vol. 15(4), pp. 81-92, 1975.

Lee, K. L. and Fitton, J. A., "Factors Affecting the Cyclic Loading Strength of Soil," Vibration Effects of Earthquakes on Soils and Foundations, ASTM STP 450, American Society for Testing and Materials, Philadelphia, PA, pp. 71-95, 1969.

Lee, K. L. and Seed, H. B., "Dynamic Strength of Anisotropically Consolidated Sand," *American Society of Civil Engineers, Journal of the Soil Mechanics and Foundations Division*, Vol. 93(SM5), pp. 169-190, 1967.

Liao, S. C. and Whitman, R. V., "Overburden Correction Factors for SPT in Sand," *American Society of Civil Engineers, Journal of the Geotechnical Engineering Division,* Vol. 112(3), pp. 373-377, 1985.

Lin, J. S. and Whitman, R.V., "Earthquake Induced Displacements of Sliding Block," *American Society of Civil Engineers, Journal of Geotechnical Engineering*, Vol. 105, No. GT12, pp. 1427-1434, 1986.

Makdisi, F. I. and Seed, H. B., "A Simplified Procedure for Estimating Earthquake Induced Deformation in Dams and Embankments," *American Society of Civil Engineers, Journal of Geotechnical Engineering,* Vol. 104, No.GT7, pp. 849-867, 1978.

Marcuson, W. F. III and Bieganousky, W. A., "Laboratory Standard Penetration Tests on Platte River Sand and Standard Concrete Sand," Research Report S-76-2, U. S. Army Engineer Waterways Experiment Station, Vicksburg, Mississippi, 1977.

Marcuson, W. F. III, Hynes, M. E., and Franklin, A. G., "Evaluation and Use of Residual Strength in Seismic Safety Analysis of Embankments" *Earthquake Spectra*, Vol. 6(3), pp. 529-572, 1990.

Marcuson, W.F. III, Hynes, M.E. and Franklin, A.G. , "Seismic Stability and Permanent Deformation analyses: the last 25 years," *Stability and Performance of Slopes and Embankments II*, Geotechnical Special Publication No. 31, American Society of Civil Engineers, Berkeley, CA, University of California, vol 1, pp. 552-592, 1992.

Marcuson, W. F. III and Franklin, A. G., "State of the Art of Undisturbed Sampling of Cohesionless Soils," Miscellaneous Paper GL-79-16, U.S. Army Engineer Waterways Experiment Station, Vicksburg, MS, 1979.

Maurenbrecher, P. M., Den Outer, A. And Luger, H. J., "Review of geotechnical investigations resulting from the Roermond April 13, 1992 earthquake," *Proceedings, 3rd International Conference on Recent Advances in Geotechnical Earthquake Engineering and Soil Dynamics,* St. Louis, MO, 645-652, 1995.

McLean, F. G., Franklin, A. G., and Dahlstrand, T. K., "Influence of Mechanical Variables on the SPT," *Proceedings, Specialty Conference on In Situ Measurement of Soil Properties, American Society of Civil Engineers*, Vol. 1, pp. 287-318, 1975.

Mitchell, J. K., and Solymar, Z. V., "Time-dependent Strength Gain in Freshly Deposited or Densified Sand," *American Society of Civil Engineers, Journal of Geotechnical Engineering,* Vol. 110(11), pp. 1559-1576, 1984.

References

Nadim, F. and Whitman, R.V. , "Seismically induced movements of retaining walls," *American Society of Civil Engineers, Journal of Geotechnical Engineering*, Vol. 109, No. GT7, pp. 915-931, 1983.

National Research Council, Liquefaction of Soils During Earthquakes, National Academy Press, Washington, D.C., 1985.

National Center for Earthquake Engineering Research, "Proceedings of the NCEER Workshop on Evaluation of Liquefaction Resistance of Soils," Report No. NCEER-97-0022, State University of New York at Buffalo, Buffalo, NY, viewable on the World Wide Web at http://mceer.buffalo.edu., 1997.

Newmark, N. M., "The Earthquake Resistance of Portage Mountain Dam," Consulting Report submitted to International Power and Engineering Consultants Limited, Vancouver, B.C., Canada, pp. 30, 1960.

Newmark, N. M., "Effects of Earthquakes on Dams and Embankments," *Geotechnique*, Vol 15, No. 2, pp. 139-160, 1965.

Obermeier, S. F., Bleuer, N. R., Munson, C. A., Munson, P. J., Martin, W. S., McWilliams, K. M., Tabaczynski, D. A., Odum, J. K., Rubin, M., and Eggert, D. L., "Evidence of Strong Earthquake Shaking in the Lower Wabash Valley from Prehistoric Liquefaction Features," Science, Vol. 251, pp. 1061-1063, 1991.

Obermeier, S. F., Gohn, G. S., Weems, R. E., Gelinas, R. L., and Rubin, M., "Geologic Evidence for Recurrent Moderate to Large Earthquakes near Charleston, South Carolina," Science, Vol. 227, pp. 408-411, 1985.

Obermeier, S. F., Weems, R. E., Jacobson, R. B., and Gohn, G. S., "Liquefaction Evidence for Repeated Holocene Earthquakes in the Coastal Region of South Carolina," Earthquake Hazards and the Design of Constructed Facilities in the Eastern United States, Annals of the New York Academy of Sciences, (eds. Jacob, K. H. and Turkstra, C. J.), Vol. 558, pp. 183-195, 1989.

Olsen, R. S., "Liquefaction Analysis using the Cone Penetrometer Test," *Proceedings of the Eighth World Conference on Earthquake Engineering*, Vol. III, Prentice-Hall Inc., Englewood Cliffs, NJ, pp. 247-254, 1984.

Olsen, R. S., "Soil Classification and Site Characterization using the Cone Penetrometer Test," *Proceedings of the First International Symposium on Penetration Testing (ISOPT-1)*, (ed. de Ruiter, J.), A. A. Balkema, Rotterdam, Netherlands, pp. 887-893, 1988.

Olsen, R. S., "Normalization and Prediction of Geotechnical Properties using the Cone Penetrometer Test (CPT)," Ph.D. Dissertation submitted to the University of California, Berkeley, May 1994 (also available as Technical Report GL-94-29, USAE Waterways Experiment Station, Vicksburg, MS 39180, August 1994), 1994.

Olsen, R. S. and Farr, J. V., "Site Characterization Using the Cone Penetrometer Test," *Proceedings, In Situ '86, American Society of Civil Engineers, Specialty Conference Use of In Situ Testing in Geotechnical Engineering*, 22-25 June, 1986, Virginia Polytechnic Institute and State University, Blacksburg, VA, pp. 854-868, 1986.

Olsen, R. S. and Koester, J. P., "Prediction of Liquefaction Resistance using the CPT," *Proceedings, International Symposium on Cone Penetrometer Testing - CPT '95*, Linkopping, Sweden, October 1989, 1995.

Olsen, R. S., Koester, J. P., and Hynes, M. E., "Evaluation of Liquefaction Potential using the CPT," *Proceedings of the 28th Joint meeting of the U.S.-Japan Cooperative Program in Natural Resources - Panel on Wind and Seismic Effects*, U.S. National Institute of Standards and Technology, Gaithersburg, Maryland, May 1996.

Olsen, R. S. and Mitchell, J. K., "CPT Stress Normalization and Prediction of Soil Classification," *Proceedings of the International Symposium on Cone Penetrometer Testing - CPT '95*, Linkopping, Sweden, October 1989, 1995.

Pillai, V. S, and Byrne, P. M., "Effect of Overburden Pressure on Liquefaction Resistance of Sands," *Canadian Geotechnical Journal*, Vol. 31, 1994.

Poulos, S. J., "The Steady State of Deformation," *American Society of Civil Engineers, Journal of Geotechnical Engineering Division,* Vol. 107(GT5), pp. 5513-5562; closure discussion in Vol. 108(GT8), pp. 1087-1091, August, 1981.

Poulos, S. J., "Liquefaction and Related Phenomena," Chapter 9 in <u>Advance Dam Engineering for Design, Construction, and Rehabilitation</u>, (ed. Jansen, R. B.), Van Nostrand Reinhold, NY, 1988.

Poulos, S. J., Castro, G., and France, J. W., "Liquefaction Evaluation Procedure," *American Society of Civil Engineers, Journal of Geotechnical Engineering,* Vol. 111(6), pp. 772-792, 1985.

Poulos, S. J., Robinsky, E. I., and Keller, T. O., "Liquefaction Resistance of Thickened Tailings," *American Society of Civil Engineers, Journal of Geotechnical Engineering,* Vol. 111(GT12), pp. 1380-1394, December, 1985.

Prakash, S. and Gupta, M. K., "Compaction of Sand under Vertical and Horizontal Vibrations," *Proceedings, Southeast Asian Regional Conference on Soil Engineering*, Bangkok, pp. 201-210, 1967.

Puri, V. K., "Liquefaction Behavior and Dynamic Properties of Loessial (Silty) Soils," Ph.D. Thesis, University of Missouri-Rolla, MO, 1984.

Pyke, R., Chan, C. K., and Seed, H. B., "Settlement and Liquefaction of Sands under Multi-Directional Shaking," Report No. EERC 74-2, Earthquake Engineering Research Center, University of California, Berkeley, CA, 1974.

Robertson, P. K., Campanella, R. G., and Wightman, A.., "SPT-CPT Correlations," *American Society of Civil Engineering, Journal of the Geotechnical Division*, Vol. 109, November 1983.

Roe, G. V., DeAlba, P. A., and Celikkol, B., "Acoustic Identification of Liquefaction Potential," *Proceedings, International Conference on Recent Advances in Geotechnical Earthquake Engineering and Soil Dynamics*, St. Louis, Missouri, Vol. 2, pp. 199-202, 1981.

Rollins, K. M., "The Influence of Buildings on Potential Liquefaction Damage," Ph.D. Thesis, University of California, Berkeley, CA, 1987.

References

Sarma, S. K., "Seismic Stability of Earth Dams & Embankments," *Geotechnique*, Vol. 25 No. 4, pp. 743-761, 1975.

Schofield, A. N., "Dynamic and Earthquake Geotechnical Centrifuge Modeling," *Proceedings, International Conference on Recent Advances in Geotechnical Earthquake Engineering and Soil Dynamics*, (ed. Prakash, S.), University of Missouri, Rolla, MO. Vol. 3, pp. 1081-1100, 1981.

Schofield, A. N., and Wroth, C. P., Critical State Soil Mechanics, McGraw-Hill Book Co., London, UK, 1968.

Scott, R. F., "Centrifuge Model Testing at Caltech," Soil Dynamics and Earthquake Engineering, Vol. 2(4), pp. 188-198, 1983.

Seed, H. B., "Evaluation of Soil Liquefaction Effects on Level Ground During Earthquakes," Liquefaction Problems in Geotechnical Engineering, Preprint No. 2752, American Society of Civil Engineers National Convention, Philadelphia, pp. 1-104, 1976.

Seed, H. B., "19th Rankine Lecture: Considerations in the Earthquake Resistant Design of Earth and Rockfill Dams," *Geotechnique*, Vol. 29(3), pp. 215-263, 1979a.

Seed, H. B., "Soil Liquefaction and Cyclic Mobility Evaluation for Level Ground During Earthquakes," *American Society of Civil Engineers, Journal of the Geotechnical Engineering Division,* New York, Vol. 105(GT2), pp. 201-255, 1979b.

Seed, H. B., "Earthquake-Resistant Design of Earth Dams," *Proceedings, Symposium on Seismic Design of Embankments and Caverns, American Society of Civil Engineers*, pp. 41-64, May 6-10, 1983.

Seed, H. B., "Design Problems in Soil Liquefaction," *American Society of Civil Engineers, Journal of the Geotechnical Engineering Division*, Vol. 113(8), 1987.

Seed, H. B., Arango, I., and Chan, C. K., "Evaluation of Soil Liquefaction Potential During Earthquakes," Report No. UCB/EERC-75/28, University of California, Berkeley, CA, 1975.

Seed, H. B. and De Alba, P., "Use of SPT and CPT Tests for Evaluating the Liquefaction Resistance of Soils," *Proceedings, Specialty Conference on the Use of In Situ Tests in Geotechnical Engineering*, Blacksburg, VA, American Society of Civil Engineers Geotechnical Special Publication No. 6, pp. 120-134, 1986.

Seed, R. B. and Harder, L. F., Jr., "SPT-Based Analysis of Cyclic Pore Pressure Generation and Undrained Residual Strength," *Proceedings, H. Bolton Seed Memorial Proceedings*, May, 1990, Berkeley, California, Bitech Publishers, Ltd., Vol. 2, pp. 351-376, 1990.

Seed, H. B. and Idriss, I. M., "Simplified Procedure for Evaluating Soil Liquefaction Potential," *American Society of Civil Engineers, Journal of the Soil Mechanics and Foundations Division*, Vol. 97(SM9), pp. 1249-1273, 1971.

Seed, H. B. and Idriss, I. M., "Evaluation of Liquefaction Potential of Sand Deposits Based on Observations of Performance in Previous Earthquakes," *Proceedings, American Society of Civil Engineers National Fall Convention*, Session No. 24, St. Louis, MO, 1981.

Seed, H. B. and Idriss, I. M., Ground Motions and Soil Liquefaction During Earthquakes, Monograph Series, Earthquake Engineering Research Institute, University of California, Berkeley, CA, 1982.

Seed, H. B., Idriss, I. M., and Arango, I., "Evaluation of Liquefaction Potential Using Field Performance Data," *American Society of Civil Engineers, Journal of Geotechnical Engineering*, Vol. 109(3), pp. 458-482, 1983.

Seed, H. B., Idriss, I. M., Makdisi, F. I., and Banerjee, N., "Representation of Irregular Stress Time Histories by Equivalent Uniform Stress Series in Liquefaction Analyses," Report No. EERC-75-29, Earthquake Engineering Research Center, University of California, Berkeley, CA, 1975.

Seed, H. B., Lee, K. L., Idriss, I. M., and Makdisi, F. I., "Analysis of the Slides in the San Fernando Dams During the Earthquake of February 9, 1971," Report No. EERC-73-2, College of Engineering, University of California, Berkeley, CA, 1973.

Seed, H. B., Tokimatsu, K., Harder, L. F., and Chung, R., "Influence of SPT Procedures in Soil Liquefaction Resistance Evaluations," *American Society of Civil Engineers, Journal of the Geotechnical Engineering Division,* Vol. 111(12), pp. 861-878, 1985.

Shannon and Wilson, Inc., and Agbabian and Associates, "Soil Behavior under Earthquake Loading Conditions," U.S. Atomic Energy Commission Report, Contract No. W-7405-eng-26, 1972.

Shibata, T., Oka, F., and Ozawa, Y., "Characteristics of ground deformation due to liquefaction," *Special Issue of Soils and Foundations*, Japanese Geotechnical Society, pp. 65-79, January, 1996.

Skempton, A. W., "Standard penetration test procedures and the effects in sands of overburden pressure, relative density, particle size, aging and overconsolidation," *Géotechnique*, Vol. 36, No. 3, pp. 425-447, 1986.

Smart, J. D. and Von Thun, J. L., "Seismic Design and Analysis of Embankment Dams-Recent Bureau of Reclamation Experience," Seismic Design of Embankments and Caverns, American Society of Civil Engineers, 1983.

Stamatopoulos, C.A. and Whitman, R.V., "Computation of Earthquake-induced permanent Deformations of Foundation on Liquefaction Susceptible Sand," Research Report No. R8705, Dept. of Civil Engineering, Massachusetts Institute of Technology, Cambridge, Mass., 1987.

Stark, T.D. and Contreras, I.A., "Fourth Avenue Landslide During 1964 Alaskan Earthquake," submitted for review and possible publication in *American Society of Civil Engineers, Journal of the Geotechnical Engineering Division,* Vol. 123, 1996a.

Stark, T.D. and Contreras, I.A., "Constant Volume Ring Shear Apparatus." ASTM *Geotechnical Testing Journal*, American Society for Testing and Materials, Vol. 19, No. 1, March, 1996, pp. 3-11, 1996b.

Stark, T. D., Olson, S. M., Kramer, S. L., and Youd, T. L., "Shear Strength of Liquefied Soil," Geotechnical Special Publication No. 75, Geotechnical Earthquake Engineering and Soil Dynamics III, (eds. Dakoulas, P., Yegian, M, and Holtz, R.), *Proceedings of a Specialty Conference, American Society of Civil Engineers Geo-Institute*, August 3-6, 1998, Seattle, WA, 1998.

References

Steedman, R. S., "Modeling the Behavior of Retaining Walls in Earthquakes," Ph.D. Thesis, Cambridge University, Cambridge, UK, 1984.

Stokoe, K. H., and Nazarian, S., "Use of Rayleigh Waves in Liquefaction Studies," *Proceedings, Measurement and Use of Shear Wave Velocity for Evaluating Dynamic Soil Properties*, American Society of Civil Engineers, held at Denver, CO, pp. 1-17, 1985.

Stokoe, K. H., Roesset, J. M., Bierschwale, J. G., and Aouad, M., "Liquefaction Potential of Sands from Shear Wave Velocity," *Proceedings, Ninth World Conference on Earthquake Engineering*, Tokyo-Kyoto, Japan, Vol. III, pp. 213-218, August, 1988.

Suzuki, Y., Koyamada K., Tokimatsu, K., Taya, Y., and Kurbota, Y., "Empirical Correlations of Soil Liquefaction based on Cone Penetrometer Test," *Proceedings, First International Conference on Earthquake Geotechnical Engineering, 1985*, (ed. Ishihara, K.), 1995a.

Suzuki, Y., Tokimatsu, K., Koyamada K., Taya, Y., and Kurbota, Y., "Field Correlation of Soil Liquefaction based on CPT Data," *Proceedings, International Symposium on Cone Penetrometer Testing - CPT '95*, Linkopping, Sweden, October 1995b.

Sy, A., "Energy Measurements and Correlations of the Standard Penetration Test (SPT) and the Becker Penetration Test (BPT)," PhD Thesis, Department of Civil Engineering, University of British Columbia, Vancouver, BC, 1993.

Sy, A., and Campanella, R. G., "Dynamic Performance of the Becker Hammer Drill and Penetration Test," *Canadian Geotechnical Journal*, Vol. 30(4), pp. 607-619, 1993.

Sy, A., and Campanella, R. G., "Becker and Standard Penetration Tests (BPT-SPT) Correlations with Consideration of Casing Friction." *Canadian Geotechnical Journal*, Vol. 31(3), pp. 343-356, 1994.

Sy, A., Campanella, R. G., and Stewart, R. A., "BPT-SPT Correlations for Evaluation of Liquefaction in Gravelly Soils," *Proceedings, American Society of Civil Engineering Annual Convention, Session on Dynamic Properties of Gravelly Soils*, San Diego, CA, October 23-27, Geotechnical Special Publication No. 56, 1995.

Sykora, D. W., Koester, J. P., and Hynes, M. E., "Seismic Stability Evaluation of Ririe Dam and Reservoir Project - Report 2 - Stability Calculations, Analysis, and Evaluations, Vol I," Technical Report GL-91-22, U.S. Army Engineer Waterways Experiment Station, Vicksburg, MS, 1991.

Szerdy, F., "Flow Slide Failure Associated with Low Level Vibrations," Ph.D. Thesis, University of California, Berkeley, CA, 1985.

Tanaka, Y., Kokusho, T., Yoshida, Y., and Kudo, K., "Dynamic Strength Evaluation of Gravelly Soils," *Proceedings, Discussion Session on Influence of Local Conditions on Seismic Response, 12th International Conference on Soil Mechanics and Foundation Engineering,* Rio de Janeiro, Brazil, as reprinted in *Proceedings, International Seminar on Dynamic Behavior of Clays, Sands, and Gravels*, Kitakyushu, Japan, November 24-25, 1989, pp. 274-282, 1989.

Taylor, D. W. And Whitman, R. V., Letter to the U.S. Army Corps of Engineers District, Los Angeles, regarding the Seismic Stability of Prado Dam (first known documentation of the sliding block method that recognizes the importance of strength reductions caused by earthquake shaking and shear movement), 1952.

Tohno, I., "Diagenesis and Mechanical Characteristics of Sediments," (in Japanese), *Geological Journal*, pp. 547-559, September, 1975.

Tokimatsu, K., and Seed, H. B., "Evaluation of Settlements in Sands Due to Earthquake Shaking," *American Society of Civil Engineers, Journal of Geotechnical Engineering*, Vol. 113, No. 8, pp. 861-878, 1987.

Tokimatsu, K. and Yoshimi, Y., "Empirical Correlation of Soil Liquefaction Based on SPT N-value and Fines Content," *Japanese Society of Soil Mechanics and Foundation Engineering, Soils and Foundations*, Vol. 15(4), pp. 81-92, 1983.

Tokimatsu, K., Yoshimi, Y., and Uchida, A., "Evaluation of Undrained Cyclic Shear Strength of Soils with Shear Wave Velocity," *Proceedings, Ninth World Conference on Earthquake Engineering*, Tokyo-Kyoto, Japan, Vol. III, pp. 207-212, August, 1988.

Torres, N., Koester, J. P., and Llopis, J. L., "Field Investigations for Foundations of Nuclear Facilities," draft contract report submitted for publication to the U.S. Nuclear Regulatory Commission, December, 1998.

Torrey, V. H., Dunbar, J. B., and Peterson R. W., "Retrogressive Failures in Sand Deposits of the Mississippi River, Report 1, Field Investigation, Laboratory Studies and Analysis of Hypothesized Failure Mechanism," Technical Report GL-88-9, U.S. Army Engineer Waterways Experiment Station, Vicksburg, MS, 1988.

Towhata, I., Tokida, K., Tamari, Y., Matsumoto, H., and Yamada, K., "Prediction of Permanent Lateral Displacement of Liquefied Ground by Means of Variational Principle," *Proceedings, 3rd Japan-U.S. Workshop on Earthquake Resistant Design of Lifeline Facilities and Countermeasures for Soil Liquefaction*, NCEER, Technical Report NCEER-91-0001, pp. 233-251, 1991.

Troncoso, J., Ishihara, K., and Verdugo, R., "Aging Effects on Cyclic Shear Strength of Tailings Materials," *Proceedings, Ninth World Conference on Earthquake Engineering*, Tokyo-Kyoto, Japan, Vol. III, pp. 121-126, August 2-9, 1988.

Tsuchida, H., "Prediction and Countermeasure Against Liquefaction in Sand Deposits," (in Japanese), Abstract of the Seminar of the Port and Harbour Research Institute, Ministry of Transport, Yokosuka, Japan, pp. 3.1-3.33, 1970.

Tuttle, M. P. and Seeber, L., "Earthquake-Induced Liquefaction in the Northeastern United States: Historical Effects and Geological Constraints," Earthquake Hazards and the Design of Constructed Facilities in the Eastern United States, Annals of the New York Academy of Sciences, (eds. Jacob, K. H. and Turkstra, C. J.), Vol. 558, pp. 196-207, 1989.

U.S. Nuclear Regulatory Commission, "Regulatory Guide 1.138: Laboratory Investigations of Soils for Engineering Analysis and Design of Nuclear Power Plants," Office of Standards Development, Washington, D.C., April, 1978.

References

U.S. Nuclear Regulatory Commission, "Regulatory Guide 1.132: Site Investigations for Foundations of Nuclear Power Plants," Revision 1, Office of Standards Development, Washington, D.C., March, 1979.

Vaid, Y. P., Byrne, P. M., and Hughes, J. M. O., "Dilation Angle and Liquefaction Potential," *Proceedings, International Conference on Recent Advances in Geotechnical Earthquake Engineering and Soil Dynamics*, St. Louis, Vol. I, pp. 179-185, 1981.

Vaid, Y. P. and Chern, J. C., "Effect of Static Shear on Resistance to Liquefaction," *Japanese Society of Soil Mechanics and Foundation Engineering, Soils and Foundations*, Vol. 23(1), pp. 47-60, 1983.

Vaid, Y. P. and Finn, W. D. L., "Static Shear and Liquefaction Potential," *American Society of Civil Engineers, Journal of the Geotechnical Division*, Vol. 105(GT10), pp. 1233-1246, 1979.

Vaid, Y. P. and Thomas, J., "Liquefaction and Post Liquefaction Behavior of Sand," *American Society of Civil Engineers, Journal of Geotechnical Engineering*, Vol. 121(2), pg. 163-173, 1995.

Walker, A. J. and Stewart, H. E., "Cyclic Undrained Behavior of Nonplastic and Low Plasticity Silts," Technical Report NCEER-89-0035, National Center for Earthquake Engineering Research, State University of New York at Buffalo, NY, July, 1989.

Wang, W. S., "Some Findings in Soil Liquefaction," Water Conservancy and Hydroelectric Power Scientific Research Institute, Beijing, China, 1979.

Wang, W. S., "Earthquake damages to earth dams and levees in relation to soil liquefaction and weakness in soft clays," *Proceedings of the International Conference on Case Histories in Geotechnical Engineering*, St. Louis, MO, Vol. 1, 511-521, 1984.

Wang, Z. Q., "Macroscopic Approach to Soil Liquefaction," *Proceedings, International Conference on Recent Advances in Geotechnical Earthquake Engineering and Soil Dynamics*, St. Louis, Vol. I, pp. 179-185, 1981.

Wesnousky, S. G., Schweig, E. S., and Pezzopane, S. K., "Extent and Character of Soil Liquefaction During the 1811-1812 New Madrid Earthquakes," Earthquake Hazards and the Design of Constructed Facilities in the Eastern United States, Annals of the New York Academy of Sciences, (eds. Jacob, K. H. and Turkstra, C. J.), Vol. 558, pp. 208-216, 1989.

Whitman, R. V., Lambe, P. C., and Kutter, B. L. "Initial Results from a Stacked Ring Apparatus for Simulation of a Soil Profile," *Proceedings, International Conference on Recent Advances in Geotechnical Engineering and Soil Dynamics*, (ed. Prakash, S.), University of Missouri, Rolla, MO, Vol. III, pp. 1105-1110, 1981.

Wood, D. M., "Laboratory Investigations of the Behavior of Soils under Cyclic Loading: A Review," Soil Mechanics - Transient and Cyclic Loads, John Wiley and Sons, Ltd., 1982.

Woods, R. D., "Measurement of Dynamic Soil Properties," *Proceedings, Earthquake Engineering and Soil Dynamics, American Society of Civil Engineers Specialty Conference*, Pasadena, Vol. I, pp. 91-178, June 19-21, 1981.

Yan, L., "Seismic Deformation Analysis of Earth Dams: a simplified method," Report No. SML 91-01, Soil Mechanics Laboratory, California Institute of Technology, Pasadena, CA, 1991.

Yasuda, S., Nagase, H., Kiku, H., and Uchida, Y., "A Simplified Procedure for the Analysis of the Permanent Ground Displacement," *Proceedings, 3rd Japan-U.S. Workshop on Earthquake Resistant Design of Lifeline Facilities and Countermeasures for Soil Liquefaction*, NCEER, Technical Report NCEER-91-0001, pp. 25-236, 1991.

Yegian, M. K., Ghahraman, V.G., and Gazetas, G., "Seismological, Geotechnical, and Structural Overview," *The Armenia Earthquake of December 1988*, Northeastern University, Boston, pp. 1-34., 1992.

Yegian, M. K., Ghahraman, V.G. and Harutiunyan, R.N., "Liquefaction and embankment failure case histories, 1988 Armenian earthquake," *Journal of Geotechnical Engineering,* ASCE, 120(3): 581-596, 1994.

Yoshimi, Y. K. and Oh-Oka, H., "Influence of Degree of Shear Stress Reversal on the Liquefaction Potential of Saturated Sand," *Japanese Society of Soil Mechanics and Foundation Engineering, Soils and Foundations*, Vol. 15(3), pp. 27-40, 1975.

Yoshimi, Y. K. and Tokimatsu, K., "Two-Dimensional Pore Pressure Changes in Sand Deposits During Earthquakes," *Proceedings, 2nd International Conference on Microzonation*, San Francisco, Vol. 2, pp. 853-863, 1978.

Youd, T. L., "Packing Changes and Liquefaction Susceptibility," *American Society of Civil Engineers, Journal of the Geotechnical Engineering Division*, 103(GT8), 918-923, 1977.

Youd, T.L. , Harp, E. L., Keefer, D. K. and Wilson, R. C., "The Borah Peak, Idaho earthquake of October 28, 1983 - liquefaction," *Earthquake Spectra*, EERI, 2(1): 71-89, 1985.

Youd, T. L., "Liquefaction-Induced Lateral Spread Displacement," Technical Note N-1862, Naval Civil Engineering Laboratory, Port Hueneme, CA., June, 1993.

Youd, T. L., "Screening Guide for Rapid Assessment of Liquefaction Hazard at Highway Bridge Sites," Technical Report MCEER-98-0005, Multidisciplinary Center for Earthquake Engineering Research, State University of New York at Buffalo, Buffalo, NY, 1998.

Youd, T. L. and Hoose, S. N., "Liquefaction Susceptibility and Geologic Setting," *Proceedings, Sixth World Conference on Earthquake Engineering*, New Delhi, India, Vol. 6, pp. 37-42, 1977.

Youd, T. L. and Perkins, D. M., "Mapping of Liquefaction Induced Ground Failure Potential," *American Society of Civil Engineers, Journal of the Geotechnical Engineering Division*, Vol. 104, No. GT4, pp. 433-446, 1978.

APPENDIX A
STEADY STATE STRENGTH TESTING

The procedure for measuring the undrained steady-state strength, S_{us}, of sands presented herein is based on Poulos, Castro, and France (1985) and Poulos (1988). The steps of the determination of in situ S_{us} values in sandy soils involve the following determinations: (1) In situ void ratio, (2) Steady state line for compacted specimens, (3) Undrained steady state strengths for "undisturbed" specimens, and (4) Correction of strengths for void ratio. Subsequent paragraphs describe each step.

Step 1: In Situ Void Ratio

Undisturbed samples should be obtained to enable estimation of the in situ S_{us}-value, which is dependent solely on the soil composition and the void ratio. The undisturbed samples should be taken in the loosest zones of the embankment or foundation to be conservative. Zones that have the lowest blowcounts, most narrowly graded soils, and most rounded grains are the zones likely to give the lowest S_{us}-values.

Currently, there are at least three satisfactory ways to obtain suitably undisturbed samples of loose sand at depth in situ: (1) fixed-piston sampling, (2) sampling in test pits, and (3) freezing of the ground and coring. A satisfactory method not only should cause minimal volume changes but should provide sufficient data to estimate the volume changes that do occur during sampling. All three methods listed above require care. For clays, it is relatively simple to measure the in situ void ratio using the procedures developed by Hvorslev (1949). For sands, considerably more care is needed. Some of the important sampling details are discussed below.

The fixed-piston sampler contains a piston that is fixed at the bottom of the hole by a rod that extends to the ground surface. One pushes a thin-wall tube into the ground past the piston while holding the piston rod fixed. The clearance ratio of the cutting edge of the sampling tube should be adjusted for the particular sand so that the ratio has the minimum value necessary for sample retention. This ratio might vary from near zero to 1 percent. The stroke length during sampling must be measured within approximately 0.2 percent. It should be corrected for rod compression if the hole is deep.

Trial sampling is needed to select the maximum hydraulic pressure that may be used without deforming the cutting edge. Short samples are acceptable for measuring void ratio and laboratory testing. **The tube should not be hammered**. Removal of the tube from the hole should be extremely slow (approximately 1 mm/sec or even slower) to reduce the vacuum at the bottom, withdrawal should occur without vibration, and the drilling water or mud should be kept above the water table. When the sample is removed from the hole, any gap between the piston and the top of the soil should be measured. This gap is caused by (1) compression of the sample during penetration, (2) downward movement as the soil fills the gap between the cutting edge and the inside wall, and (3) sample slippage during removal from the hole. To be conservative, it is usually assumed that, except for item 3, the gap is caused entirely by sample compression.

The volume of a tube sample is computed as the product of stroke length and the area of the tube inside the cutting edge. The measured gap is prorated to each specimen tested. Thus when one knows the specimen dry weight, specific gravity of solids, and specimen volume, one can calculate the void ratio it had in situ. Use of the above values to compute void ratio without accounting for possible downward slippage of the soil in the tube during removal from the hole is conservative. If slippage occurs, the void ratio will be overestimated. At present there is no satisfactory way for estimating slippage except when it is large enough that the calculated void ratio is unreasonable. Thus trial sampling with various clearance ratios is helpful in judging the clearance ratio needed to control slippage.

Step 2: Steady State Line for Compacted Specimens

"Undisturbed" samples of loose sand almost always have a lower void ratio in the laboratory than in situ. Therefore, a procedure for correcting laboratory measured steady state strengths to the in situ void ratio is required. For sands the S_{us}-value is quite sensitive to void ratio; therefore, conservative techniques for making this correction are important.

In practice it has been found that the volume changes during sampling are relatively small compared to those occurring during consolidation in the triaxial cell. Even if a sample is obtained by freezing the ground and coring, the density may increase significantly during reconsolidation in the laboratory to in situ stresses.

In subsequent discussions the term "steady state line" will be used. It is the line drawn through points that show the steady state void ratio versus the effective minor principal stress during steady state deformation. The effective stress may be plotted on an arithmetic or logarithmic scale.

The procedure for correcting laboratory-measured undrained steady state strengths to the in situ void ratio is based on two observations: (1) the slope of the steady state line on a semi-log plot is affected chiefly by the shape of the grains in a given soil, and (2) the vertical position of the steady state line is affected even by small differences in grain-size distribution (Poulos, Castro, and France, 1985 and Castro et al., 1982).

The correction procedure requires that the steady state line be obtained by testing five or six compacted specimens of identical soil. Any suitable test method may be used. For clean, narrowly graded sands, the triaxial test is satisfactory. It is advisable to check the steady state line using a second type of test, for example, a rotation shear test or a direct sample shear test. For soils with a substantial percentage of fines, it is often necessary to use a rotation shear test to achieve steady state deformation. For clays the vane test can be used (Poulos, Robinsky, and Keller, 1985).

The soil used should be as nearly as possible the same soil as that in the ground. Often several "undisturbed" samples from the upper part of sampling tubes can be thoroughly mixed, as these zones may be more disturbed than the lower samples, which are used for subsequent steps. At this stage only the grain shape distribution need be well preserved because it has the major effect on the slope of the steady state line. It is also desirable to preserve the grain-size distribution. The slope of the steady state line for the compacted specimens will then be as close as possible to that for the associated undisturbed specimens to be tested in Step 3.

Each compacted specimen should be placed in the test apparatus at a void ratio and effective stress combination that is well above the steady state line. Such a specimen will be highly contractive, and the strain needed to reach steady state will be minimized.

Figure A-1 gives plots of the data for one undrained test. These graphs are suggested as a standard method for plotting stress-strain data.

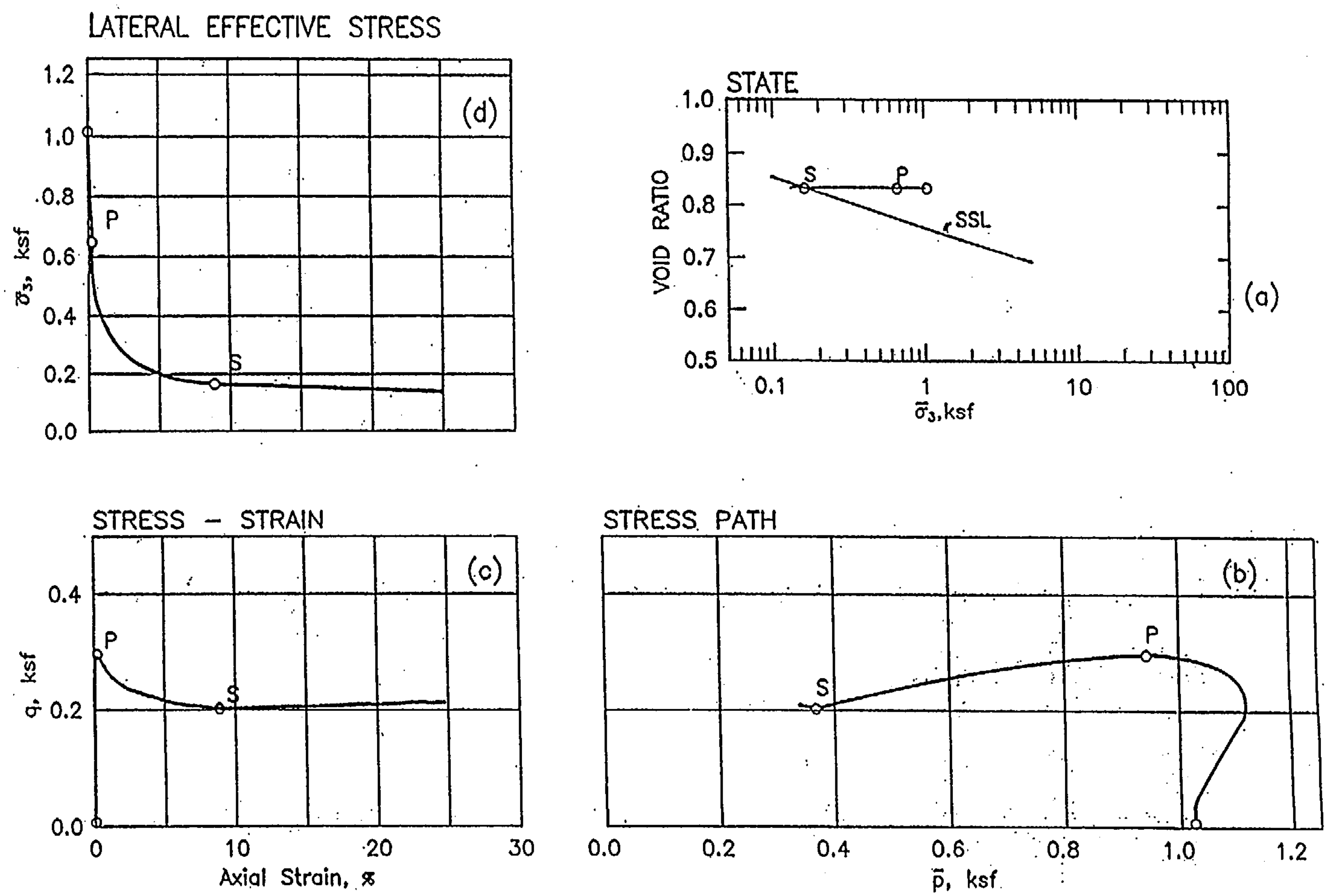

SOIL	STRUCTURE	STATE	LOADING
Batch Mix Poorly graded SAND with clay (SP – SC).	Compacted moist at 6% water content in 8 layers.	$\bar{\sigma}_{3c}$ = 1.02 ksf $q_c/\bar{\sigma}_{3c}$ = 0 γ_{dc} = 91.3 pcf B_c = 0.98 e_c = 0.832 D_c = 2.63 inch H_c = 5.97 inch	Undrained monotonic axial compression at 0.11%/min.

Figure A-1. Typical undrained triaxial test result on loose sand (Castro, Poulos, and France, 1985, reprinted with permission from ASCE)

A typical stress-strain curve from an undrained triaxial test on a contractive specimen is shown in Figure A-1c. The steady state is reached at that strain where the shear stress and the effective minor principal stress are no longer changing as deformation continues. This is point S in graphs (a) and (c) of Figure A-1. Note that the strain at peak shear stress, point **P** in Figure A-1c, must be exceeded greatly to reach the steady state of deformation.

The results of the tests on compacted specimens are plotted on one "state diagram," such as Figure A-2. The best fit line through the points representing the steady state is the steady state line. Each point on this line represents a condition of continuous deformation. The original structure is completely remolded at the steady state. Therefore, the method of specimen preparation, which controls the original structure, has no influence on the position or slope of the steady state line for the particular soil used.

As it is the steady state shear strength that is needed for liquefaction analysis by this procedure, it is convenient to plot the results of the undrained triaxial tests in terms of void ratio versus undrained steady state shear strength on the failure plane, S_{us}, as shown in Figure A-2. To compute S_{us} from the results of each consolidated undrained triaxial test, one uses the following equations:

$$S_{us} = q_s \cos \phi_s \tag{A-1}$$

and:

$$\sin \phi_s = \frac{q_s}{\sigma_{3s} + q_s} = \frac{q_s}{(\sigma_{3c} - u_s) + q_s} \tag{A-2}$$

for

$$q_s = (\sigma_{1s} - \sigma_{3s})/2 \tag{A-3}$$

where

$\bar{\sigma}_{1s} - \bar{\sigma}_{3s}$ = Principal stress difference at the steady state from the triaxial test
$\bar{\sigma}_{3s}$ = Effective minor principal stress at the steady state
$\bar{\sigma}_{3c}$ = Effective minor principal stress at start of shear (after consolidation)
u_s = Pore pressure induced in the test specimen at the steady state of deformation
ϕ_s = Steady state friction angle

The quantities q_s, $\bar{\sigma}_{3c}$, and u_s are obtained directly during triaxial tests.

The steady state strength line (Figure A-2) obtained from the compacted specimens is used to correct the strengths of "undisturbed" specimens, which are determined in the following step.

Step 3: Undrained Steady State Strengths for "Undisturbed" Specimens

A series of consolidated undrained triaxial or other appropriate tests is performed on "undisturbed" specimens from the zone being evaluated. Sufficient tests are needed to determine the average steady state strength reliably.

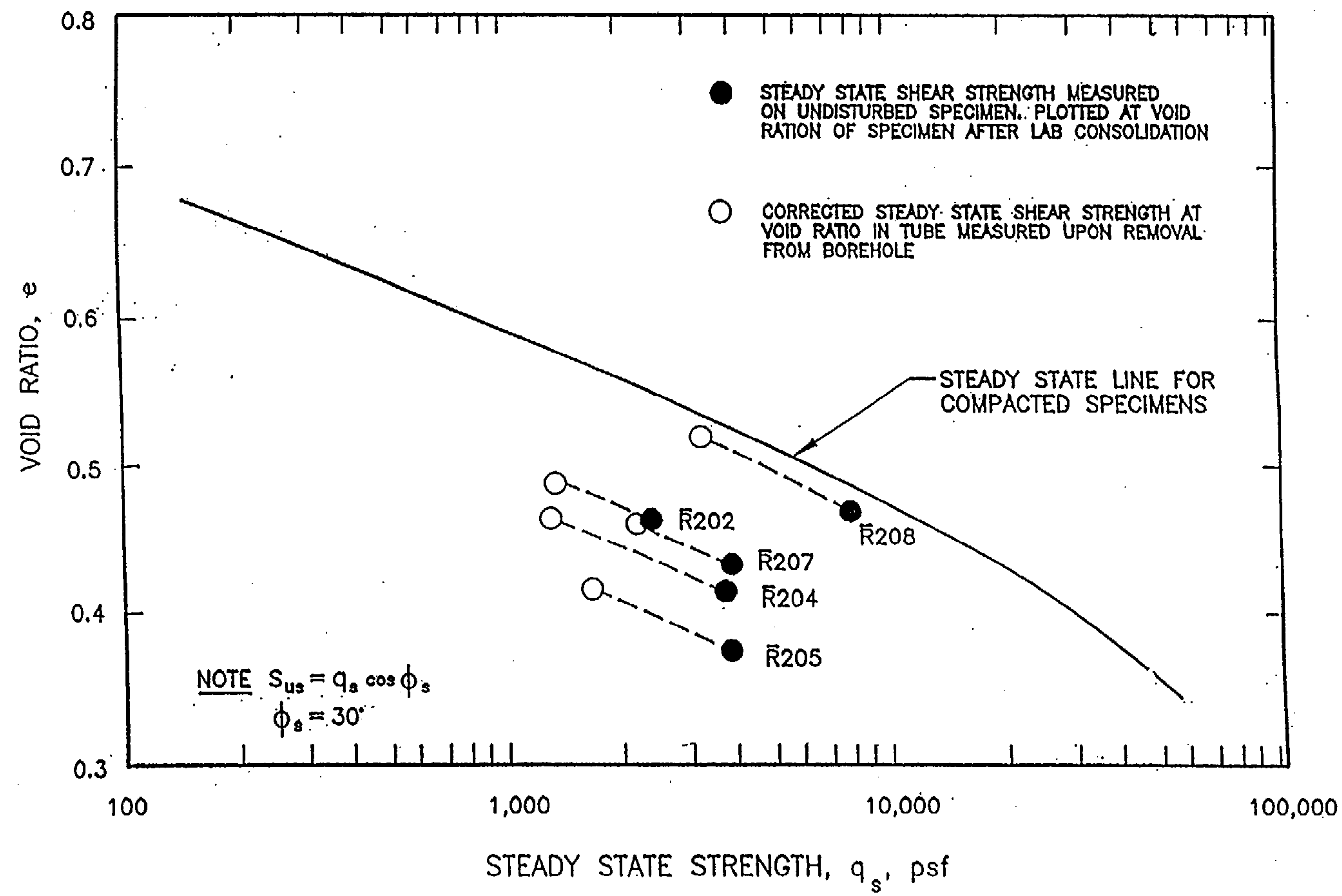

Figure A-2. State diagram for compacted specimens (Castro, Poulos, and France, 1985, reprinted with permission from ASCE)

To define the steady state well in a triaxial test - at strains achievable in that test - it is best to ensure that the undisturbed specimen is contractive, just as was done for the compacted specimens. One procedure is to consolidate the undisturbed specimens to high effective stresses (but not so high that the correction needed in Step 4 becomes excessive). At high effective stresses, sandy soils are more contractive than at low effective stresses. If the stresses used are not high enough to make the specimens contractive, the steady state still can be determined. However, the accuracy of the measurement is poorer than for contractive specimens, because more redistribution of void ratio probably occurs during tests on dilative specimens and the strain required to reach steady state are larger.

The stress-strain data for the tests on contractive, undisturbed specimens are similar to those shown in Figure A-1. The steady state point for each "undisturbed" specimen is plotted on the state diagram, together with the steady state line for the compacted specimens, as shown in Figure A-2. The vertical distance between the individual points and the steady state line for compacted specimens is assumed to be due chiefly to minor differences in grain-size distribution. For the case in Figure A-2, all of the tests results on undisturbed specimens plotted below the steady state line for the compacted specimens. However, they may plot above and/or below in other cases, and it is more common for the undisturbed specimens to plot above the steady state line for the remolded specimens.

The undrained steady state shear strengths shown by the solid dots in Figure A-2 were obtained at the void ratio after consolidation, not at the in situ void ratio. Therefore, correction of the results to the in situ void ratio must be made, as described in the next, and final, step.

Step 4: Correction of Strengths for Void Ratio

The final, and most significant, step in this procedure is to compute the in situ void ratio for each of the tested "undisturbed" specimens from the measurements made during undisturbed sampling. Using the in situ void ratio, the correction procedure given in Figure A-3 is applied for each test in Figure A-2 on the undisturbed specimens. The dashed line is drawn through the point that shows the measured undrained steady state strength of the "undisturbed" specimen at its void ratio in the laboratory. The dashed line is drawn parallel to the steady state strength line for the compacted specimens.

A horizontal line is drawn from the ordinate axis starting at the calculated in situ void ratio to intersect the dashed line for the test on that undisturbed specimen. The estimated in situ undrained steady state strength is selected from the abscissa. This strong dependence of the steady state strength approach on void ratio, which has been confirmed by many investigators, is the main source of uncertainty in evaluating the undrained steady state strength (S_{us}). Note that the uncertainty is present in any method to evaluate S_{us}, whether it is explicitly considered, as in the method just described, or not, such as in the empirical method. In other words, it is a clear experimental fact that minor changes in void ratio in the *in situ* soil represent significant changes in S_{us}, and thus index tests such as blowcounts that are not very sensitive to void ratio are themselves suspect to inaccuracy in measurement of S_{us}.

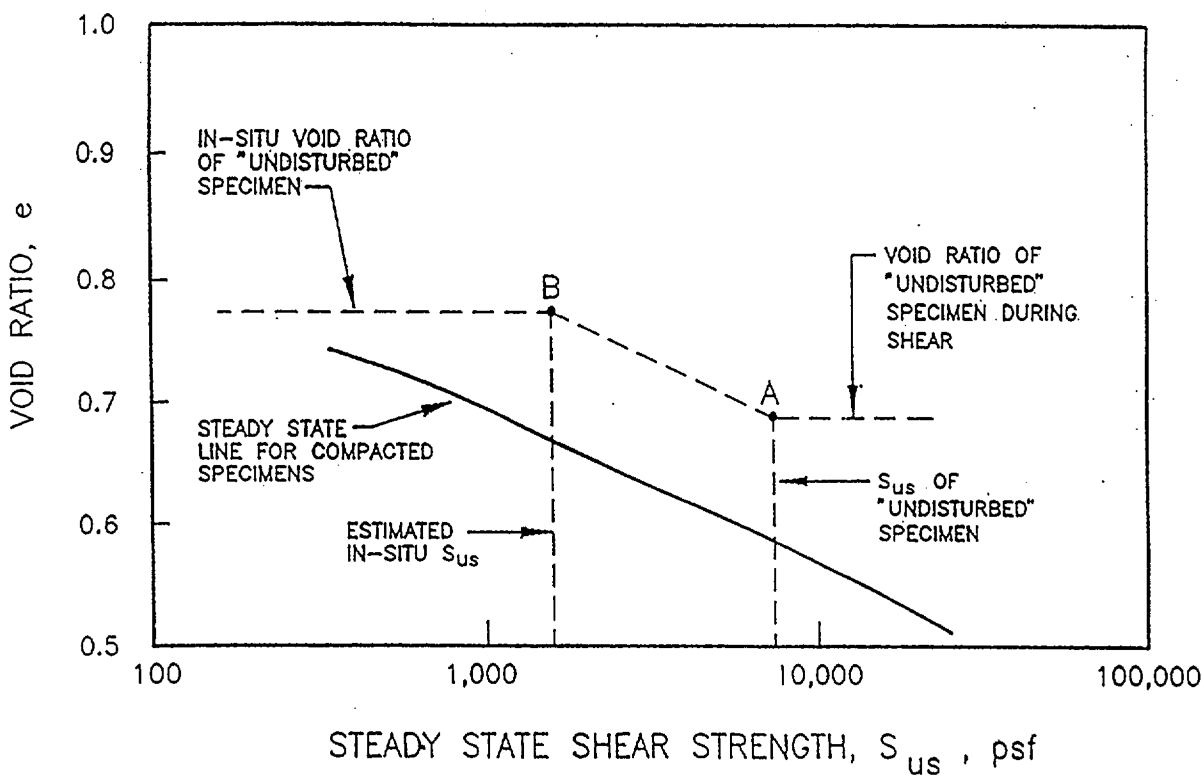

Figure A-3. Correction of steady state strength for void ratio changes (Castro, Poulos, and France, 1985, reprinted with permission from ASCE)

NRC FORM 335 (2-89) NRCM 1102, 3201, 3202 — U.S. NUCLEAR REGULATORY COMMISSION **BIBLIOGRAPHIC DATA SHEET** *(See instructions on the reverse)*	1. REPORT NUMBER (Assigned by NRC, Add Vol., Supp., Rev., and Addendum Numbers, if any.) NUREG/CR-5741
2. TITLE AND SUBTITLE Technical Bases for Regulatory Guide for Soil Liquefaction	3. DATE REPORT PUBLISHED MONTH: March YEAR: 2000 4. FIN OR GRANT NUMBER W6246
5. AUTHOR(S) J.P. Koester, M.K. Sharp, M.E. Hynes	6. TYPE OF REPORT Technical 7. PERIOD COVERED *(Inclusive Dates)* June 1995 - July 1999

8. PERFORMING ORGANIZATION - NAME AND ADDRESS *(If NRC, provide Division, Office or Region, U.S. Nuclear Regulatory Commission, and mailing address; if contractor, provide name and mailing address.)*

U.S. Army Corps of Engineers
Waterways Experiment Station
3909 Halls Ferry Road
Vicksburg, MS 39180-6199

9. SPONSORING ORGANIZATION - NAME AND ADDRESS *(If NRC, type "Same as above"; if contractor, provide NRC Division, Office or Region, U.S. Nuclear Regulatory Commission, and mailing address.)*

Division of Engineering Technology
Office of Nuclear Regulatory Research
U.S. Nuclear Regulatory Commission
Washington, DC 20555-0001

10. SUPPLEMENTARY NOTES

E. Zurflueh, NRC Project Manager

11. ABSTRACT *(200 words or less)*

This document provides technical bases for developing a new Regulatory Guide for evaluating the potential for earthquake-induced liquefaction at nuclear facility sites, compiling current and state of the art techniques. A historical perspective is provided to define liquefaction phenomena observed during earthquakes and to support identification of soil characteristics associated with liquefaction. Guidance is presented for site characterization studies, including the various in situ tests available for liquefaction potential evaluation. Screening techniques and progressively more detailed procedures are presented for investigations necessary to identify soils that may pose a hazard to important facilities. Only deterministic procedures are described; probabilistic approaches are detailed in a separate report.

An example problem illustrates the evaluation of liquefaction triggering and estimation of residual strength of liquefied soils. Current practice for evaluating and estimating permanent deformations to earthen structures is discussed. Deformations accompanying liquefaction are included, but limited to those resulting from inertial forces during shaking. Estimation of very large deformations is not a well-established process and is a subject of ongoing research.

12. KEY WORDS/DESCRIPTORS *(List words or phrases that will assist researchers in locating the report.)*	13. AVAILABILITY STATEMENT
Deterministic Procedures Liquefaction Potential Displacement Analysis	unlimited 14. SECURITY CLASSIFICATION *(This Page)* unclassified *(This Report)* unclassified 15. NUMBER OF PAGES 16. PRICE

UNITED STATES
NUCLEAR REGULATORY COMMISSION
WASHINGTON, D.C. 20555-0001

1975 25 2000
years